

Transverse Centroid and Envelope Descriptions of Beam Evolution*

Prof. Steven M. Lund
Physics and Astronomy Department
Facility for Rare Isotope Beams (FRIB)
Michigan State University (MSU)

US Particle Accelerator School (USPAS) Lectures on
“Beam Physics with Intense Space-Charge”

Steven M. Lund and John J. Barnard

US Particle Accelerator School Winter Session
Old Dominion University, 19-30 January, 2015
(Version 20170105)

* Research supported by:

FIRB/MSU, 2014 onward via: U.S. Department of Energy Office of Science Cooperative Agreement DE-SC0000661 and National Science Foundation Grant No. PHY-1102511 and

LLNL/LBNL, before 2014 via: US Dept. of Energy Contract Nos. DE-AC52-07NA27344 and DE-AC02-05CH11231

Transverse Centroid and Envelope Model: Outline

Overview

Derivation of Centroid and Envelope Equations of Motion

Centroid Equations of Motion

Envelope Equations of Motion

Matched Envelope Solutions

Envelope Perturbations

Envelope Modes in Continuous Focusing

Envelope Modes in Periodic Focusing

Transport Limit Scaling Based on Envelope Models

Centroid and Envelope Descriptions via 1st Order Coupled Moment Equations

References

Comments:

- ◆ Some of this material related to J.J. Barnard lectures:
 - Transport limit discussions ([Introduction](#))
 - Transverse envelope modes ([Continuous Focusing Envelope Modes and Halo](#))
 - Longitudinal envelope evolution ([Longitudinal Beam Physics III](#))
 - 3D Envelope Modes in a Bunched Beam ([Cont. Focusing Envelope Modes and Halo](#))
- ◆ Specific transverse topics will be covered in more detail here for s -varying focusing
- ◆ Extensive Review paper covers envelope mode topics presented in more detail:

Lund and Bukh, “Stability properties of the transverse envelope equations
describing intense ion beam transport,” PRSTAB **7** 024801 (2004)

Transverse Centroid and Envelope Model: Detailed Outline

1) Overview

2) Derivation of Centroid and Envelope Equations of Motion

Statistical Averages

Particle Equations of Motion

Distribution Assumptions

Self-Field Calculation: Direct and Image

Coupled Centroid and Envelope Equations of Motion

3) Centroid Equations of Motion

Single Particle Limit: Oscillation and Stability Properties

Effect of Driving Errors

Effect of Image Charges

4) Envelope Equations of Motion

KV Envelope Equations

Applicability of Model

Properties of Terms

5) Matched Envelope Solution

Construction of Matched Solution

Symmetries of Matched Envelope: Interpretation via KV Envelope Equations

Examples

Detailed Outline - 2

6) Envelope Perturbations

Perturbed Equations

Matrix Form: Stability and Mode Symmetries

Decoupled Modes

General Mode Limits

7) Envelope Modes in Continuous Focusing

Normal Modes: Breathing and Quadrupole Modes

Driven Modes

Appendix A: Particular Solution for Driven Envelope Modes

8) Envelope Modes in Periodic Focusing

Solenoidal Focusing

Quadrupole Focusing

Launching Conditions

9) Transport Limit Scaling Based on Envelope Models

Overview

Example for a Periodic Quadrupole FODO Lattice

Discussion and Application of Formulas in Design

Results of More Detailed Models

Detailed Outline - 3

10) Centroid and Envelope Descriptions via 1st Order Coupled Moment Equations

Formulation

Example Illustration -- Familiar KV Envelope Model

Contact Information

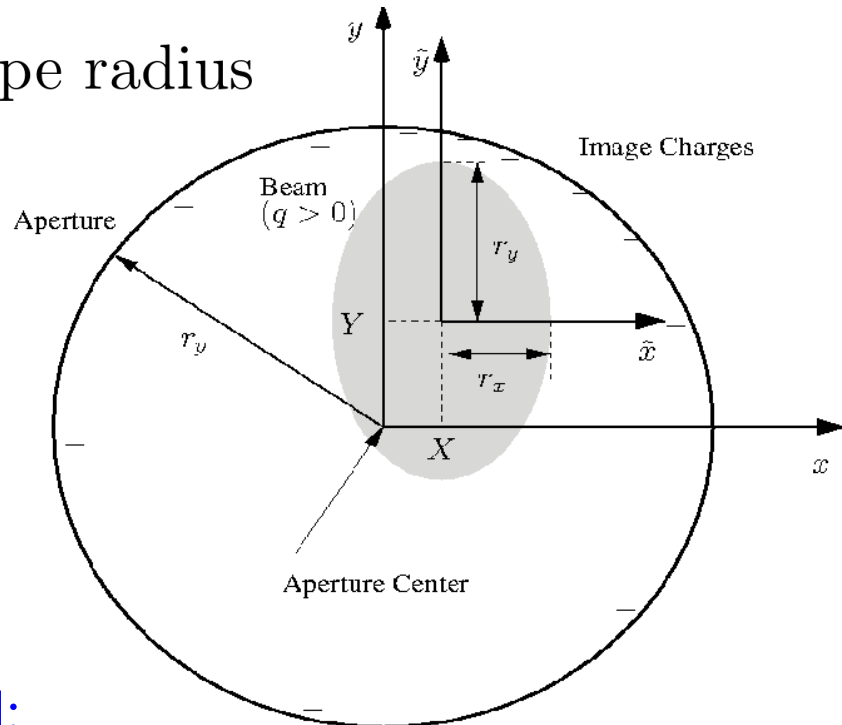
References

Acknowledgments

S1: Overview

Analyze **transverse centroid** and **envelope** properties of an unbunched ($\partial/\partial z = 0$) beam

r_p = pipe radius



Centroid:

$$X = \langle x \rangle_{\perp}$$

$$Y = \langle y \rangle_{\perp}$$

x - and y -coordinates
of beam “center of mass”

Envelope: (edge measure)

$$r_x = 2\sqrt{\langle (x - X)^2 \rangle_{\perp}}$$

$$r_y = 2\sqrt{\langle (y - Y)^2 \rangle_{\perp}}$$

x - and y -principal axis radii
of an elliptical beam envelope

- Apply to general f_{\perp} but base on uniform density f_{\perp}
- Factor of 2 results from dimensionality (diff 1D and 3D)

Expect for linearly focused beam with intense space-charge:

- Beam to look roughly elliptical in shape
- Nearly uniform density within fairly sharp edge

Transverse averages:

$$\langle \dots \rangle_{\perp} \equiv \frac{\int d^2x_{\perp} \int d^2x'_{\perp} \dots f_{\perp}}{\int d^2x_{\perp} \int d^2x'_{\perp} f_{\perp}}$$

Oscillations in the statistical beam centroid and envelope radii are the *lowest-order* collective responses of the beam

Centroid Oscillations: Associated with errors and are suppressed to the extent possible:

- ◆ Error Sources seeding/driving oscillations:
 - Beam distribution assymmetries (even emerging from injector: born offset)
 - Dipole bending terms from imperfect applied field optics
 - Dipole bending terms from imperfect mechanical alignment
- ◆ Exception: Large centroid oscillations desired when the beam is kicked (insertion or extraction) into or out of a transport channel as is often done in rings

Envelope Oscillations: Can have two components in periodic focusing lattices

1) **Matched Envelope:** Periodic “flutter” synchronized to period of focusing lattice to maintain best radial confinement of the beam

- ◆ Properly tuned flutter essential in Alternating Gradient quadrupole lattices

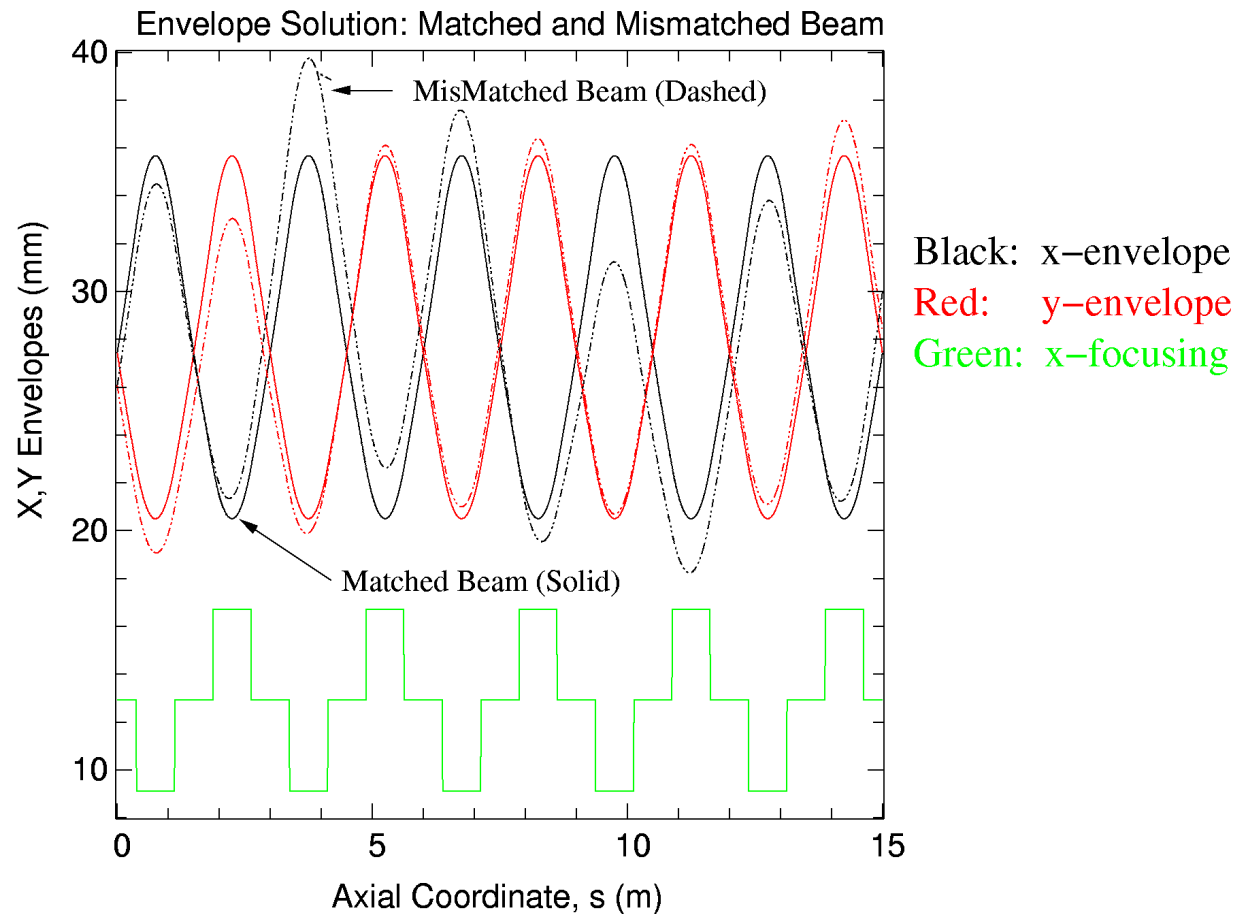
2) **Mismatched Envelope:** Excursions deviate from matched flutter motion and are seeded/driven by errors

Limiting maximum beam-edge excursions is desired for economical transport

- Reduces cost by Limiting material volume needed to transport an intense beam
- Reduces generation of halo and associated particle loses

Mismatched beams have larger envelope excursions and have more collective stability and beam halo problems since mismatch adds another source of free energy that can drive statistical increases in particle amplitudes
 (see: J.J. Barnard lectures on [Envelopes and Halo](#))

Example: FODO Quadrupole Transport Channel



- ◆ Larger machine aperture is needed to confine a mismatched beam

Centroid and Envelope oscillations are the *most important collective modes* of an intense beam

- ◆ Force balances based on matched beam envelope equation predict scaling of transportable beam parameters
 - Used to design transport lattices
- ◆ Instabilities in beam centroid and/or envelope oscillations can prevent reliable transport
 - Parameter locations of instability regions should be understood and avoided in machine design/operation

Although it is *necessary* to avoid envelope and centroid instabilities in designs, it is not alone *sufficient* for effective machine operation

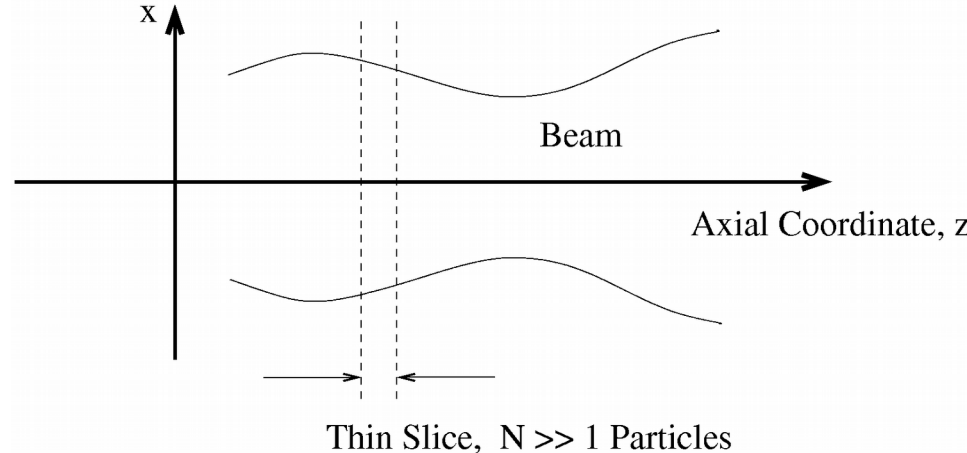
- ◆ Higher-order kinetic and fluid instabilities not expressed in the low-order envelope models can degrade beam quality and control and must also be evaluated
 - To be covered (see: S.M. Lund, lectures on Kinetic Stability)

S2: Derivation of Transverse Centroid and Envelope Equations of Motion

Analyze centroid and envelope properties of an unbunched ($\partial/\partial z = 0$) beam

Transverse Statistical Averages:

Let N be the number of particles in a thin axial slice of the beam at axial coordinate s .



Averages can be equivalently defined in terms of the discrete **particles** making up the beam or the continuous model transverse Vlasov **distribution function**:

particles: $\langle \dots \rangle_{\perp} \equiv \frac{1}{N} \sum_{i=1}^N \Big|_{\text{slice}} \dots$

distribution: $\langle \dots \rangle_{\perp} \equiv \frac{\int d^2x_{\perp} \int d^2x'_{\perp} \dots f_{\perp}}{\int d^2x_{\perp} \int d^2x'_{\perp} f_{\perp}}$

- ◆ Averages can be generalized to include axial momentum spread

Transverse Particle Equations of Motion

Consistent with earlier analysis [lectures on **Transverse Particle Dynamics**], take:

$$x'' + \frac{(\gamma_b \beta_b)'}{(\gamma_b \beta_b)} x' + \kappa_x x = -\frac{q}{m \gamma_b^3 \beta_b^2 c^2} \frac{\partial \phi}{\partial x}$$

$$y'' + \frac{(\gamma_b \beta_b)'}{(\gamma_b \beta_b)} y' + \kappa_y y = -\frac{q}{m \gamma_b^3 \beta_b^2 c^2} \frac{\partial \phi}{\partial y}$$

$$\nabla_{\perp}^2 \phi = \left(\frac{\partial^2}{\partial x^2} + \frac{\partial^2}{\partial y^2} \right) \phi = -\frac{\rho}{\epsilon_0}$$

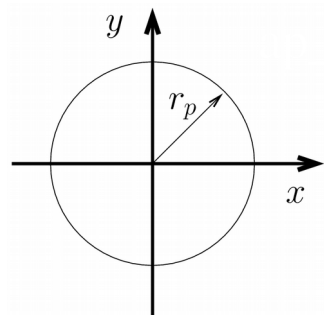
$$\rho = q \int d^2 x'_{\perp} f_{\perp} \quad \phi|_{\text{aperture}} = 0$$

Assume:

- ◆ Unbunched beam
- ◆ No axial momentum spread
- ◆ Linear applied focusing fields described by κ_x, κ_y
- ◆ Possible acceleration: $\gamma_b \beta_b$ need not be constant

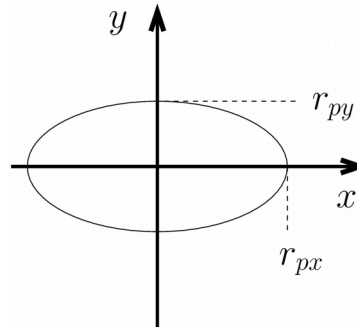
Various apertures are possible influence solution for ϕ . Some simple examples:

Round Pipe



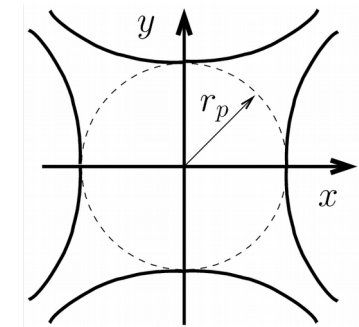
Linac magnetic quadrupoles,
acceleration cells,

Elliptical Pipe



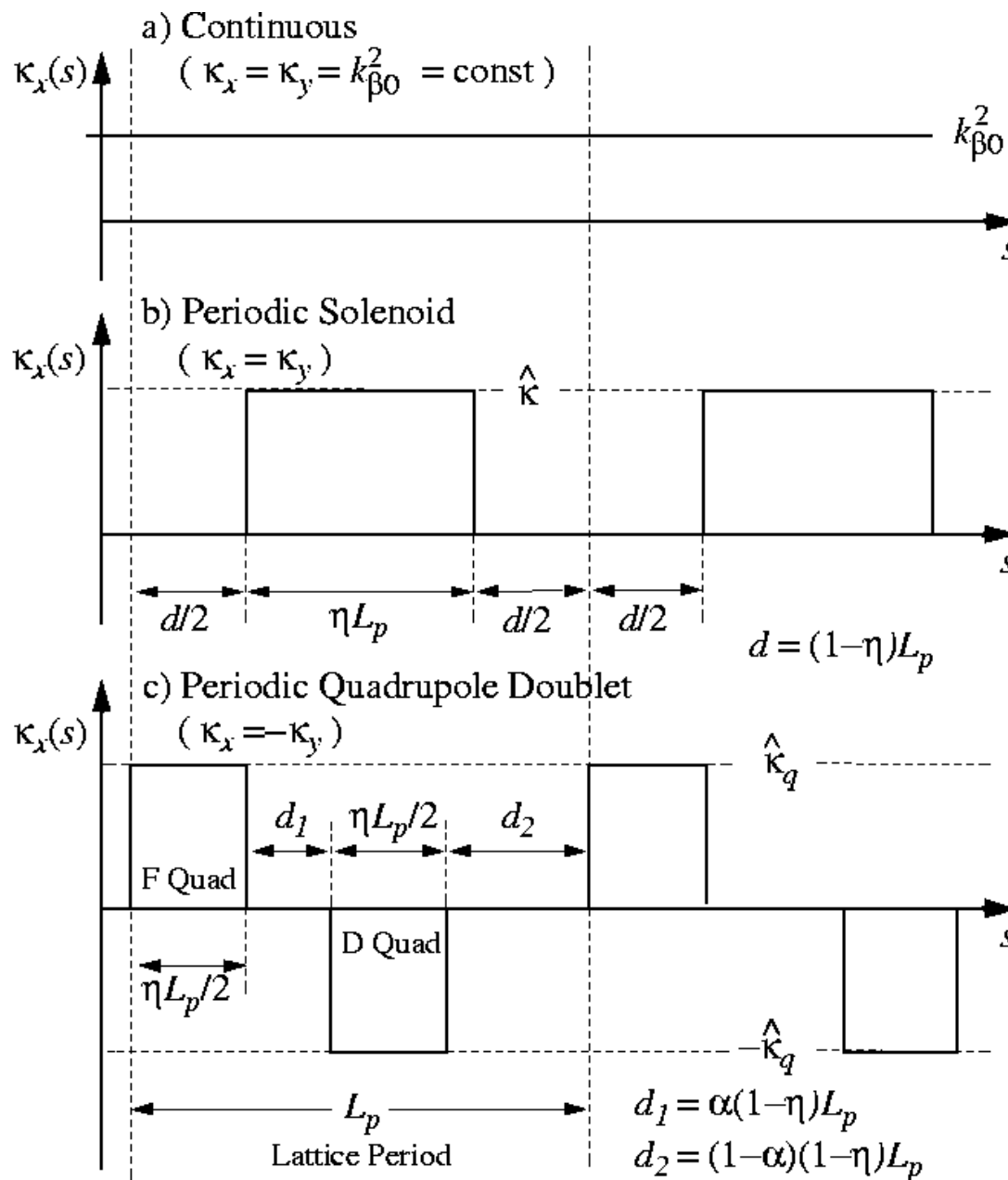
In rings with dispersion:
in drifts, magnetic optics,

Hyperbolic Sections



Electric quadrupoles

Review: Focusing lattices we will take in examples: Continuous and piecewise constant periodic solenoid and quadrupole doublet



Lattice Period L_p

Occupancy η

$$\eta \in [0, 1]$$

Solenoid description
carried out implicitly in
Larmor frame

[see: S.M. Lund lectures on
Transverse Particle Dynamics]

Syncopation Factor α

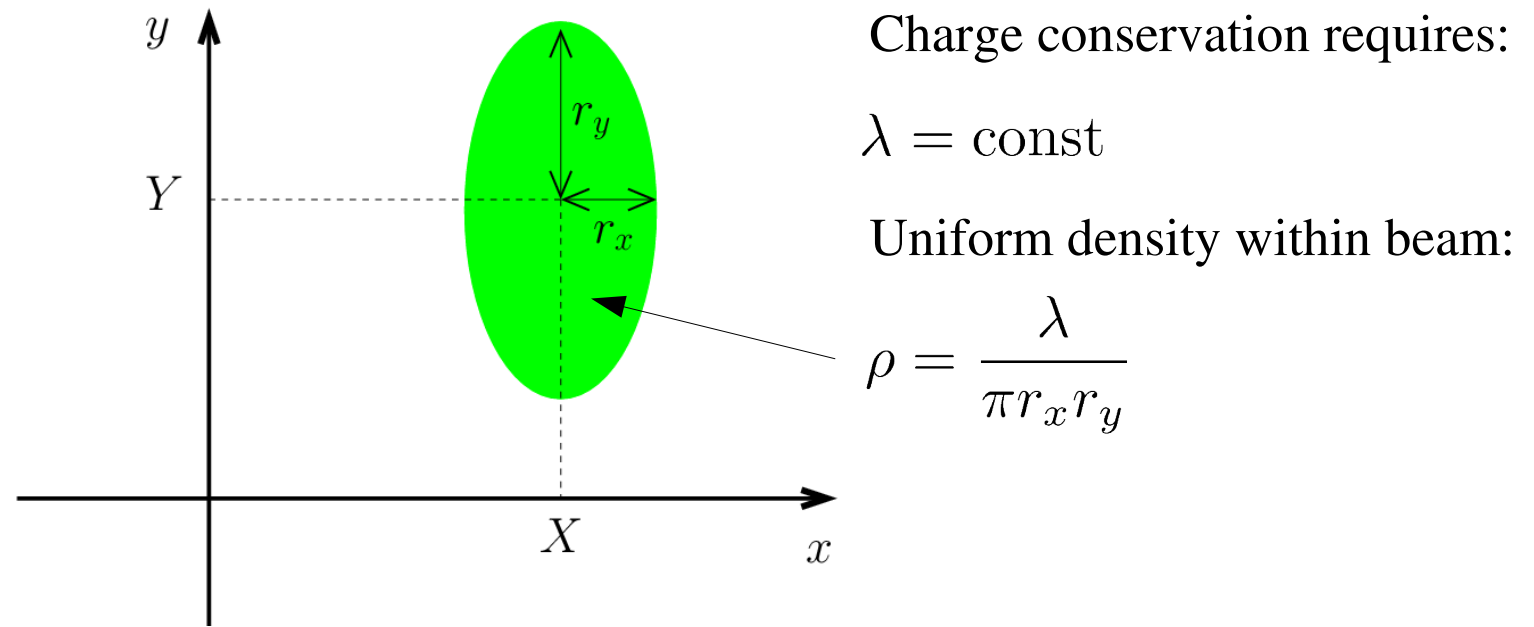
$$\alpha \in [0, \frac{1}{2}]$$

$$\alpha = \frac{1}{2} \implies \text{FODO}$$

Distribution Assumptions

To lowest order, linearly focused intense beams are **expected to be nearly uniform in density** within the core of the beam out to an spatial edge where the density falls rapidly to zero

- ◆ See S.M. Lund lectures on **Transverse Equilibrium Distributions**



$$\rho(x, y) = q \int d^2x'_\perp f_\perp \simeq \begin{cases} \frac{\lambda}{\pi r_x r_y}, & (x - X)^2/r_x^2 + (y - Y)^2/r_y^2 < 1 \\ 0, & (x - X)^2/r_x^2 + (y - Y)^2/r_y^2 > 1 \end{cases}$$

$$\lambda = q \int d^2x_\perp \int d^2x'_\perp f_\perp = \int d^2x \rho = \text{const}$$

Comments:

- ◆ Nearly uniform density out to a sharp spatial beam edge expected for near equilibrium structure beam with strong space-charge due to Debye screening
 - see: S.M. Lund, lectures on **Transverse Equilibrium Distributions**
- ◆ Simulations support that uniform density model is a good approximation for stable non-equilibrium beams when space-charge is high
 - Variety of initial distributions launched and, where stable, rapidly relax to a fairly uniform charge density core
 - Low order core oscillations may persist with little problem evident
 - See S.M. Lund lectures on **Transverse Kinetic Stability**
- ◆ Assumption of a fixed form of distribution essentially closes the infinite hierarchy of moments that are needed to describe a general beam distribution
 - Need only describe shape/edge and center for uniform density beam to fully specify the distribution!
 - Analogous to closures of fluid theories using assumed equations of state etc.

Self-Field Calculation

Temporarily, we will consider an *arbitrary* beam charge distribution within an arbitrary aperture to formulate the problem.

Electrostatic field of a line charge in free-space

$$\mathbf{E}_\perp = \frac{\lambda_0}{2\pi\epsilon_0} \frac{(\mathbf{x}_\perp - \tilde{\mathbf{x}})}{|\mathbf{x}_\perp - \tilde{\mathbf{x}}|^2}$$

λ_0 = line charge

$\mathbf{x}_\perp = \tilde{\mathbf{x}}$ = coordinate of charge

Resolve the field of the beam into direct (free space) and image terms:

$$\mathbf{E}_\perp^s = -\frac{\partial\phi}{\partial\mathbf{x}_\perp} = \mathbf{E}_\perp^d + \mathbf{E}_\perp^i$$

and superimpose free-space solutions for direct and image contributions

Direct Field

$$\mathbf{E}_\perp^d(\mathbf{x}_\perp) = \frac{1}{2\pi\epsilon_0} \int d^2\tilde{\mathbf{x}}_\perp \frac{\rho(\tilde{\mathbf{x}}_\perp)(\mathbf{x}_\perp - \tilde{\mathbf{x}}_\perp)}{|\mathbf{x}_\perp - \tilde{\mathbf{x}}_\perp|^2}$$

$\rho(\mathbf{x})$ = beam charge density

Image Field

$$\mathbf{E}_\perp^i(\mathbf{x}_\perp) = \frac{1}{2\pi\epsilon_0} \int d^2\tilde{\mathbf{x}}_\perp \frac{\rho^i(\tilde{\mathbf{x}}_\perp)(\mathbf{x}_\perp - \tilde{\mathbf{x}}_\perp)}{|\mathbf{x}_\perp - \tilde{\mathbf{x}}_\perp|^2}$$

$\rho^i(\mathbf{x})$ = beam image charge density induced on aperture

// Aside: 2D Field of Line-Charges in Free-Space

$$\nabla_{\perp} \cdot \mathbf{E} = \frac{\rho}{\epsilon_0} \quad \rho(r) = \lambda \frac{\delta(r)}{2\pi r}$$

Line charge at origin, apply Gauss' Law to obtain:

$$E_r = \frac{\lambda}{2\pi\epsilon_0 r} \quad \mathbf{E}_{\perp} = \hat{\mathbf{r}} E_r$$

For a line charge at $\mathbf{x}_{\perp} = \tilde{\mathbf{x}}_{\perp}$, shift coordinates and employ vector notation:

$$\mathbf{E}_{\perp} = \frac{\lambda}{2\pi\epsilon_0} \frac{\mathbf{x}_{\perp} - \tilde{\mathbf{x}}_{\perp}}{|\mathbf{x}_{\perp} - \tilde{\mathbf{x}}_{\perp}|^2}$$

Use this and linear superposition for the field due to direct and image charges

- ◆ Metallic aperture replaced by collection of images external to the aperture in free-space to calculate consistent fields interior to the aperture

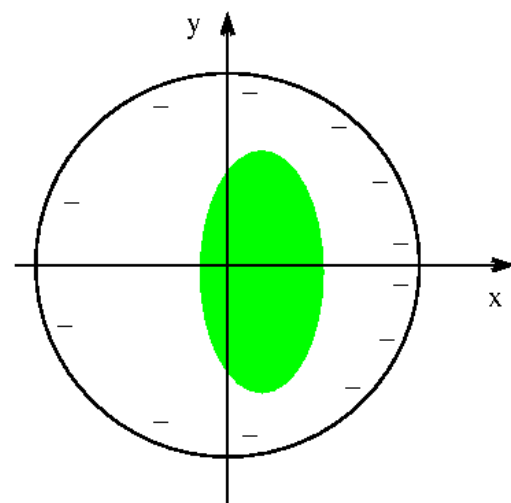
$$\mathbf{E}_{\perp} = \frac{1}{2\pi\epsilon_0} \int d^2 x_{\perp} \rho(\tilde{\mathbf{x}}_{\perp}) \frac{\mathbf{x}_{\perp} - \tilde{\mathbf{x}}_{\perp}}{|\mathbf{x}_{\perp} - \tilde{\mathbf{x}}_{\perp}|^2}$$

Comment on Image Fields

Actual charges on the conducting aperture are induced on a thin (surface charge density) layer on the inner aperture surface. In the method of images, these are replaced by a distribution of charges outside the aperture in vacuum that meet the conducting aperture boundary conditions

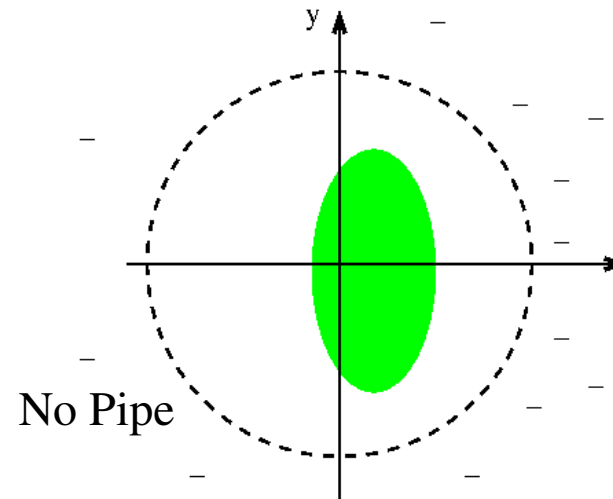
- ◆ Field within aperture can be calculated using the images in vacuum
- ◆ Induced charges on the inner aperture often called “image charges”
- ◆ Magnitude of induced charge on aperture is equal to beam charge and the total charge of the images

Physical



Images

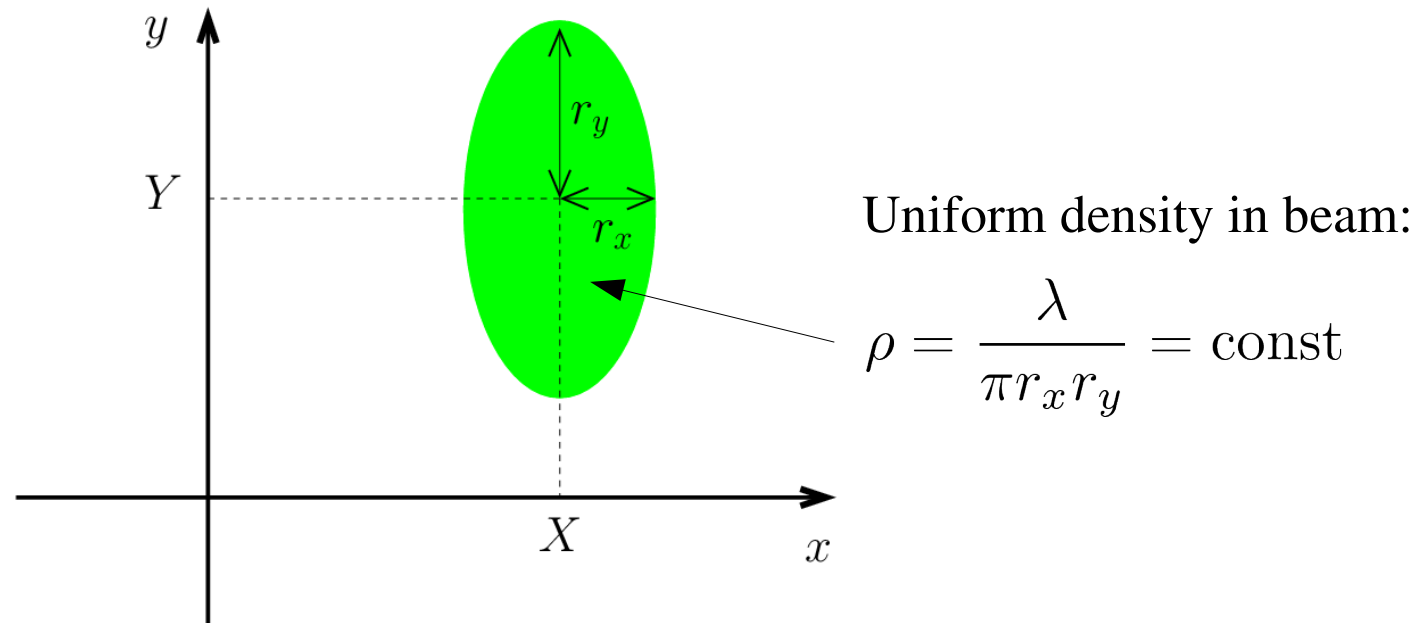
- ◆ No pipe
- ◆ Schematic only (really continuous image dist)



Direct Field:

The direct field solution for a uniform density beam in free-space was calculated for the KV equilibrium distribution

- see: S.M. Lund, lectures on **Transverse Equilibrium Distributions, S3**

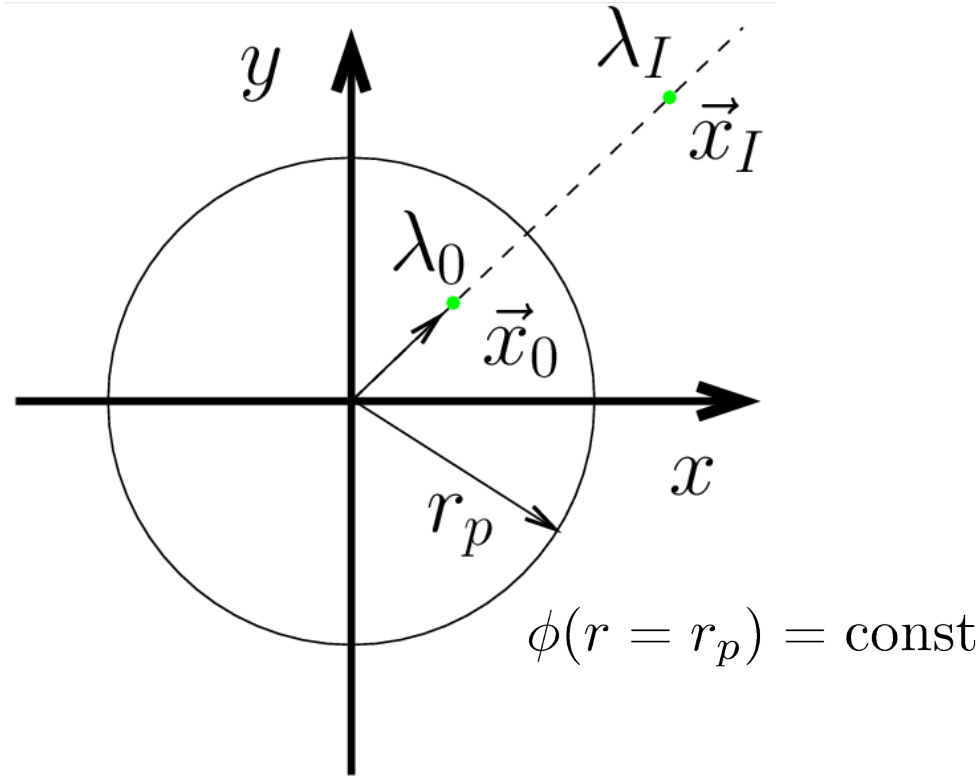


$$E_x^d = \frac{\lambda}{\pi \epsilon_0} \frac{x - X}{(r_x + r_y) r_x}$$
$$E_y^d = \frac{\lambda}{\pi \epsilon_0} \frac{y - Y}{(r_x + r_y) r_y}$$

Expressions are valid only within the elliptical density beam -- where they will be applied in taking averages

Image Field:

Image structure depends on the aperture. Assume a round pipe (most common case) for simplicity.



$$\lambda_I = -\lambda_0 \quad \text{image charge}$$

$$\mathbf{x}_I = \frac{r_p^2}{|\mathbf{x}_0|^2} \mathbf{x}_0 \quad \text{image location}$$

Will be derived in the
the problem sets.

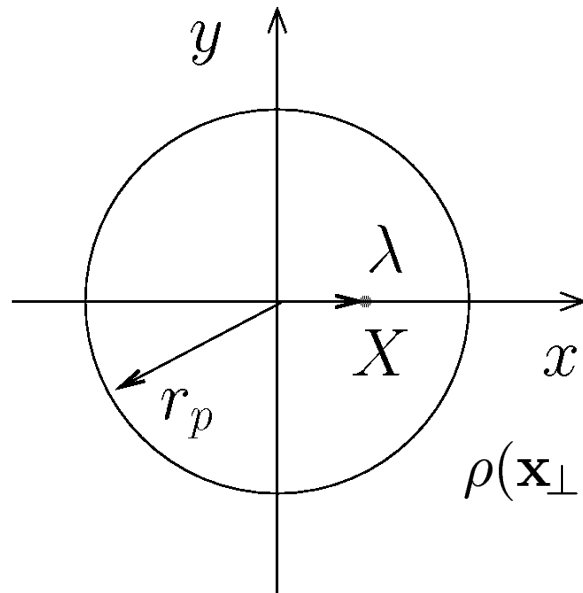
Superimpose all images of beam to obtain the image contribution in aperture:

$$\mathbf{E}_{\perp}^i(\mathbf{x}_{\perp}) = -\frac{1}{2\pi\epsilon_0} \int_{\text{pipe}} d^2 \tilde{\mathbf{x}}_{\perp} \frac{\rho(\tilde{\mathbf{x}}_{\perp})(\mathbf{x}_{\perp} - r_p^2 \tilde{\mathbf{x}}_{\perp}/|\tilde{\mathbf{x}}_{\perp}|^2)}{|\mathbf{x}_{\perp} - r_p^2 \tilde{\mathbf{x}}_{\perp}/|\tilde{\mathbf{x}}_{\perp}|^2|^2}$$

- Difficult to calculate even for ρ corresponding to a uniform density beam

Examine limits of the image field to build intuition on the range of properties:

1) Line charge along x -axis:



choose coordinates to
make true

$$\rho(\mathbf{x}_\perp) = \lambda \delta(\mathbf{x}_\perp - X \hat{\mathbf{x}})$$

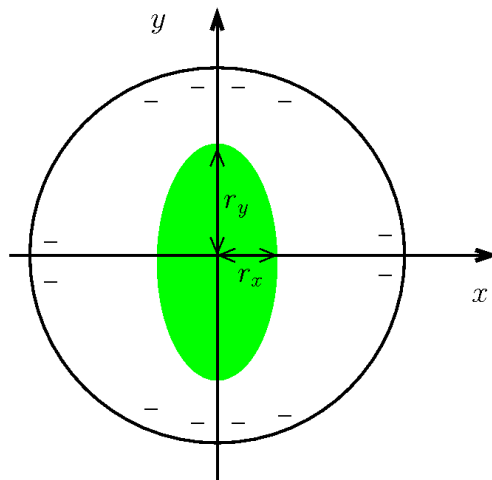
Plug this density in the image charge expression for a round-pipe aperture:

- ♦ Need only evaluate at $\mathbf{x}_\perp = X \hat{\mathbf{x}}$ since beam is at that location

$$\boxed{\mathbf{E}_\perp^i(\mathbf{x}_\perp = X \hat{\mathbf{x}}) = \frac{\lambda}{2\pi\epsilon_0(r_p^2/X - X)} \hat{\mathbf{x}}}$$

- ♦ Generates **nonlinear field** at position of direct charge
- ♦ Field creates **attractive force** between direct and image charge
 - Therefore image charge should be expected to “drag” centroid further off
 - Amplitude of centroid oscillations expected to increase if not corrected (steering)

2) Centered, uniform density elliptical beam:



$$\rho(\mathbf{x}_\perp) = \begin{cases} \frac{\lambda}{\pi r_x r_y}, & x^2/r_x^2 + y^2/r_y^2 < 1 \\ 0, & x^2/r_x^2 + y^2/r_y^2 > 1 \end{cases}$$

Expand using complex coordinates starting from the general image expression:

- ◆ Image field is in vacuum aperture so complex methods help calculation
- ◆ Follow procedures in **Transverse Particle Dynamics, Sec 3D: Multipole Models**

$$\underline{E}^i = E_x^i - iE_y^i = \sum_{n=2,4,\dots}^{\infty} \underline{c}_n \underline{z}^{n-1} \quad \underline{c}_n = \frac{1}{2\pi\epsilon_0} \int_{\text{pipe}} d^2x_\perp \rho(\mathbf{x}_\perp) \frac{(x - iy)^n}{r_p^{2n}}$$

$$\underline{z} = x + iy \quad i = \sqrt{-1} \quad = \frac{\lambda n!}{2\pi\epsilon_0 2^n (n/2 + 1)! (n/2)!} \left(\frac{r_x^2 - r_y^2}{r_p^4} \right)^{n/2}$$

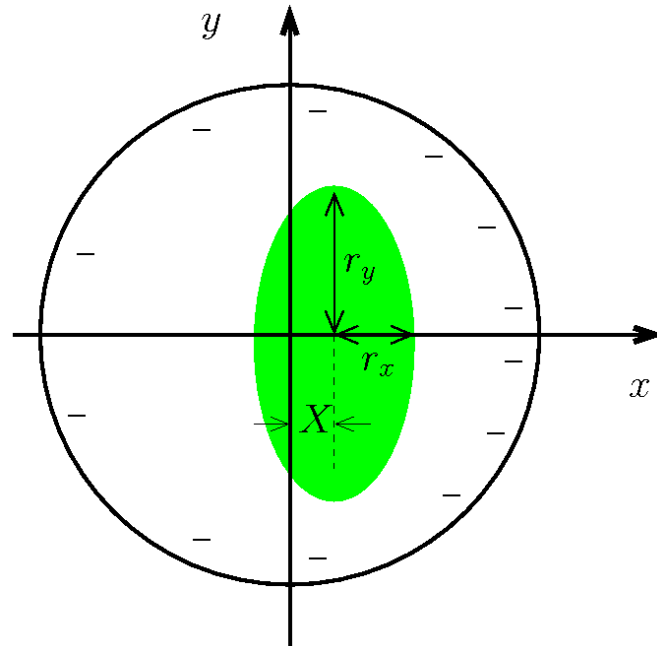
The linear ($n = 2$) components of this expansion give:

$$E_x^i = \frac{\lambda}{8\pi\epsilon_0} \frac{r_x^2 - r_y^2}{r_p^4} x, \quad E_y^i = -\frac{\lambda}{8\pi\epsilon_0} \frac{r_x^2 - r_y^2}{r_p^4} y$$

- ◆ Rapidly vanish (higher order n terms more rapidly) as beam becomes more round
- ◆ Case will be analyzed further in the problem sets

3) Uniform density elliptical beam with a small displacement along the x -axis:

$$Y = 0 \quad |X|/r_p \ll 1$$



Expand using complex coordinates starting from the general image expression:

- ◆ Complex coordinates help simplify very messy calculation

E.P. Lee, E. Close, and L. Smith, Nuclear Instruments and Methods, 1126 (1987)

Leading order terms expanded in $|X|/r_p$ without assuming small ellipticity obtain:

$$E_x^i = \frac{\lambda}{2\pi\epsilon_0 r_p^2} [f \cdot (x - X) + g \cdot X] + \Theta\left(\frac{X}{r_p}\right)^3$$

$$E_y^i = -\frac{\lambda}{2\pi\epsilon_0 r_p^2} f \cdot y + \Theta\left(\frac{X}{r_p}\right)^3$$

Where f and g are focusing and bending coefficients that can be calculated in terms of X, Y, r_x, r_y (which all may vary in s) as:

Focusing Term:

$$f = \frac{r_x^2 - r_y^2}{4r_p^2} + \frac{X^2}{r_p^2} \left[1 + \frac{3}{2} \left(\frac{r_x^2 - r_y^2}{r_p^2} \right) + \frac{3}{8} \left(\frac{r_x^2 - r_y^2}{r_p^2} \right)^2 \right]$$

Bending Term:

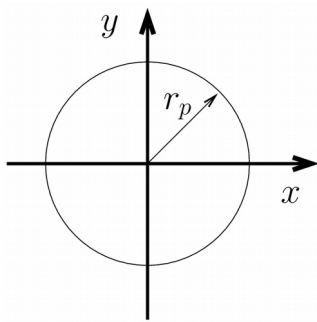
$$g = 1 + \frac{r_x^2 - r_y^2}{4r_p^2} + \frac{X^2}{r_p^2} \left[1 + \frac{3}{4} \left(\frac{r_x^2 - r_y^2}{r_p^2} \right) + \frac{1}{8} \left(\frac{r_x^2 - r_y^2}{r_p^2} \right)^2 \right]$$

- ◆ Expressions become even more complicated with simultaneous x - and y -displacements and more complicated aperture geometries !
- ◆ f quickly become weaker as the beam becomes more round and/or for a larger pipe
- ◆ Similar comments apply to g other than it has a term that remains for a round beam

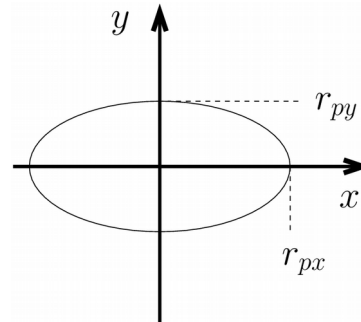
Comments on images:

- ◆ Sign is generally such that it will tend to increase beam centroid displacements
 - Also (usually) weak linear focusing corrections for an elliptical beam
- ◆ Can be very difficult to calculate explicitly
 - Even for simple case of circular pipe
 - Special cases of simple geometry and case formulas help clarify scaling
 - Generally suppress by making the beam small relative to characteristic aperture dimensions and keeping the beam steered near-axis
 - Simulations typically applied
- ◆ Depend strongly on the aperture geometry
 - Generally varies as a function of s in the machine aperture due to changes in accelerator lattice elements and/or as beam symmetries evolve

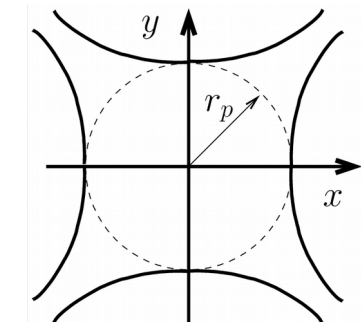
Round Pipe



Elliptical Pipe



Hyperbolic Sections



Coupled centroid and envelope equations of motion

Consistent with the assumed structure of the distribution (uniform density elliptical beam), denote:

Beam Centroid:

$$\begin{aligned} X &\equiv \langle x \rangle_{\perp} & X' &= \langle x' \rangle_{\perp} \\ Y &\equiv \langle y \rangle_{\perp} & Y' &= \langle y' \rangle_{\perp} \end{aligned}$$

Coordinates with respect to centroid:

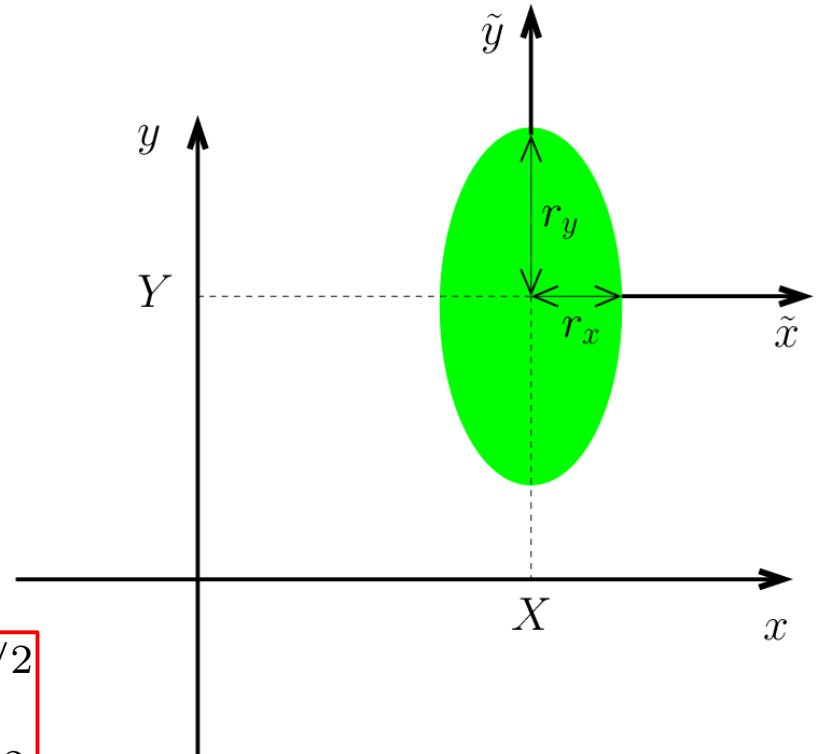
$$\begin{aligned} \tilde{x} &\equiv x - X & \tilde{x}' &= x' - X' \\ \tilde{y} &\equiv y - Y & \tilde{y}' &= y' - Y' \end{aligned}$$

Envelope Edge Radii:

$$\begin{aligned} r_x &\equiv 2\sqrt{\langle \tilde{x}^2 \rangle_{\perp}} & r'_x &= 2\langle \tilde{x}\tilde{x}' \rangle_{\perp}/\langle \tilde{x}^2 \rangle_{\perp}^{1/2} \\ r_y &\equiv 2\sqrt{\langle \tilde{y}^2 \rangle_{\perp}} & r'_y &= 2\langle \tilde{y}\tilde{y}' \rangle_{\perp}/\langle \tilde{y}^2 \rangle_{\perp}^{1/2} \end{aligned}$$

With the *assumed* uniform elliptical beam, **all moments** can be calculated in terms of: X, Y, r_x, r_y

- Such truncations follow whenever the form of the distribution is “frozen”



//Aside: Edge Radius Measures and Dimension

The coefficient of rms edge measures of “radii” of a uniform density beam depends on dimension:

1D: Uniform Sheet Beam:

- ◆ For accelerator equivalent model details see:
Lund, Friedman, Bazouin PRSTAB**14**, 054201 (2011)

$$x_{\text{width}} \equiv \sqrt{3} \langle \tilde{x}^2 \rangle^{1/2}$$

2D: Uniform Elliptical Cross-Section:

- ◆ See lectures on **Transverse Equilibrium Distributions** and homework problems

$$r_x \equiv 2 \langle \tilde{x}^2 \rangle_{\perp}^{1/2}$$

$$r_y \equiv 2 \langle \tilde{y}^2 \rangle_{\perp}^{1/2}$$

3D: Uniformly Filled Ellipsoid:

- ◆ See JJ Barnard Lectures on a mismatched ellipsoidal bunch and
and Barnard and Lund, PAC 9VO18 (1997)
Axisymmetric Transverse

$$r_{\perp} \equiv \sqrt{5/2} \langle \tilde{x}^2 + \tilde{y}^2 \rangle^{1/2}$$

$$r_z \equiv \sqrt{5} \langle \tilde{z}^2 \rangle^{1/2}$$

3D

$$r_x \equiv \sqrt{5} \langle \tilde{x}^2 \rangle^{1/2}$$

$$r_y \equiv \sqrt{5} \langle \tilde{y}^2 \rangle^{1/2}$$

$$r_z \equiv \sqrt{5} \langle \tilde{z}^2 \rangle^{1/2}$$

///

Derive centroid equations: First use the self-field resolution for a uniform density beam, then the equations of motion for a particle within the beam are:

$x'' + \frac{(\gamma_b \beta_b)'}{(\gamma_b \beta_b)} x' + \kappa_x x - \frac{2Q}{(r_x + r_y)r_x} (x - X) = \frac{q}{m\gamma_b^3 \beta_b^2 c^2} E_x^i$	$y'' + \frac{(\gamma_b \beta_b)'}{(\gamma_b \beta_b)} y' + \kappa_y y - \frac{2Q}{(r_x + r_y)r_y} (y - Y) = \frac{q}{m\gamma_b^3 \beta_b^2 c^2} E_y^i$
Direct Terms	Image Terms

Perveance:

$$Q \equiv \frac{q\lambda}{2\pi\epsilon_0 m \gamma_b^3 \beta_b^2 c^2} \quad (\text{not necessarily constant if beam accelerates})$$

average equations using: $\langle x' \rangle_{\perp} = \langle x \rangle'_{\perp} = X'$ etc., to obtain:

Centroid Equations:

$X'' + \frac{(\gamma_b \beta_b)'}{(\gamma_b \beta_b)} X' + \kappa_x X = Q \left[\frac{2\pi\epsilon_0}{\lambda} \langle E_x^i \rangle_{\perp} \right]$	$Y'' + \frac{(\gamma_b \beta_b)'}{(\gamma_b \beta_b)} Y' + \kappa_y Y = Q \left[\frac{2\pi\epsilon_0}{\lambda} \langle E_y^i \rangle_{\perp} \right]$
--	--

Note: the electric image field will cancel the coefficient $2\pi\epsilon_0/\lambda$

- ♦ $\langle E_x^i \rangle_{\perp}$ will generally depend on: X, Y and r_x, r_y

//Aside: Steps in deriving the x -centroid equation

Start with equation of motion:

$$x'' + \frac{(\gamma_b \beta_b)'}{(\gamma_b \beta_b)} x' + \kappa_x x - \frac{2Q}{(r_x + r_y)r_x} (x - X) = \frac{q}{m\gamma_b^3 \beta_b^2 c^2} E_x^i$$

Average pulling through terms that depend on s :

$$\langle x'' \rangle_{\perp} + \left\langle \frac{(\gamma_b \beta_b)'}{(\gamma_b \beta_b)} x' \right\rangle_{\perp} + \langle \kappa_x x \rangle_{\perp} - \left\langle \frac{2Q}{(r_x + r_y)r_x} (x - X) \right\rangle_{\perp} = \left\langle \frac{q}{m\gamma_b^3 \beta_b^2 c^2} E_x^i \right\rangle_{\perp}$$

$$\begin{aligned} \langle x \rangle_{\perp}'' + \frac{(\gamma_b \beta_b)'}{(\gamma_b \beta_b)} \langle x' \rangle_{\perp} + \kappa_x \langle x \rangle_{\perp} - \frac{2Q}{(r_x + r_y)r_x} \langle x - X \rangle_{\perp} \\ = \frac{q\lambda}{2\pi\epsilon_0 m \gamma_b^3 \beta_b^2 c^2} \left[\frac{2\pi\epsilon_0}{\lambda} \right] \langle E_x^i \rangle_{\perp} \end{aligned}$$

Use:

$$X = \langle x \rangle_{\perp} \quad X' = \langle x' \rangle_{\perp} \quad Q \equiv \frac{q\lambda}{2\pi\epsilon_0 m \gamma_b^3 \beta_b^2 c^2}$$

$$\langle x - X \rangle_{\perp} = X - X = 0$$

$$\implies \boxed{X'' + \frac{(\gamma_b \beta_b)'}{(\gamma_b \beta_b)} X' + \kappa_x X = Q \left[\frac{2\pi\epsilon_0}{\lambda} \langle E_x^i \rangle_{\perp} \right]}$$

///

To derive equations of motion for the envelope radii, first subtract the centroid equations from the particle equations of motion ($\tilde{x} \equiv x - X$) to obtain:

$$\begin{aligned}\tilde{x}'' + \frac{(\gamma_b \beta_b)'}{(\gamma_b \beta_b)} \tilde{x}' + \kappa_x \tilde{x} - \frac{2Q\tilde{x}}{(r_x + r_y)r_x} &= \frac{q}{m\gamma_b^3 \beta_b^2 c^2} [E_x^i - \langle E_x^i \rangle_{\perp}] \\ \tilde{y}'' + \frac{(\gamma_b \beta_b)'}{(\gamma_b \beta_b)} \tilde{y}' + \kappa_y \tilde{y} - \frac{2Q\tilde{y}}{(r_x + r_y)r_x} &= \frac{q}{m\gamma_b^3 \beta_b^2 c^2} [E_y^i - \langle E_y^i \rangle_{\perp}]\end{aligned}$$

Differentiate the equation for the envelope radius (y -equations analogous):

$$r_x = 2\langle \tilde{x}^2 \rangle_{\perp}^{1/2} \implies r'_x = \frac{2\langle \tilde{x}\tilde{x}' \rangle_{\perp}}{\langle \tilde{x}^2 \rangle_{\perp}^{1/2}} = \frac{4\langle \tilde{x}\tilde{x}' \rangle_{\perp}}{r_x}$$

Define (motivated the KV equilibrium results) a statistical rms edge emittance:

$$\varepsilon_x \equiv 4\varepsilon_{x,\text{rms}} \equiv 4 [\langle \tilde{x}^2 \rangle_{\perp} \langle \tilde{x}'^2 \rangle_{\perp} - \langle \tilde{x}\tilde{x}' \rangle_{\perp}^2]^{1/2}$$

Differentiate the equation for r'_x again and use the emittance definition:

$$\begin{aligned}r''_x &= 4 \frac{\langle \tilde{x}\tilde{x}'' \rangle_{\perp}}{r_x} + \frac{16[\langle \tilde{x}^2 \rangle_{\perp} \langle \tilde{x}'^2 \rangle_{\perp} - \langle \tilde{x}\tilde{x}' \rangle_{\perp}^2]}{r_x^3} \\ &= 4 \frac{\langle \tilde{x}\tilde{x}'' \rangle_{\perp}}{r_x} + \frac{\varepsilon_x^2}{r_x^3}\end{aligned}$$

and then employ the equations of motion to eliminate \tilde{x}'' in $\langle \tilde{x}\tilde{x}'' \rangle_{\perp}$ to obtain:

//Aside: Additional steps in deriving the x -envelope equation

Using the equation of motion:

$$\tilde{x}'' + \frac{(\gamma_b \beta_b)'}{(\gamma_b \beta_b)} \tilde{x}' + \kappa_x \tilde{x} - \frac{2Q\tilde{x}}{(r_x + r_y)r_x} = \frac{q}{m\gamma_b^3 \beta_b^2 c^2} [E_x^i - \langle E_x^i \rangle_{\perp}]$$

Multiply the equation by \tilde{x} , average, and pull s -varying coefficients and constants through the average terms:

$$\begin{aligned} \langle \tilde{x}\tilde{x}'' \rangle_{\perp} + \frac{(\gamma_b \beta_b)'}{(\gamma_b \beta_b)} \langle \tilde{x}\tilde{x}' \rangle_{\perp} + \kappa_x \langle \tilde{x}^2 \rangle_{\perp} - \frac{2Q\langle \tilde{x}^2 \rangle_{\perp}}{(r_x + r_y)r_x} \\ = \frac{q}{m\gamma_b^3 \beta_b^2 c^2} [\langle \tilde{x}E_x^i \rangle_{\perp} - \langle \tilde{x}\langle E_x^i \rangle_{\perp} \rangle_{\perp}] \end{aligned}$$

$\nearrow 0$

$$\langle \tilde{x}\langle E_x^i \rangle_{\perp} \rangle_{\perp} = \langle \tilde{x} \rangle_{\perp} \langle E_x^i \rangle_{\perp} = 0$$

Giving:

$$\langle \tilde{x}\tilde{x}'' \rangle_{\perp} + \frac{(\gamma_b \beta_b)'}{(\gamma_b \beta_b)} \langle \tilde{x}\tilde{x}' \rangle_{\perp} + \kappa_x \langle \tilde{x}^2 \rangle_{\perp} - \frac{2Q\langle \tilde{x}^2 \rangle_{\perp}}{(r_x + r_y)r_x} = \frac{q}{m\gamma_b^3 \beta_b^2 c^2} \langle \tilde{x}E_x^i \rangle_{\perp}$$

Using this moment in the equation for r_x'' and the definition of the emittance ε_x then gives the envelope equation in the form given with the image charge term:

///

Envelope Equations:

$$r_x'' + \frac{(\gamma_b \beta_b)'}{(\gamma_b \beta_b)} r_x' + \kappa_x r_x - \frac{2Q}{r_x + r_y} - \frac{\varepsilon_x^2}{r_x^3} = 8Q \left[\frac{\pi \epsilon_0}{\lambda} \langle \tilde{x} E_x^i \rangle_{\perp} \right]$$

$$r_y'' + \frac{(\gamma_b \beta_b)'}{(\gamma_b \beta_b)} r_y' + \kappa_y r_y - \frac{2Q}{r_x + r_y} - \frac{\varepsilon_y^2}{r_y^3} = 8Q \left[\frac{\pi \epsilon_0}{\lambda} \langle \tilde{y} E_y^i \rangle_{\perp} \right]$$

- $\langle \tilde{x} E_x^i \rangle_{\perp}$ will generally depend on: X , Y and r_x , r_y

Comments on Centroid/Envelope equations:

- Centroid and envelope equations are *coupled* and must be solved simultaneously when image terms on the RHS cannot be neglected
- Image terms contain nonlinear terms that can be difficult to evaluate explicitly
 - Aperture geometry changes image correction
- The formulation is not self-consistent because a frozen form (uniform density) charge profile is assumed
 - Uniform density choice motivated by KV results and Debye screening
see: S.M. Lund, lectures on **Transverse Equilibrium Distributions**
 - The assumed distribution form not evolving represents a fluid model closure
 - Typically find with simulations that uniform density frozen form distribution models can provide reasonably accurate approximate models for centroid and envelope evolution

Comments on Centroid/Envelope equations (Continued):

- Constant (normalized when accelerating) emittances are generally assumed
 - For strong space charge emittance terms small and limited emittance evolution does not strongly influence evolution outside of final focus
 - See: S.M. Lund, lectures on **Transverse Particle Dynamics** and **Transverse Kinetic Theory** to motivate when this works well

$\beta_b, \gamma_b, \lambda$ s -variation set by acceleration schedule

$$\begin{aligned}\varepsilon_{nx} &= \gamma_b \beta_b \varepsilon_x = \text{const} \\ \varepsilon_{ny} &= \gamma_b \beta_b \varepsilon_y = \text{const}\end{aligned} \quad \longrightarrow \quad \text{used to calculate } \varepsilon_x, \varepsilon_y$$

$$Q = \frac{q\lambda}{2\pi m \epsilon_0 \gamma_b^3 \beta_b^2 c^2}$$

S3: Centroid Equations of Motion

Single Particle Limit: Oscillation and Stability Properties

Neglect image charge terms, then the centroid equation of motion becomes:

$$X'' + \frac{(\gamma_b \beta_b)'}{(\gamma_b \beta_b)} X' + \kappa_x X = 0$$
$$Y'' + \frac{(\gamma_b \beta_b)'}{(\gamma_b \beta_b)} Y' + \kappa_y Y = 0$$

- Usual **Hill's equation** with acceleration term
- Single particle form. Apply results from S.M. Lund lectures on **Transverse Particle Dynamics**: phase amplitude methods, Courant-Snyder invariants, and stability bounds, ...

Assume that applied lattice focusing is tuned for constant phase advances with normalized coordinates and/or that acceleration is weak and can be neglected.

Then single particle stability results give immediately:

$$\frac{1}{2} |\text{Tr } \mathbf{M}_x(s_i + L_p | s_i)| \leq 1$$
$$\frac{1}{2} |\text{Tr } \mathbf{M}_y(s_i + L_p | s_i)| \leq 1$$

$$\sigma_{0x} < 180^\circ$$
$$\sigma_{0y} < 180^\circ$$

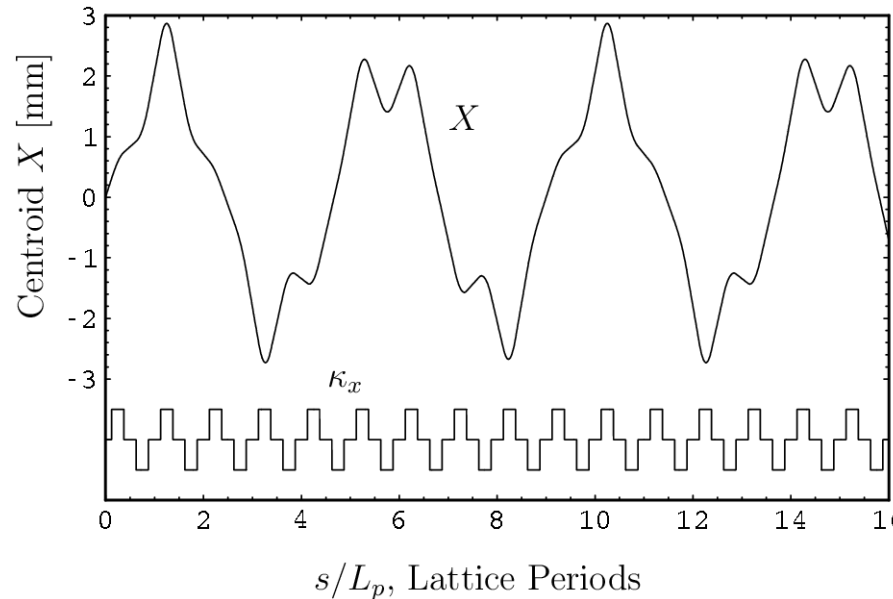
centroid stability
1st stability condition

/// Example: FODO channel centroid evolution for a coasting beam

Mid-drift
launch:

$$X(0) = 0 \text{ mm}$$

$$X'(0) = 1 \text{ mrad}$$



lattice/beam
parameters:

$$\gamma_b \beta_b = \text{const}$$

$$\sigma_{0x} = 80^\circ$$

$$L_p = 0.5 \text{ m}$$

$$\eta = 0.5$$

- ◆ Centroid exhibits expected characteristic stable betatron oscillations
 - Stable so oscillation amplitude does not grow
 - Courant-Snyder invariant (i.e, initial centroid phase-space area set by initial conditions) and betatron function can be used to bound oscillation
- ◆ Motion in y -plane analogous

///

Designing a lattice for single particle stability by limiting undepressed phases advances to less than 180 degrees per period means that the centroid will be stable

- ◆ Situation could be modified in very extreme cases due to image couplings

Effect of Driving Errors

The reference orbit is **ideally tuned for zero centroid excursions**. But there will *always* be driving errors that can cause the centroid oscillations to accumulate with beam propagation distance:

$$X'' + \frac{(\gamma_b \beta_b)'}{(\gamma_b \beta_b)} X' + \sum_n \frac{G_n}{G_0} \kappa_n(s) X = \sum_n \frac{G_n}{G_0} \kappa_n(s) \Delta_{xn}$$

$\kappa_q(s) = \sum \kappa_n(s)$ $\kappa_n(s)$ nominal gradient function, n th quadrupole

$\frac{G_n}{G_0} =$ n th quadrupole gradient error (unity for no error; s -varying)

$\Delta_{xn} =$ n th quadrupole transverse displacement error (s -varying)

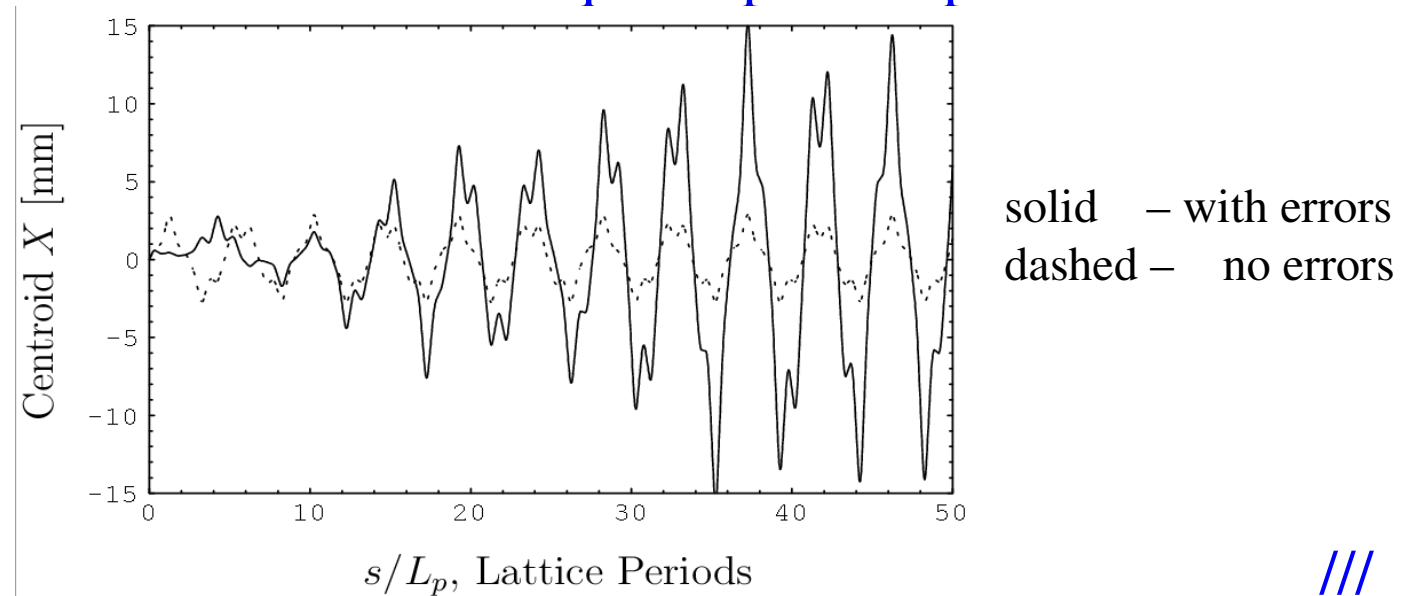
/// Example: FODO channel centroid with quadrupole displacement errors

$$\frac{G_n}{G_0} = 1$$

$$\Delta_{xn} = [-0.5, 0.5] \text{ mm}$$

(uniform dist)

same lattice and initial condition as previous



Errors will result in a characteristic random walk increase in oscillation amplitude due to the (generally random) driving terms

- ◆ Can also be systematic errors with different (not random walk) characteristics depending on the nature of the errors

Control by:

- ◆ Synthesize small applied dipole fields to regularly steer the centroid back on-axis to the reference trajectory: $X = 0 = Y$, $X' = 0 = Y'$
- ◆ Fabricate and align focusing elements with higher precision
- ◆ Employ a sufficiently large aperture to contain the oscillations and limit detrimental nonlinear image charge effects

Economics dictates the optimal strategy

- Usually sufficient control achieved by a combination of methods

Effects of Image Charges

Model the beam as a displaced line-charge in a circular aperture. Then using the previously derived image charge field, the equations of motion reduce to:

$$X'' + \frac{(\gamma_b \beta_b)'}{(\gamma_b \beta_b)} X' + \kappa_x X = \frac{QX}{r_p^2 - X^2}$$

examine oscillation
along x -axis

$$\frac{QX}{r_p^2 - X^2} \simeq \frac{Q}{r_p^2} X + \frac{Q}{r_p^4} X^3$$

linear correction

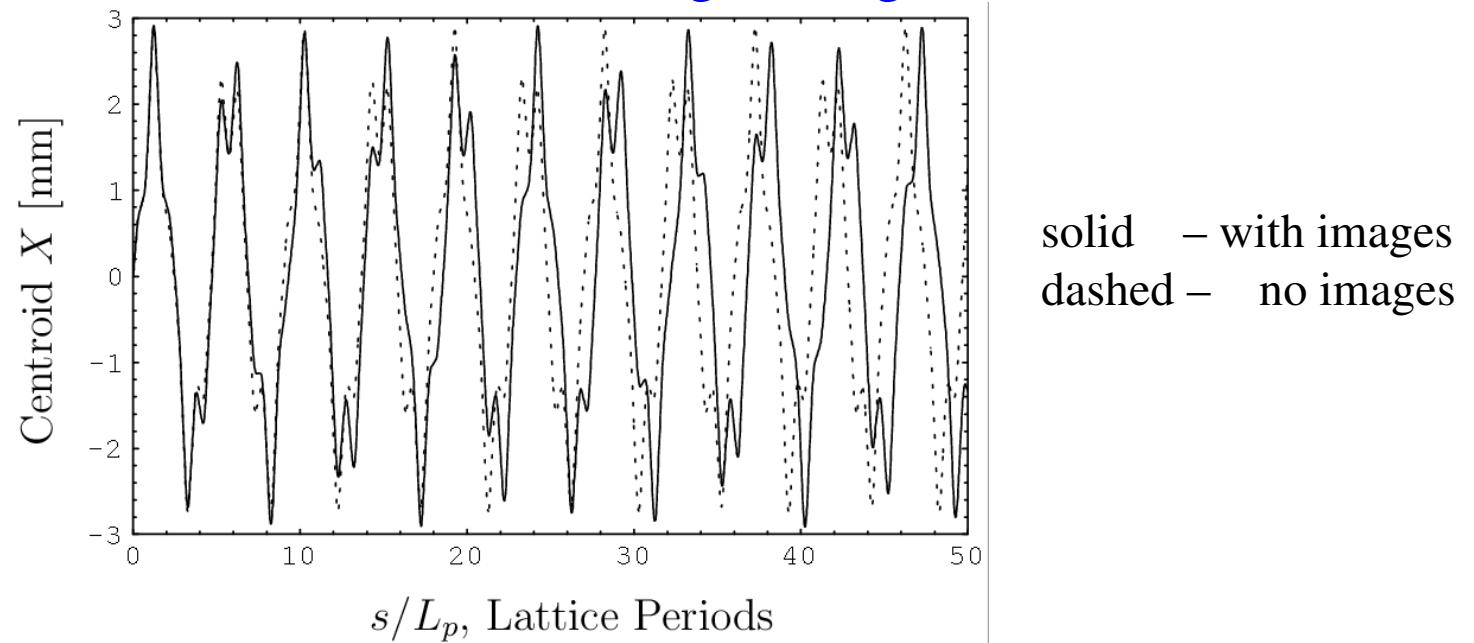
Nonlinear correction (smaller)

Example: FODO channel centroid with image charge corrections

$$r_p = 30 \text{ mm}$$

$$Q = 2 \times 10^{-4}$$

same lattice
as previous



Main effect of images is typically an **accumulated phase error of the centroid orbit**

- ◆ This will complicate extrapolations of errors over many lattice periods

Control by:

- ◆ Keeping centroid displacements X, Y small by correcting
- ◆ Make aperture (pipe radius) larger

Comments:

- ◆ Images contributions to centroid excursions generally less problematic than misalignment errors in focusing elements
- ◆ More detailed analysis show that the coupling of the envelope radii r_x, r_y to the centroid evolution in X, Y is often weak
- ◆ Fringe fields are more important for accurate calculation of centroid orbits since orbits are not part of a matched lattice
 - Single orbit vs a bundle of orbits, so more sensitive to the timing of focusing impulses imparted by the lattice
- ◆ Over long path lengths many nonlinear terms can also influence oscillation phase
- ◆ Lattice errors are not often known so one must often analyze characteristic error distributions to see if centroids measured are consistent with expectations
 - Often model a uniform distribution of errors or Gaussian with cutoff tails since quality checks should render the tails of the Gaussian inconceivable to realize

S4: Envelope Equations of Motion

Overview: Reduce equations of motion for r_x, r_y

- ◆ Find that couplings to centroid coordinates X, Y are weak
 - Centroid ideally zero in a well tuned system
- ◆ Envelope eqns are most important in designing transverse focusing systems
 - Expresses average radial force balance (see following discussion)
 - Can be difficult to analyze analytically for scaling properties
 - “Systems” or design scoping codes often written using envelope equations, stability criteria, and practical engineering constraints
- ◆ Instabilities of the envelope equations in periodic focusing lattices must be avoided in machine operation
 - Instabilities are strong and real: not washed out with realistic distributions without frozen form
 - Represent lowest order “KV” modes of a full kinetic theory
- ◆ Previous derivation of envelope equations relied on Courant-Snyder invariants in linear applied and self-fields. Analysis shows that the same force balances result for a uniform elliptical beam with no image couplings.
 - Debye screening arguments suggest assumed uniform density model taken should be a good approximation for intense space-charge

KV/rms Envelope Equations: Properties of Terms

The envelope equation reflects low-order force balances:

$$\begin{aligned}
 r''_x + \frac{(\gamma_b \beta_b)'}{(\gamma_b \beta_b)} r'_x &+ \kappa_x r_x - \frac{2Q}{r_x + r_y} - \frac{\varepsilon_x^2}{r_x^3} = 0 \\
 r''_y + \frac{(\gamma_b \beta_b)'}{(\gamma_b \beta_b)} r'_y &+ \kappa_y r_y - \frac{2Q}{r_x + r_y} - \frac{\varepsilon_y^2}{r_y^3} = 0
 \end{aligned}$$

Applied Streaming Terms: Inertial Applied Acceleration Lattice Space-Charge Defocusing Lattice Thermal Defocusing Emittance

The “acceleration schedule” specifies both $\gamma_b \beta_b$ and λ
then the equations are integrated with:

$$\gamma_b \beta_b \varepsilon_x = \text{const}$$

$$\gamma_b \beta_b \varepsilon_y = \text{const}$$

normalized emittance conservation
(set by initial value)

$$Q = \frac{q\lambda}{2\pi\epsilon_0 m \gamma_b^3 \beta_b^2 c^2}$$

specified permeance

Reminder: It was shown for a coasting beam that the envelope equations remain valid for elliptic charge densities suggesting more general validity [Sacherer, IEEE Trans. Nucl. Sci. **18**, 1101 (1971), J.J. Barnard, **Intro. Lectures**]

For any beam with **elliptic symmetry** charge density in each transverse slice:

$$\rho = \rho \left(\frac{x^2}{r_x^2} + \frac{y^2}{r_y^2} \right)$$

Based on:

$$\langle x \frac{\partial \phi}{\partial x} \rangle_{\perp} = -\frac{\lambda}{4\pi\epsilon_0} \frac{r_x}{r_x + r_y}$$

the KV envelope equations

$$r_x''(s) + \kappa_x(s)r_x(s) - \frac{2Q}{r_x(s) + r_y(s)} - \frac{\varepsilon_x^2(s)}{r_x^3(s)} = 0$$

$$r_y''(s) + \kappa_y(s)r_y(s) - \frac{2Q}{r_x(s) + r_y(s)} - \frac{\varepsilon_y^2(s)}{r_y^3(s)} = 0$$

See

- ◆ J.J. Barnard, **Intro. Lectures**
- ◆ **Transverse Equilibrium Distributions, S3 App. A**

remain valid when (averages taken with the full distribution):

$$Q = \frac{q\lambda}{2\pi\epsilon_0 m \gamma_b^3 \beta_b^2 c^2} = \text{const}$$

$$\lambda = q \int d^2x_{\perp} \rho = \text{const}$$

$$r_x = 2\langle x^2 \rangle_{\perp}^{1/2}$$

$$\varepsilon_x = 4[\langle x^2 \rangle_{\perp} \langle x'^2 \rangle_{\perp} - \langle xx' \rangle_{\perp}^2]^{1/2}$$

$$r_y = 2\langle y^2 \rangle_{\perp}^{1/2}$$

$$\varepsilon_y = 4[\langle y^2 \rangle_{\perp} \langle y'^2 \rangle_{\perp} - \langle yy' \rangle_{\perp}^2]^{1/2}$$

◆ Evolution changes often small in $\varepsilon_x, \varepsilon_y$

Properties of Envelope Equation Terms:

Inertial: r_x'' , r_y''

Applied Focusing: $\kappa_x r_x$, $\kappa_y r_y$ and Acceleration: $\frac{(\gamma_b \beta_b)'}{(\gamma_b \beta_b)} r_x'$, $\frac{(\gamma_b \beta_b)'}{(\gamma_b \beta_b)} r_y'$

- ◆ Analogous to single-particle orbit terms in **Transverse Particle Dynamics**
- ◆ Contributions to beam envelope essentially the same as in single particle case
- ◆ Have strong s dependence, *can be both focusing and defocusing*
 - Act only in focusing elements and acceleration gaps
 - Net tendency to damp oscillations with energy gain

Perveance: $\frac{2Q}{r_x + r_y}$

Scale $\sim \frac{1}{\text{Env. Radius}}$

- ◆ Acts continuously in s , *always defocusing*
- ◆ Becomes stronger (relatively to other terms) when the beam expands in cross-sectional area

Emittance: $\frac{\varepsilon_x^2}{r_x^3}$

Scale $\sim \frac{1}{(\text{Env. Radius})^3}$

- ◆ Acts continuously in s , *always defocusing*
- ◆ Becomes stronger (relatively to other terms) when the beam becomes small in cross-sectional area
- ◆ Scaling makes clear why it is necessary to inhibit emittance growth for applications where small spots are desired on target

As the beam expands, perveance term will eventually dominate emittance term:
 [see: Lund and Bukh, PRSTAB 7, 024801 (2004)]

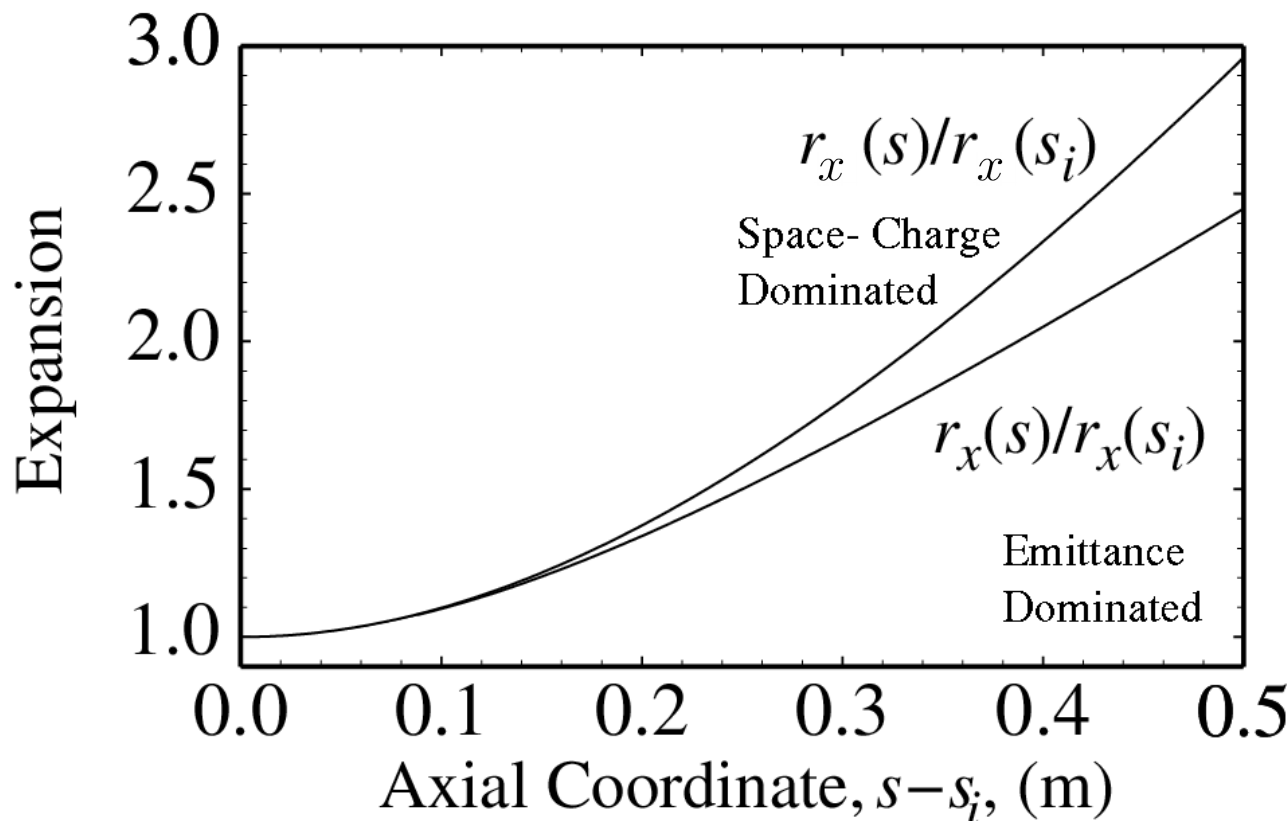
Consider a free expansion ($\kappa_x = \kappa_y = 0$) for a coasting beam with $\gamma_b \beta_b = \text{const}$

Initial conditions:

$$\begin{aligned} r_x(s_i) &= r_y(s_i) \\ r'_x(s_i) &= r'_y(s_i) = 0 \\ Q &= \frac{\varepsilon_x^2}{r_x^2(s_i)} = 10^{-3} \end{aligned}$$

Cases:

Space-Charge Dominated: $\varepsilon_x = 0$
 Emittance Dominated: $Q = 0$



See next page: solution is analytical in bounding limits shown

Parameters are chosen such that initial defocusing forces in two limits are equal to compare case

For an **emittance dominated** beam in free-space, the envelope equation becomes:

$$\frac{Q}{r_x + r_y} \ll \frac{\varepsilon_{x,y}^2}{r_{x,y}^3} \implies r_j'' - \frac{\varepsilon_j^2}{r_j^3} = 0 \quad j = x, y$$

The envelope Hamiltonian gives:

$$\frac{1}{2} r_j'^2 + \frac{\varepsilon_j^2}{2r_j^2} = \text{const}$$

which can be integrated from the initial envelope at $s = s_i$ to show that:

Emittance Dominated Free-Expansion ($Q = 0$)

$$r_j(s) = r_j(s_i) \sqrt{1 + \frac{2r'_j(s_i)}{r_j(s_i)}(s - s_i) + \left[1 + \frac{r_j^2(s_i)r_j'^2(s_i)}{\varepsilon_j^2}\right] \frac{\varepsilon_j^2}{r_j^4(s_i)}(s - s_i)^2}$$

$$j = x, y$$

Conversely, for a **space-charge dominated** beam in free-space, the envelope equation becomes:

$$\frac{Q}{r_x + r_y} \gg \frac{\varepsilon_{x,y}^2}{r_{x,y}^3} \implies \begin{aligned} r_+'' - \frac{Q}{r_+} &= 0 \\ r_-'' &= 0 \end{aligned} \quad r_{\pm} \equiv \frac{1}{2}(r_x \pm r_y)$$

The equations of motion

$$r''_+ - \frac{Q}{r_+} = 0$$

$$r''_- = 0$$

can be integrated from the initial envelope at $s = s_i$ to show that:

- ◆ r_- equation solution trivial
- ◆ r_+ equation solution exploits Hamiltonian $\frac{1}{2}r'^2_+ - Q \ln r_+ = \text{const}$

Space-Charge Dominated Free-Expansion ($\varepsilon_x = \varepsilon_y = 0$)

$$r_+(s) = r_+(s_i) \exp \left(-\frac{r'^2_+(s_i)}{2Q} + \left[\text{erfi}^{-1} \left\{ \text{erfi} \left[\frac{r'_+(s_i)}{\sqrt{2Q}} \right] + \sqrt{\frac{2Q}{\pi}} e^{\frac{r'^2_+(s_i)}{2Q}} \frac{(s - s_i)}{r_+(s_i)} \right\} \right]^2 \right)$$

$$r_-(s) = r_-(s_i) + r'_-(s_i)(s - s_i)$$

Imaginary Error Function

$$r_{\pm} = \frac{1}{2}(r_x \pm r_y)$$

$$\text{erfi}(z) \equiv \frac{\text{erf}(iz)}{i} \equiv \frac{2}{\sqrt{\pi}} \int_0^z dt \exp(t^2)$$

$$i \equiv \sqrt{-1}$$

The free-space expansion solutions for emittance and space-charge dominated beams will be explored more in the problems

Neglect acceleration ($\gamma_b \beta_b = \text{const}$) or use transformed variables:

$$r_x''(s) + \kappa_x(s)r_x(s) - \frac{2Q}{r_x(s) + r_y(s)} - \frac{\varepsilon_x^2}{r_x^3(s)} = 0$$

$$r_y''(s) + \kappa_y(s)r_y(s) - \frac{2Q}{r_x(s) + r_y(s)} - \frac{\varepsilon_y^2}{r_y^3(s)} = 0$$

$$r_x(s + L_p) = r_x(s) \quad r_x(s) > 0$$

$$r_y(s + L_p) = r_y(s) \quad r_y(s) > 0$$

Matching involves finding specific initial conditions for the envelope to have the **periodicity of the lattice**:

Find Values of:

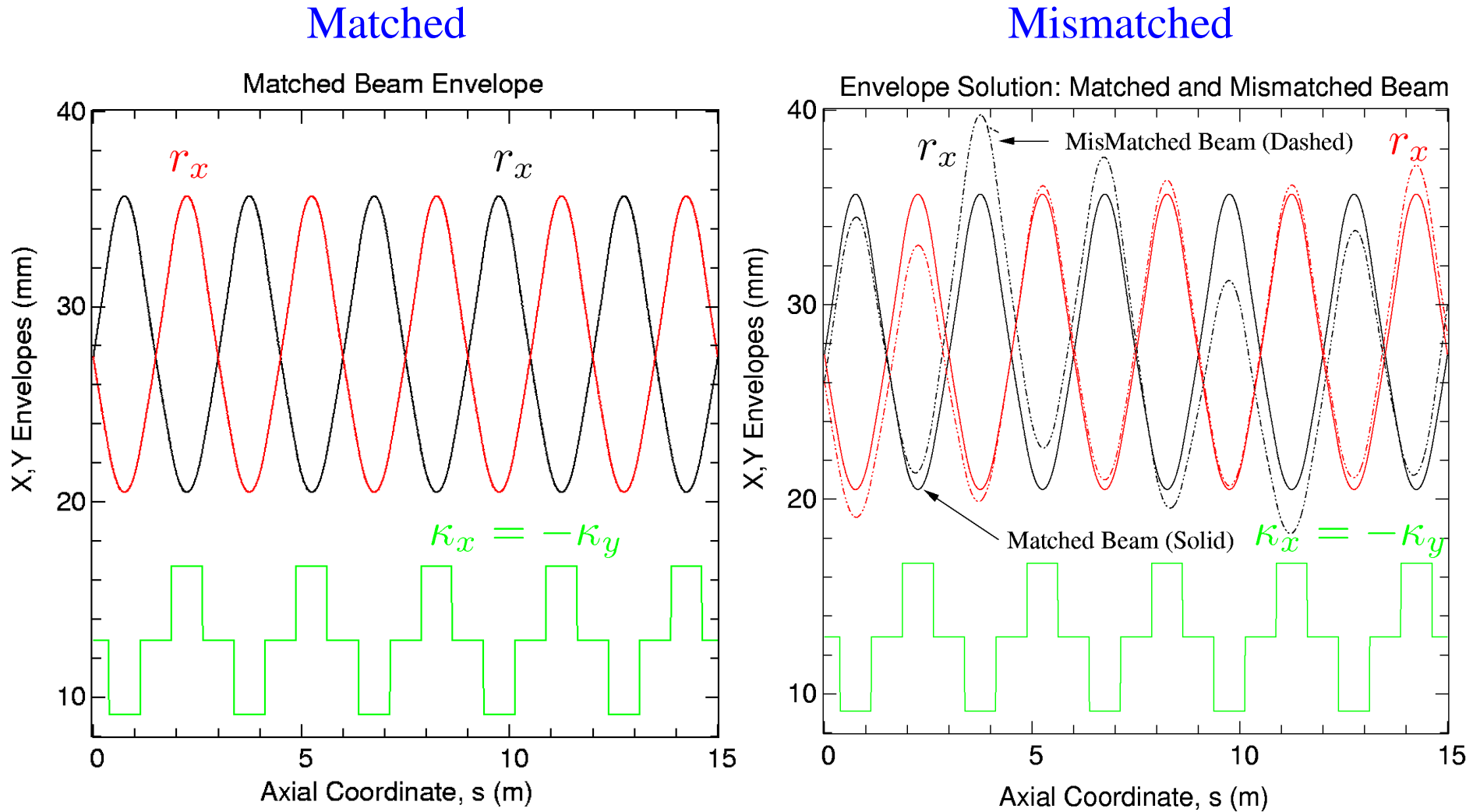
$r_x(s_i)$	$r'_x(s_i)$
$r_y(s_i)$	$r'_y(s_i)$

Such That: (periodic)

$r_x(s_i + L_p) = r_x(s_i)$	$r'_x(s_i + L_p) = r'_x(s_i)$
$r_y(s_i + L_p) = r_y(s_i)$	$r'_y(s_i + L_p) = r'_y(s_i)$

- ◆ Typically constructed with numerical root finding from estimated/guessed values
 - Can be surprisingly difficult for complicated lattices (high σ_0) with strong space-charge
- ◆ Iterative technique developed to numerically calculate without root finding;
 - Lund, Chilton and Lee, PRSTAB 9, 064201 (2006)
 - Method exploits Courant-Snyder invariants of depressed orbits within the beam

Typical Matched vs Mismatched solution for FODO channel:



The matched beam is the most radially compact solution to the envelope equations rendering it highly important for beam transport

- ◆ Matching uses optics most efficiently to maintain radial beam confinement

The matched solution to the KV envelope equations reflects the symmetry of the focusing lattice and must, in general, be calculated numerically

Envelope equation very nonlinear

$$r_x(s + L_p) = r_x(s)$$

$$r_y(s + L_p) = r_y(s)$$

$$\varepsilon_x = \varepsilon_y$$

Parameters

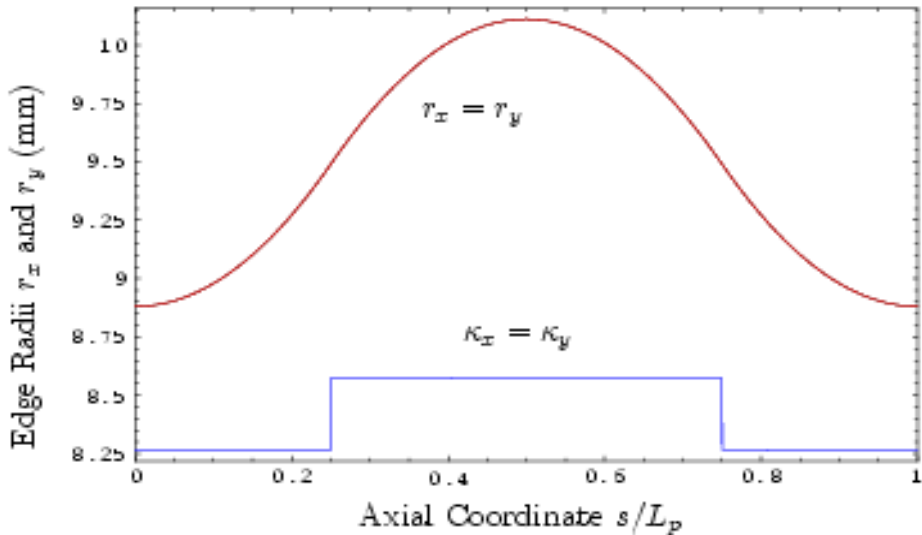
$$L_p = 0.5 \text{ m}, \quad \sigma_0 = 80^\circ, \quad \eta = 0.5$$

$$\varepsilon_x = 50 \text{ mm-mrad}$$

$\sigma/\sigma_0 = 0.2$ Perveance Q iterated to obtain matched solution with this tune depression

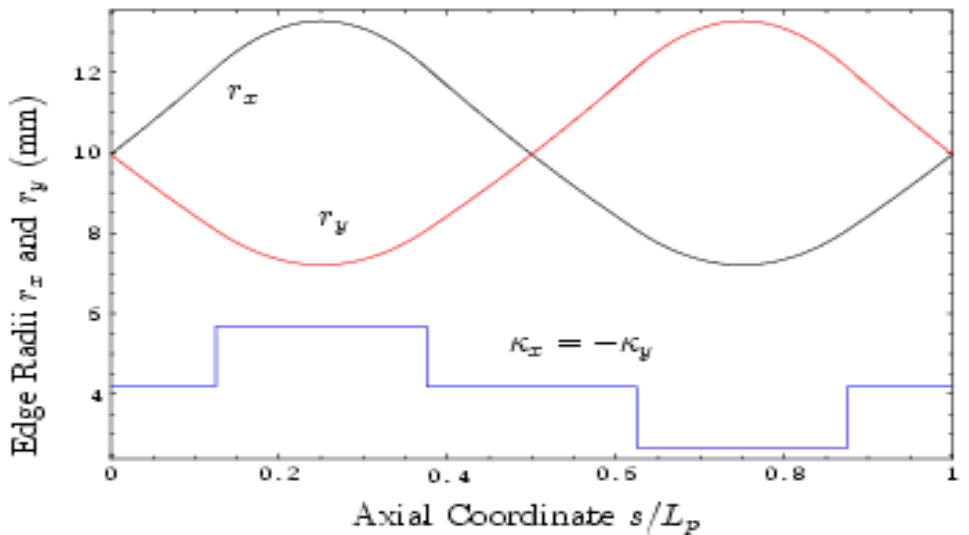
Solenoidal Focusing

$$(Q = 6.6986 \times 10^{-4})$$



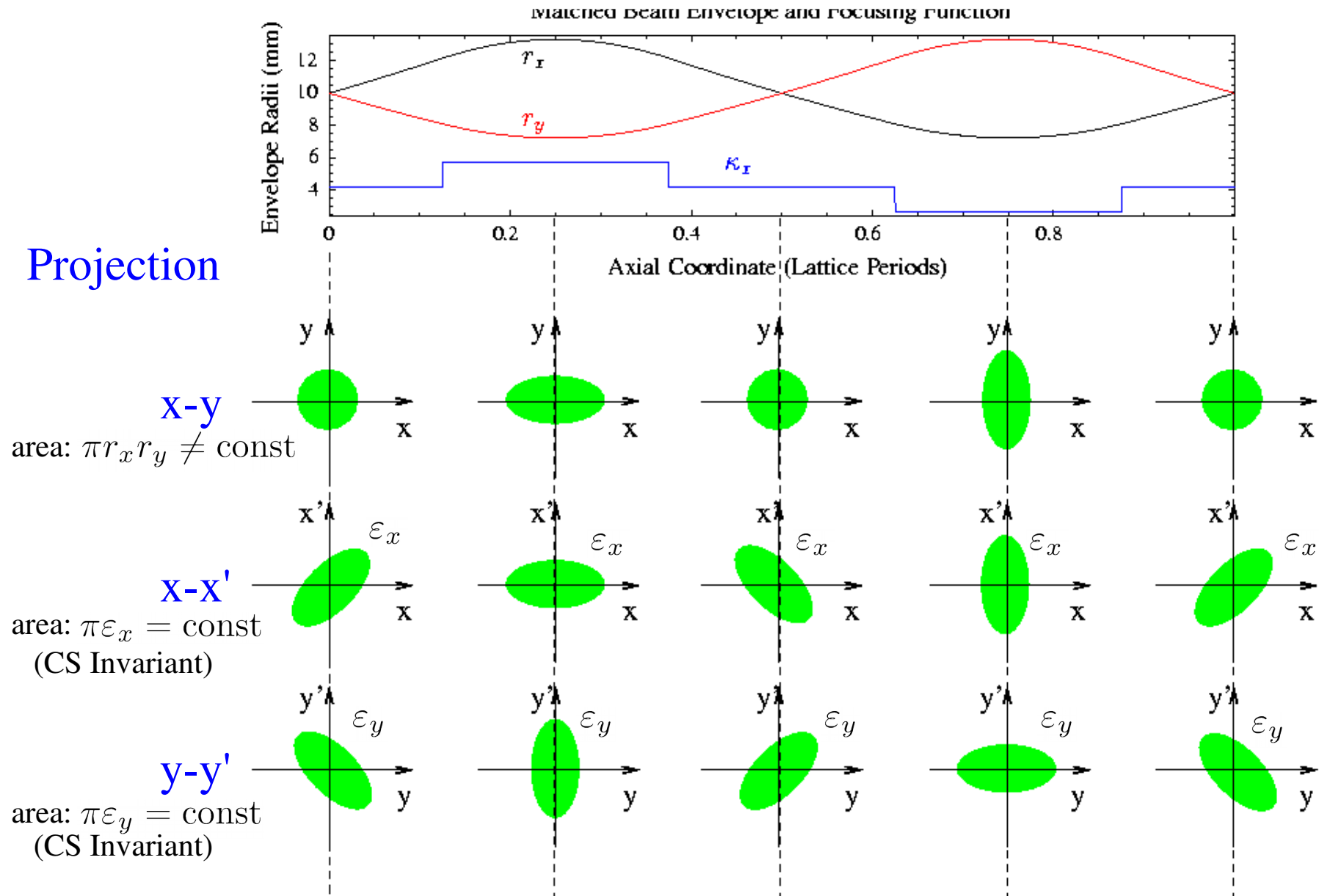
FODO Quadrupole Focusing

$$(Q = 6.5614 \times 10^{-4})$$



Symmetries of a matched beam are interpreted in terms of a local rms equivalent KV beam and moments/projections of the KV distribution
[see: S.M. Lund, lectures on [Transverse Equilibrium Distributions](#)]

Projection



Iterative Numerical Matching Code implemented in Mathematica provided
Lund, Chilton, and Lee, PRSTAB **9**, 064201 (2006)

IM (Iterated Matching) Method

- IM Method uses fail-safe numerical iteration technique without root finding to construct matched envelope solutions in periodic focusing lattices

- Based on projections of Courant-Snyder invariants of depressed orbits in beam
 - Applies to arbitrarily complicated lattices (with user input focusing functions)
 - Works even where matched envelope is unstable

- Can find matched solutions under a variety of parameterizations:

$$\text{Case -1} \quad \kappa_x, \kappa_y, L_p \quad (\sigma_{0x}, \sigma_{0y})^T \quad Q, \quad \varepsilon_x, \quad \varepsilon_y \quad + \quad r_{xi}, \quad r_{yi}, \quad r'_{xi}, \quad r'_{yi}$$

Case 0: (standard) κ_x, κ_y, L_p (σ_{0x}, σ_{0y}) $Q, \varepsilon_x, \varepsilon_y$

Case 1: κ_x, κ_y, L_p (σ_{0x}, σ_{0y}) Q, σ_x, σ_y (find consit: $\varepsilon_x, \varepsilon_y$)

Case 2: κ_x, κ_y, L_p (σ_{0x}, σ_{0y}) $\varepsilon_x = \varepsilon_y, \sigma_x = \sigma_y$ (find constitutive Q)

Note: Case 0 is only applied to integrate from an initial condition and does NOT generate a matched beam.

- ◆ Optional packages include additional information:

- Characteristic undepressed and depressed particle orbits within beam
 - Matched envelope stability properties (covered later in these lectures)

- ◆ Program employed to make many example figures in this course

- Many highly nontrivial to make without this code !

To Obtain code:

- Package files placed in directory “env_match_code” with this lecture note set
- Package maintained/updated presently using git software maintenance tools.
Can obtain full distribution on unix-like system from a terminal window using:

```
% git clone https://github.com/smlund/iterative_match
```

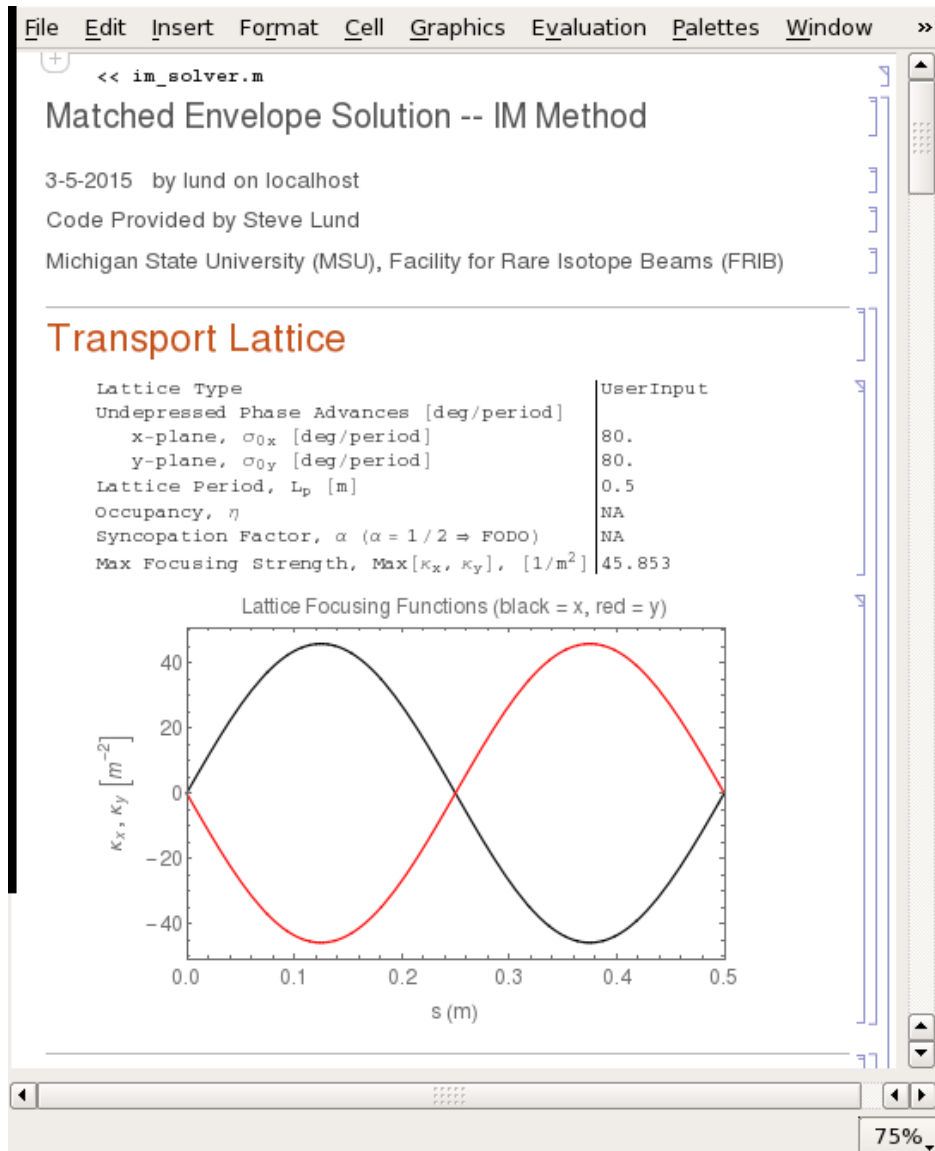
To Run code: see readme.txt file with source code for more details

- 1) Place “im_*.m” program files in directory and set parameters (text editor) in “im_inputs.m”
- 2) Open Mathematica Notebook in directory
- 3) Run in notebook by typing: << im_solver.m [shift-return]

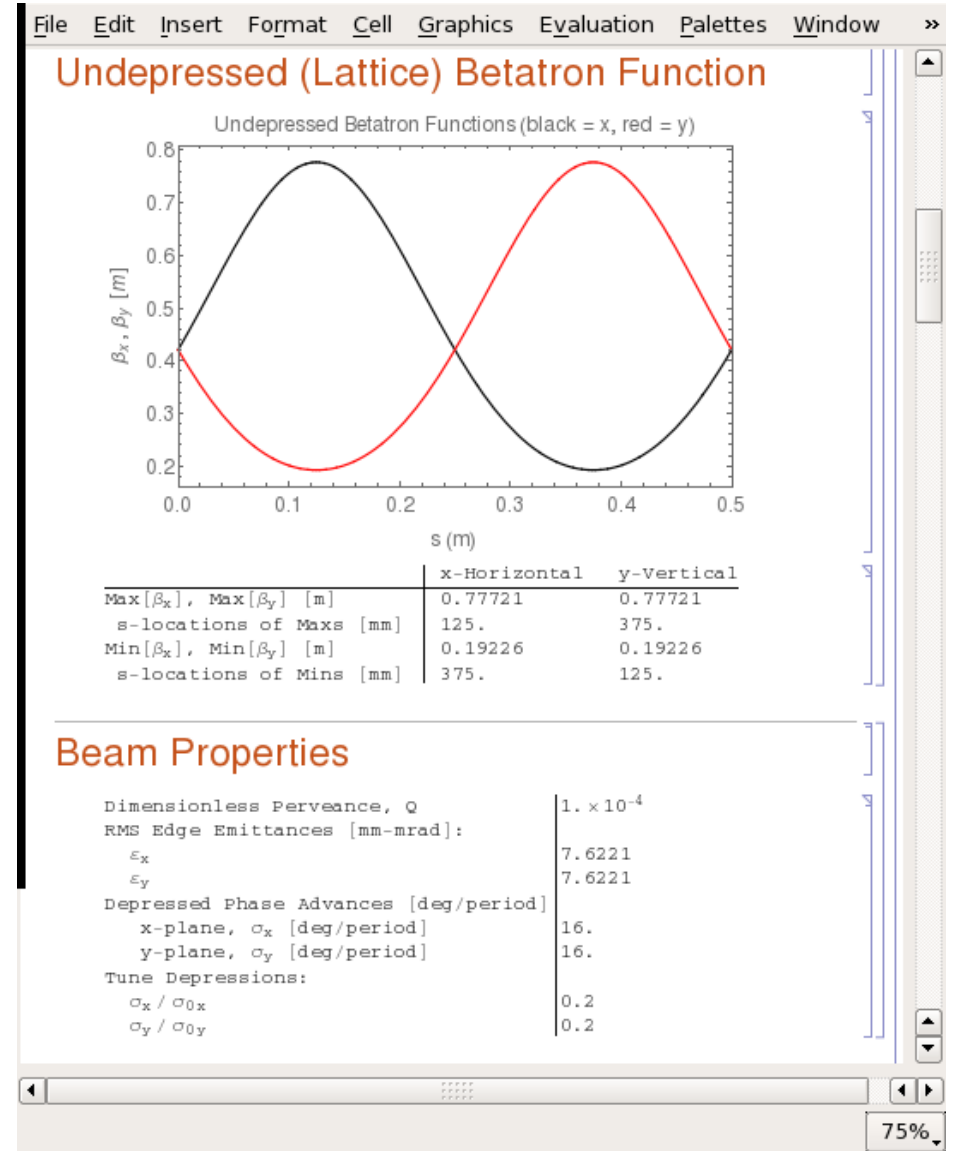
Example Run: sinusoidally varying quadrupole lattice with $\kappa_x = -\kappa_y$

- ♦ See “examples/user” subdirectory in source code distribution (other examples also)

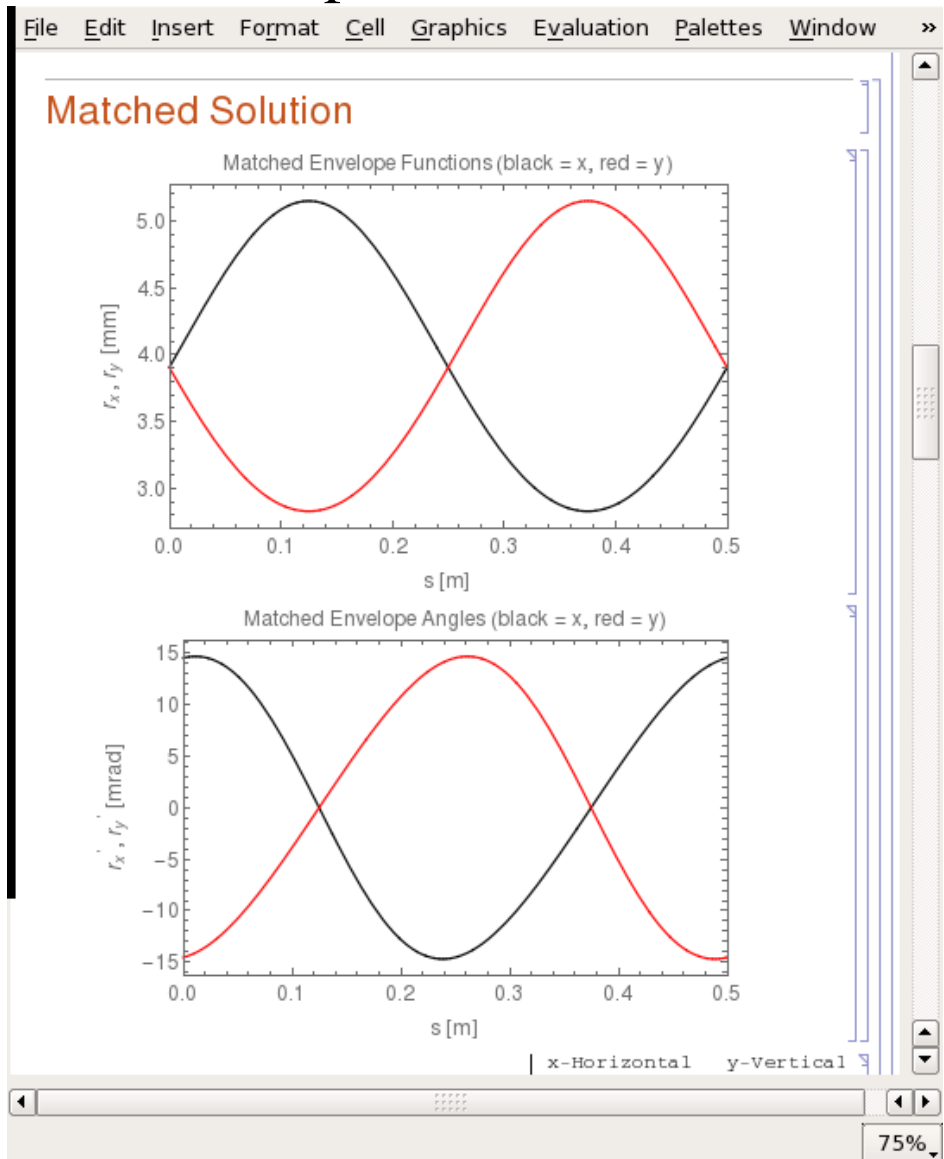
Output: 1st



Output: 2^{ndt}



Output: 3rd



Output: 4th

File Edit Insert Format Cell Graphics Evaluation Palettes Window »

	x-Horizontal	y-Vertical
Radii, $r_x = 2(x^2)^{1/2}$, $r_y = 2(y^2)^{1/2}$:	3.947	3.947
Avg (Lattice Period), \bar{r}_x , \bar{r}_y [mm]	5.1485	5.1485
Max, Max[r _x], Max[r _y] [mm]	125.	375.
s-locations of Maxs [mm]	2.8298	2.8298
Min, Min[r _x], Min[r _y] [mm]	375.	125.
s-locations of Mins [mm]		
Angles, r_x' , r_y' :		
Max, Max[r _x '], Max[r _y '] [mrad]	14.685	14.685
s-locations of Maxs [mm]	11.317	261.32
Min, Min[r _x '], Min[r _y '] [mrad]	-14.685	-14.685
s-locations of Mins [mm]	238.66	488.67
Matching Conditions:		
Radii, $r_x[0]$, $r_y[0]$ [mm]	3.9049	3.9049
Angles, $r_x'[0]$, $r_y'[0]$ [mrad]	14.533	-14.533
Average Radius Measures:		
$\sqrt{r_x r_y}$ [mm]	3.8612	
$(\bar{r}_x + \bar{r}_y) / 2$ [mm]	3.947	

Matched Solution -- Numerical Parameters

Parameterization Case	1
Specified Fractional Tolerance	1×10^{-6}
Achieved Fractional Tolerance	2.6884×10^{-7}
Iterations Needed	7
CPU Time for Solution [sec]	15.9703

Characteristic x- and y-Plane Orbits

Single Particle CS Invariants (includes space-charge):	
ϵ_x [mm-mrad]	2.744
ϵ_y [mm-mrad]	2.744
Axial Coordinates:	
Initial s_i [m]	0.
Final s_f [m]	11.25

75%

+ More on particle orbits and
matched envelope stability

In the envelope equations take:

Envelope Perturbations:

$$\begin{aligned} r_x(s) &= r_{xm}(s) + \delta r_x(s) \\ r_y(s) &= r_{ym}(s) + \delta r_y(s) \end{aligned}$$

Matched Mismatch
Envelope Perturbations

Driving Perturbations:

$\kappa_x(s) \rightarrow \kappa_x(s) + \delta\kappa_x(s)$	Focus
$\kappa_y(s) \rightarrow \kappa_y(s) + \delta\kappa_y(s)$	Perveance
$Q \rightarrow Q + \delta Q(s)$	Emittance
$\varepsilon_x \rightarrow \varepsilon_x + \delta\varepsilon_x(s)$	
$\varepsilon_y \rightarrow \varepsilon_y + \delta\varepsilon_y(s)$	

Perturbations in envelope radii are about a matched solution:

$$r_{xm}(s + L_p) = r_{xm}(s) \quad r_{xm}(s) > 0$$

$$r_{ym}(s + L_p) = r_{ym}(s) \quad r_{ym}(s) > 0$$

Perturbations in envelope radii are small relative to matched solution and driving terms are consistently ordered:

$$\begin{aligned} r_{xm}(s) &\gg |\delta r_x(s)| \\ r_{ym}(s) &\gg |\delta r_y(s)| \end{aligned}$$

← Amplitudes defined in terms of
producing small envelope perturbations

- ◆ Driving perturbations and distribution errors generate/pump envelope perturbations
 - Arise from many sources: focusing errors, lost particles, emittance growth,

The **matched solution** satisfies:

- ◆ Add subscript m to denote matched envelope solution and distinguish from other evolutions

$$r_x \rightarrow r_{xm}$$

For matched beam envelope

$$r_y \rightarrow r_{ym}$$

with periodicity of lattice

$$r''_{xm}(s) + \kappa_x(s)r_{xm}(s) - \frac{2Q}{r_{xm}(s) + r_{ym}(s)} - \frac{\varepsilon_x^2}{r_{xm}^3(s)} = 0$$

$$r''_{ym}(s) + \kappa_y(s)r_{ym}(s) - \frac{2Q}{r_{xm}(s) + r_{ym}(s)} - \frac{\varepsilon_y^2}{r_{ym}^3(s)} = 0$$

$$r_{xm}(s + L_p) = r_{xm}(s)$$

$$r_{xm}(s) > 0$$

$$r_{ym}(s + L_p) = r_{ym}(s)$$

$$r_{ym}(s) > 0$$

Matching is usually cast in terms of finding 4 “initial” envelope phase-space values where the envelope solution satisfies the periodicity constraint for specified focusing, perveance, and emittances:

$$r_{xm}(s_i) \quad r'_{xm}(s_i)$$

$$r_{ym}(s_i) \quad r'_{ym}(s_i)$$

Linearized Perturbed Envelope Equations:

- ♦ Neglect all terms of order δ^2 and higher: $(\delta r_x)^2, \delta r_x \delta r_y, \delta Q \delta r_x, \dots$

$$\begin{aligned} \delta r''_x + \kappa_x \delta r_x + \frac{2Q}{(r_{xm} + r_{ym})^2} (\delta r_x + \delta r_y) + \frac{3\varepsilon_x^2}{r_{xm}^4} \delta r_x \\ = -r_{xm} \delta \kappa_x + \frac{2}{r_{xm} + r_{ym}} \delta Q + \frac{2\varepsilon_x}{r_{xm}^3} \delta \varepsilon_x \end{aligned}$$

$$\begin{aligned} \delta r''_y + \kappa_y \delta r_y + \frac{2Q}{(r_{xm} + r_{ym})^2} (\delta r_x + \delta r_y) + \frac{3\varepsilon_y^2}{r_{ym}^4} \delta r_y \\ = -r_{ym} \delta \kappa_y + \frac{2}{r_{xm} + r_{ym}} \delta Q + \frac{2\varepsilon_y}{r_{ym}^3} \delta \varepsilon_y \end{aligned}$$

Homogeneous Equations:

- ♦ Linearized envelope equations with driving terms set to zero

$$\begin{aligned} \delta r''_x + \kappa_x \delta r_x + \frac{2Q}{(r_{xm} + r_{ym})^2} (\delta r_x + \delta r_y) + \frac{3\varepsilon_x^2}{r_{xm}^4} \delta r_x = 0 \\ \delta r''_y + \kappa_y \delta r_y + \frac{2Q}{(r_{xm} + r_{ym})^2} (\delta r_x + \delta r_y) + \frac{3\varepsilon_y^2}{r_{ym}^4} \delta r_y = 0 \end{aligned}$$

Derivation steps for terms in the linearized envelope equation:

Inertial: $r_x'' \rightarrow r_{xm}'' + \delta r_{xm}''$

Focusing: $\kappa_x r_x \rightarrow (\kappa_x + \delta \kappa_x)(r_{xm} + \delta r_x)$
 $\simeq \kappa_x r_{xm} + \kappa_x \delta r_{xm} + \delta \kappa_x r_{xm} + \Theta(\delta^2)$

Perveance: $\frac{2Q}{r_x + r_y} \rightarrow \frac{2Q + 2\delta Q}{r_{xm} + r_{ym} + \delta r_x + \delta r_y}$
 $\simeq \frac{2Q}{r_{xm} + r_{ym}} \left[1 - \frac{\delta r_x + \delta r_y}{r_{xm} + r_{ym}} \right]$
 $+ \frac{2\delta Q}{r_{xm} + r_{ym}} + \Theta(\delta^2)$

Emittance: $\frac{\varepsilon_x^2}{r_x^3} \rightarrow \frac{(\varepsilon_x + \delta \varepsilon_x)^2}{(r_{xm} + \delta r_x)^3}$
 $\simeq \frac{2\varepsilon_x \delta \varepsilon_x}{r_{xm}^3} + \frac{\varepsilon_x^2}{r_{xm}^3} \left[1 - 3 \frac{\delta r_x}{r_{xm}} \right] + \Theta(\delta^2)$

Martix Form of the Linearized Perturbed Envelope Equations:

$$\boxed{\frac{d}{ds} \delta \mathbf{R} + \mathbf{K} \cdot \delta \mathbf{R} = \delta \mathbf{P}}$$

$$\delta \mathbf{R} \equiv \begin{pmatrix} \delta r_x \\ \delta r'_x \\ \delta r_y \\ \delta r'_y \end{pmatrix}$$

Coordinate vector

$$\mathbf{K} \equiv \begin{pmatrix} 0 & -1 & 0 & 0 \\ k_{xm} & 0 & k_{0m} & 0 \\ 0 & 0 & 0 & -1 \\ k_{0m} & 0 & k_{ym} & 0 \end{pmatrix}$$

$$\delta \mathbf{P} \equiv \begin{pmatrix} 0 \\ -\delta \kappa_x r_{xm} + 2 \frac{\delta Q}{r_{xm} + r_{ym}} + 2 \frac{\varepsilon_x \delta \varepsilon_x}{r_{xm}^3} \\ 0 \\ -\delta \kappa_y r_{ym} + 2 \frac{\delta Q}{r_{xm} + r_{ym}} + 2 \frac{\varepsilon_y \delta \varepsilon_y}{r_{ym}^3} \end{pmatrix}$$

Coefficient matrix

$$k_{0m} = \frac{2Q}{(r_{xm} + r_{ym})^2}$$

$$k_{jm} = \kappa_j + 3 \frac{\varepsilon_j^2}{r_{jm}^4} + k_{0m} \quad j = x, y$$

Has periodicity
of the lattice period

Driving perturbation vector

Expand solution into homogeneous and particular parts:

$$\delta \mathbf{R} = \delta \mathbf{R}_h + \delta \mathbf{R}_p$$

$\delta \mathbf{R}_h$ = homogeneous solution

$\delta \mathbf{R}_p$ = particular solution

$$\boxed{\frac{d}{ds} \delta \mathbf{R}_h + \mathbf{K} \cdot \delta \mathbf{R}_h = 0}$$

$$\boxed{\frac{d}{ds} \delta \mathbf{R}_p + \mathbf{K} \cdot \delta \mathbf{R}_p = \delta \mathbf{P}}$$

Homogeneous Solution: Normal Modes

- ◆ Describes normal mode oscillations
- ◆ Original analysis by Struckmeier and Reiser [Part. Accel. **14**, 227 (1984)]

Particular Solution: Driven Modes

- ◆ Describes action of driving terms
- ◆ Characterize in terms of projections on homogeneous response (on normal modes)

Homogeneous solution expressible as a map:

$$\delta\mathbf{R}(s) = \mathbf{M}_e(s|s_i) \cdot \delta\mathbf{R}(s_i)$$

$$\delta\mathbf{R}(s) = (\delta r_x, \delta r'_x, \delta r_y, \delta r'_y)$$

$\mathbf{M}_e(s|s_i)$ = 4×4 transfer map

Now 4×4 system, but analogous to the 2×2 analysis of Hill's equation via transfer matrices: see S.M. Lund lectures on **Transverse Particle Dynamics**

Eigenvalues and eigenvectors of map through one period characterize normal modes and stability properties:

$$\mathbf{M}_e(s_i + L_p|s_i) \cdot \mathbf{E}_n(s_i) = \lambda_n \mathbf{E}_n(s_i)$$

Stability Properties

$\lambda_n = \gamma_n e^{i\sigma_n}$ $\sigma_n \rightarrow$ mode phase advance (real)

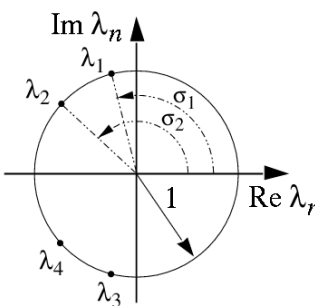
$\gamma_n \rightarrow$ mode growth/damp factor (real)

Mode Expansion/Launching

$$\delta\mathbf{R}(s_i) = \sum_{n=1}^4 \alpha_n \mathbf{E}_n(s_i)$$
$$\alpha_n = \text{const (complex)}$$

Eigenvalue/Eigenvector Symmetry Classes:

a) Stable



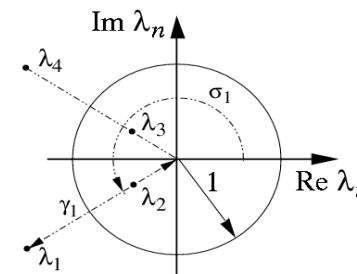
Eigenvalues

$$\begin{aligned}\lambda_1 &= e^{i\sigma_1} \\ \lambda_2 &= e^{i\sigma_2} \\ \lambda_3 &= 1/\lambda_1 = \lambda_1^* = e^{-i\sigma_1} \\ \lambda_4 &= 1/\lambda_2 = \lambda_2^* = e^{-i\sigma_2}\end{aligned}$$

Eigenvectors

$$\begin{aligned}\vec{E}_1 \\ \vec{E}_2 \\ \vec{E}_3 = \vec{E}_1^* \\ \vec{E}_4 = \vec{E}_2^*\end{aligned}$$

b) Unstable, Confluent Resonance



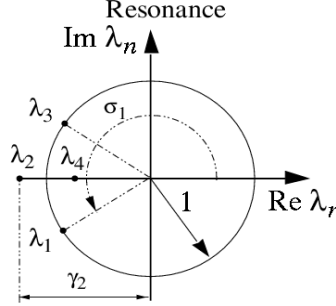
Eigenvalues

$$\begin{aligned}\lambda_1 &= \gamma_1 e^{i\sigma_1} \\ \lambda_2 &= 1/\lambda_1^* = (1/\gamma_1) e^{-i\sigma_1} \\ \lambda_3 &= 1/\lambda_1 = (1/\gamma_1) e^{-i\sigma_1} \\ \lambda_4 &= \lambda_1^* = \gamma_1 e^{-i\sigma_1}\end{aligned}$$

Eigenvectors

$$\begin{aligned}\vec{E}_1 \\ \vec{E}_2 \\ \vec{E}_3 = \vec{E}_2^* \\ \vec{E}_4 = \vec{E}_1^*\end{aligned}$$

c) Unstable, Lattice Resonance



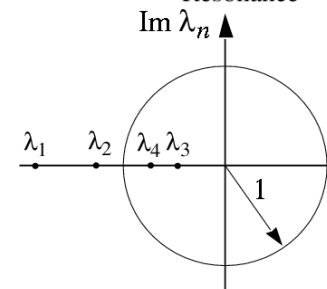
Eigenvalues

$$\begin{aligned}\lambda_1 &= e^{i\sigma_1} \\ \lambda_2 &= \gamma_2 e^{i\pi} \\ \lambda_3 &= \lambda_1^* = e^{-i\sigma_1} \\ \lambda_4 &= 1/\lambda_2 = (1/\gamma_2) e^{i\pi}\end{aligned}$$

Eigenvectors

$$\begin{aligned}\vec{E}_1 \\ \vec{E}_2 \text{ (real)} \\ \vec{E}_3 = \vec{E}_1^* \\ \vec{E}_4 \text{ (real)}\end{aligned}$$

d) Unstable, Double Lattice Resonance



Eigenvalues

$$\begin{aligned}\lambda_1 &= \gamma_1 e^{i\pi} \\ \lambda_2 &= \gamma_2 e^{i\pi} \\ \lambda_3 &= 1/\lambda_1 = (1/\gamma_1) e^{i\pi} \\ \lambda_4 &= 1/\lambda_2 = (1/\gamma_2) e^{i\pi}\end{aligned}$$

Eigenvectors

$$\begin{aligned}\vec{E}_1 \text{ (real)} \\ \vec{E}_2 \text{ (real)} \\ \vec{E}_3 \text{ (real)} \\ \vec{E}_4 \text{ (real)}\end{aligned}$$

Symmetry classes of eigenvalues/eigenvectors:

- ◆ Determine normal mode symmetries
- ◆ Hamiltonian dynamics allow only 4 distinct classes of eigenvalue symmetries
 - See A. Dragt, Lectures on Nonlinear Orbit Dynamics, in Physics of High Energy Particle Accelerators, (AIP Conf. Proc. No. 87, 1982, p. 147)
- ◆ Envelope mode symmetries discussed fully in PRSTAB review
- ◆ Caution: Textbook by Reiser makes errors in quadrupole mode symmetries and mislabels/identifies dispersion characteristics and branch choices

Pure mode launching conditions:

Launching conditions for distinct normal modes corresponding to the eigenvalue classes illustrated:

A_ℓ = mode amplitude (real) ℓ = mode index

ψ_ℓ = mode launch phase (real) *C.C.* = complex conjugate

Case	Mode	Launching Condition	Lattice Period Advance
(a) Stable	1 - Stable Osc.	$\delta\mathbf{R}_1 = A_1 e^{i\psi_1} \mathbf{E}_1 + \text{C.C.}$	$\mathbf{M}_e \delta\mathbf{R}_1(\psi_1) = \delta\mathbf{R}_1(\psi_1 + \sigma_1)$
	2 - Stable Osc.	$\delta\mathbf{R}_2 = A_2 e^{i\psi_2} \mathbf{E}_2 + \text{C.C.}$	$\mathbf{M}_e \delta\mathbf{R}_2(\psi_2) = \delta\mathbf{R}_2(\psi_2 + \sigma_2)$
(b) Unstable Confluent Res.	1 - Exp. Growth	$\delta\mathbf{R}_1 = A_1 e^{i\psi_1} \mathbf{E}_1 + \text{C.C.}$	$\mathbf{M}_e \delta\mathbf{R}_1(\psi_1) = \gamma_1 \delta\mathbf{R}_1(\psi_1 + \sigma_1)$
	2 - Exp. Damping	$\delta\mathbf{R}_2 = A_2 e^{i\psi_2} \mathbf{E}_2 + \text{C.C.}$	$\mathbf{M}_e \delta\mathbf{R}_2(\psi_2) = (1/\gamma_1) \delta\mathbf{R}_2(\psi_2 + \sigma_1)$
(c) Unstable Lattice Res.	1 - Stable Osc.	$\delta\mathbf{R}_1 = A_1 e^{i\psi_1} \mathbf{E}_1 + \text{C.C.}$	$\mathbf{M}_e \delta\mathbf{R}_1(\psi_1) = \delta\mathbf{R}_1(\psi_1 + \sigma_1)$
	2 - Exp. Growth	$\delta\mathbf{R}_2 = A_2 \mathbf{E}_2$	$\mathbf{M}_e \delta\mathbf{R}_2 = -\gamma_2 \delta\mathbf{R}_2$
	3 - Exp. Damping	$\delta\mathbf{R}_3 = A_3 \mathbf{E}_4$	$\mathbf{M}_e \delta\mathbf{R}_3 = -(1/\gamma_2) \delta\mathbf{R}_3$
(d) Unstable Double Lattice Resonance	1 - Exp. Growth	$\delta\mathbf{R}_1 = A_1 \mathbf{E}_1$	$\mathbf{M}_e \delta\mathbf{R}_1 = -\gamma_1 \delta\mathbf{R}_1$
	2 - Exp. Growth	$\delta\mathbf{R}_2 = A_2 \mathbf{E}_2$	$\mathbf{M}_e \delta\mathbf{R}_2 = -\gamma_2 \delta\mathbf{R}_2$
	3 - Exp. Damping	$\delta\mathbf{R}_3 = A_3 \mathbf{E}_3$	$\mathbf{M}_e \delta\mathbf{R}_3 = -(1/\gamma_1) \delta\mathbf{R}_3$
	4 - Exp. Damping	$\delta\mathbf{R}_4 = A_4 \mathbf{E}_4$	$\mathbf{M}_e \delta\mathbf{R}_4 = -(1/\gamma_2) \delta\mathbf{R}_4$

$$\delta\mathbf{R}_\ell \equiv \delta\mathbf{R}_\ell(s_i) \quad \mathbf{E}_\ell \equiv \mathbf{E}_\ell(s_i) \quad \mathbf{M}_e \equiv \mathbf{M}_e(s_i + L_p | s_i)$$

$$\delta\mathbf{R}(s) = \begin{cases} A_1[\mathbf{E}_1(s)e^{i\psi_1(s)} + \mathbf{E}_1^*(s)e^{-i\psi_1(s)}] + A_2[\mathbf{E}_2(s)e^{i\psi_2(s)} + \mathbf{E}_2^*(s)e^{-i\psi_2(s)}], & \text{cases (a) and (b)} \\ A_1[\mathbf{E}_1(s)e^{i\psi_1(s)} + \mathbf{E}_1^*(s)e^{-i\psi_1(s)}] + A_2\mathbf{E}_2(s) + A_3\mathbf{E}_4(s), & \text{case (c)} \\ A_1\mathbf{E}_1(s) + A_2\mathbf{E}_2(s) + A_3\mathbf{E}_3(s) + A_4\mathbf{E}_4(s), & \text{case (d)} \end{cases}$$

Decoupled Modes

In a **continuous or periodic solenoidal** focusing channel

$$\kappa_x(s) = \kappa_y(s) = \kappa(s)$$

with a round matched-beam solution

$$\varepsilon_x = \varepsilon_y \equiv \varepsilon = \text{const}$$

$$r_{xm}(s) = r_{ym}(s) \equiv r_m(s)$$

envelope perturbations are simply decoupled with:

Breathing Mode: $\delta r_+ \equiv \frac{\delta r_x + \delta r_y}{2}$

Quadrupole Mode: $\delta r_- \equiv \frac{\delta r_x - \delta r_y}{2}$

The resulting decoupled envelope equations are:

Breathing Mode:

$$\delta r''_+ + \kappa \delta r_+ + \frac{Q}{r_m^2} \delta r_+ + \frac{3\varepsilon^2}{r_m^4} \delta r_+ = -r_m \left(\frac{\delta \kappa_x + \delta \kappa_y}{2} \right) + \frac{1}{r_m} \delta Q + \frac{2\varepsilon}{r_m^3} \left(\frac{\delta \varepsilon_x + \delta \varepsilon_y}{2} \right)$$

Quadrupole Mode:

$$\delta r''_- + \kappa \delta r_- + \frac{3\varepsilon^2}{r_m^4} \delta r_- = -r_m \left(\frac{\delta \kappa_x - \delta \kappa_y}{2} \right) + \frac{2\varepsilon}{r_m^3} \left(\frac{\delta \varepsilon_x - \delta \varepsilon_y}{2} \right)$$

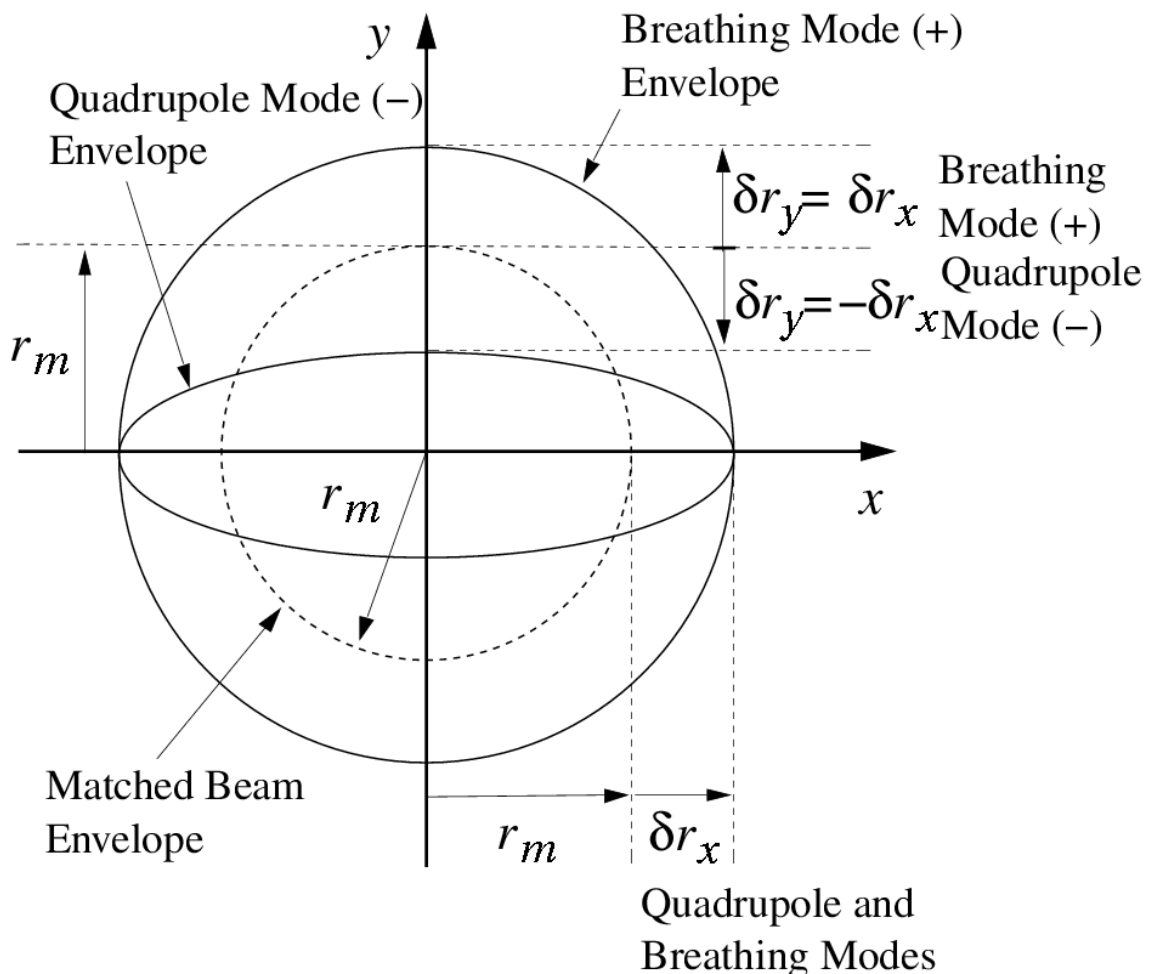
Graphical interpretation of mode symmetries:

Breathing Mode:

$$\delta r_+ = \frac{\delta r_x + \delta r_y}{2}$$

Quadrupole Mode:

$$\delta r_- = \frac{\delta r_x - \delta r_y}{2}$$



Decoupled Mode Properties:

Space charge terms $\sim Q$ only directly expressed in equation for $\delta r_+(s)$

- ♦ Indirectly present in both equations from matched envelope $r_m(s)$

Homogeneous Solution:

- ♦ Restoring term for $\delta r_+(s)$ larger than for $\delta r_-(s)$
 - Breathing mode should oscillate faster than the quadrupole mode

Particular Solution:

- ♦ Misbalances in focusing and emittance driving terms can project onto either mode
 - nonzero perturbed $\kappa_x(s) + \kappa_y(s)$ and $\varepsilon_x(s) + \varepsilon_y(s)$ project onto breathing mode
 - nonzero perturbed $\kappa_x(s) - \kappa_y(s)$ and $\varepsilon_x(s) - \varepsilon_y(s)$ project onto quadrupole mode
- ♦ Perveance driving perturbations project *only* on breathing mode

Previous symmetry classes greatly reduce for decoupled modes:

Previous homogeneous 4x4 solution map:

$$\delta\mathbf{R}(s) = \mathbf{M}_e(s|s_i) \cdot \delta\mathbf{R}(s_i)$$

$$\delta\mathbf{R}(s) = (\delta r_x, \delta r'_x, \delta r_y, \delta r'_y)$$

$\mathbf{M}_e(s|s_i)$ = 4 × 4 transfer map

Reduces to two independent 2x2 maps with greatly simplified symmetries:

$$\delta\mathbf{R} \equiv (\delta r_+, \delta r'_+, \delta r_-, \delta r'_-)$$

$$\mathbf{M}_e(s_i + L_p|s_i) = \begin{bmatrix} \mathbf{M}_+(s_i + L_p|s_i) & 0 \\ 0 & \mathbf{M}_-(s_i + L_p|s_i) \end{bmatrix}$$

Here \mathbf{M}_{\pm} denote the 2x2 map solutions to the uncoupled Hills equations for δr_{\pm} :

$$\delta r_{\pm} + \kappa_{\pm} \delta r_{\pm} = 0$$

$$\kappa_+ \equiv \kappa + \frac{Q}{r_m^2} + \frac{3\varepsilon^2}{r_m^4}$$

$$\kappa_- \equiv \kappa + \frac{3\varepsilon^2}{r_m^4}$$

$$\begin{pmatrix} \delta r_{\pm} \\ \delta r'_{\pm} \end{pmatrix} = \mathbf{M}_{\pm}(s|s_i) \cdot \begin{pmatrix} \delta r_{\pm} \\ \delta r'_{\pm} \end{pmatrix}_i$$

The corresponding 2D eigenvalue problems:

$$\mathbf{M}_{\pm}(s_i + L_p|s_i) \cdot \mathbf{E}_n(s_i) = \lambda_{\pm} \mathbf{E}_n(s_i)$$

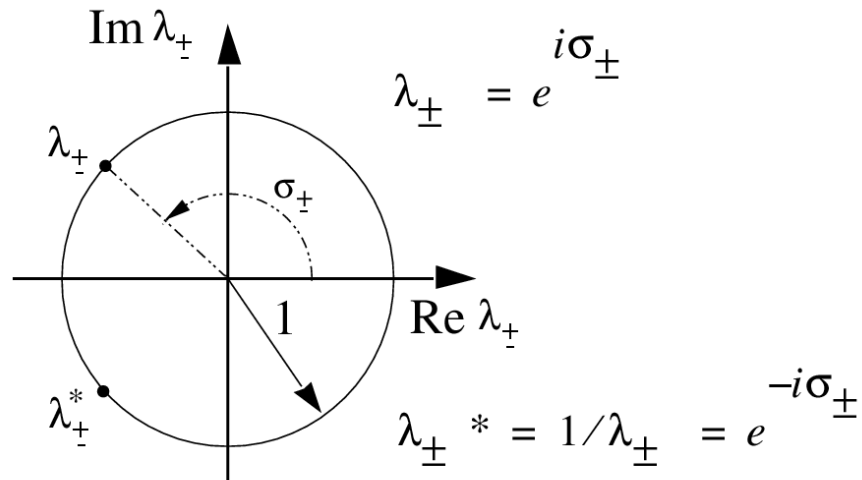
Familiar results from analysis of Hills equation (see: S.M. Lund lectures on **Transverse Particle Dynamics**) can be immediately applied to the decoupled case, for example:

$$\frac{1}{2} |\text{Tr } \mathbf{M}_{\pm}(s_i + L_p|s_i)| \leq 1 \iff \text{mode stability}$$

Eigenvalue symmetries give decoupled mode launching conditions

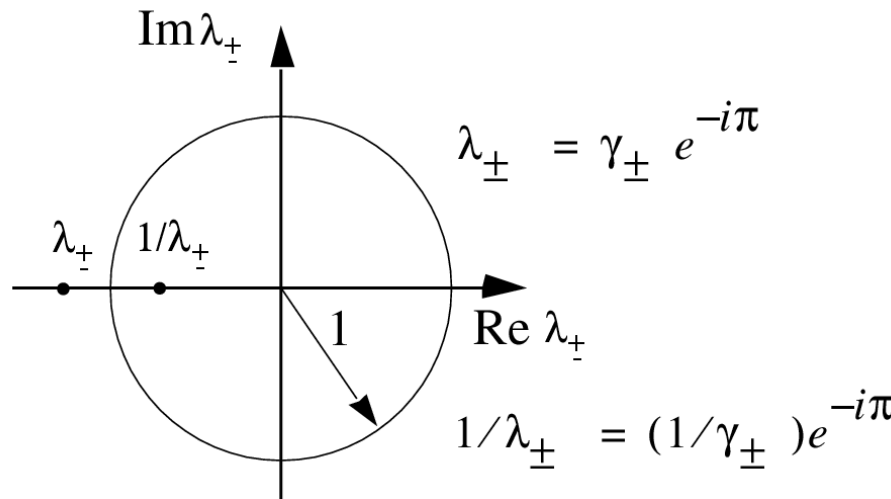
Eigenvalue Symmetry 1:

Stable

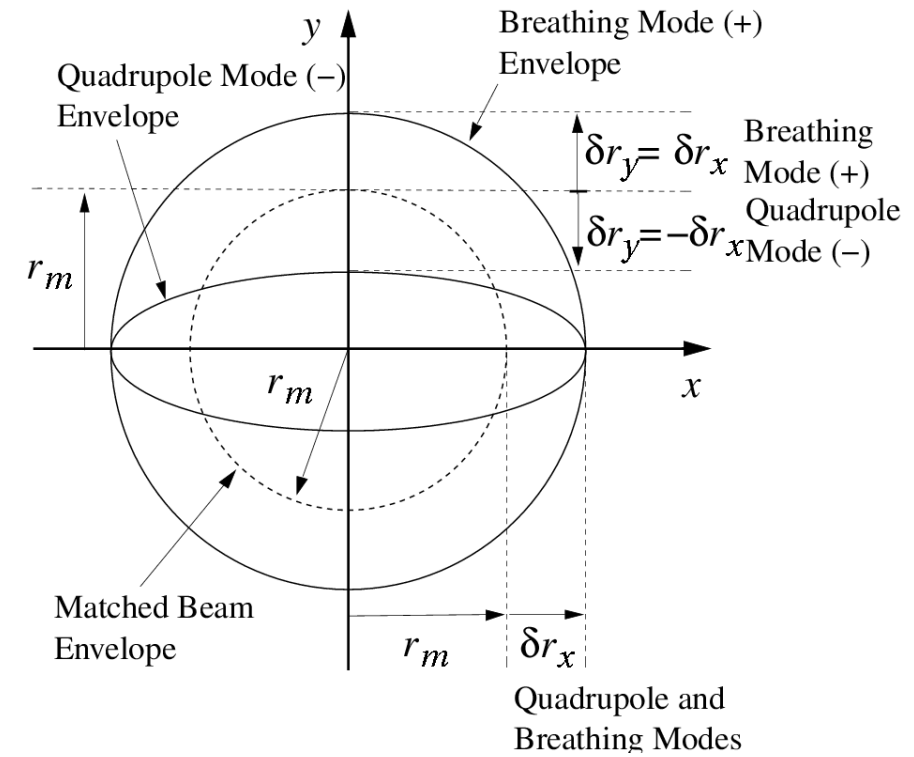


Eigenvalue Symmetry 2:

Unstable, Lattice Resonance



Launching Condition / Projections



General Envelope Mode Limits

Using phase-amplitude analysis can show for any linear focusing lattice:

1) Phase advance of any normal mode satisfies the zero space-charge limit:

$$\lim_{Q \rightarrow 0} \sigma_\ell = 2\sigma_0$$

2) Pure normal modes (not driven) evolve with a quadratic phase-space (Courant-Snyder) invariant in the normal coordinates of the mode

Simply expressed for decoupled modes with $\kappa_x = \kappa_y, \varepsilon_x = \varepsilon_y$

$$\left[\frac{\delta r_\pm(s)}{w_\pm(s)} \right]^2 + [w'_\pm(s)\delta r_\pm(s) - w_\pm(s)\delta r'_\pm(s)]^2 = \text{const}$$

where

$$w''_+ + \kappa w_+ + \frac{Q}{r_m^2} w_+ + \frac{3\varepsilon^2}{r_m^4} w_+ - \frac{1}{w_+^3} = 0$$

$$w''_- + \kappa w_- + \frac{3\varepsilon^2}{r_m^4} w_- - \frac{1}{w_-^3} = 0$$

$$w_\pm(s + L_p) = w_\pm(s)$$

Analogous results for coupled modes [See Edwards and Teng, IEEE Trans Nuc. Sci. **20**, 885 (1973)]

◆ But typically much more complex expression due to coupling

S7: Envelope Modes in Continuous Focusing

Lund and Bukh, PRSTAB 7, 024801 (2004)

Focusing: $\kappa_x(s) = \kappa_y(s) = k_{\beta 0}^2 = \left(\frac{\sigma_0}{L_p}\right)^2 = \text{const}$

Matched beam: $\varepsilon_x = \varepsilon_y = \varepsilon = \text{const}$

symmetric beam: $r_{xm}(s) = r_{ym}(s) = r_m = \text{const}$

matched envelope: $k_{\beta 0}^2 r_m - \frac{Q}{r_m} - \frac{\varepsilon^2}{r_m^3} = 0$

depressed phase advance: $\sigma = \sqrt{\sigma_0^2 - \frac{Q}{(r_m/L_p)^2}} = \frac{\varepsilon L_p}{r_m^2}$

one parameter needed for scaled solution:

Decoupled Modes: $\frac{k_{\beta 0}^2 \varepsilon^2}{Q^2} = \frac{\sigma_0^2 \varepsilon^2}{Q^2 L_p^2} = \frac{(\sigma/\sigma_0)^2}{[1 - (\sigma/\sigma_0)^2]^2}$

$$\delta r_{\pm}(s) = \frac{\delta r_x(s) \pm \delta r_y(s)}{2}$$

Envelope equations of motion become:

$$L_p^2 \frac{d^2}{ds^2} \left(\frac{\delta r_+}{r_m} \right) + \sigma_+^2 \left(\frac{\delta r_+}{r_m} \right) = -\frac{\sigma_0^2}{2} \left(\frac{\delta \kappa_x}{k_{\beta 0}^2} + \frac{\delta \kappa_y}{k_{\beta 0}^2} \right) + (\sigma_0^2 - \sigma^2) \frac{\delta Q}{Q} + \sigma^2 \left(\frac{\delta \varepsilon_x}{\varepsilon} + \frac{\delta \varepsilon_y}{\varepsilon} \right)$$

$$L_p^2 \frac{d^2}{ds^2} \left(\frac{\delta r_-}{r_m} \right) + \sigma_-^2 \left(\frac{\delta r_-}{r_m} \right) = -\frac{\sigma_0^2}{2} \left(\frac{\delta \kappa_x}{k_{\beta 0}^2} - \frac{\delta \kappa_y}{k_{\beta 0}^2} \right) + \sigma^2 \left(\frac{\delta \varepsilon_x}{\varepsilon} - \frac{\delta \varepsilon_y}{\varepsilon} \right)$$

$$\sigma_+ \equiv \sqrt{2\sigma_0^2 + 2\sigma^2} \quad \text{"breathing" mode phase advance}$$

$$\sigma_- \equiv \sqrt{\sigma_0^2 + 3\sigma^2} \quad \text{"quadrupole" mode phase advance}$$

Homogeneous equations for normal modes:

$$\frac{d^2}{ds^2} \delta r_{\pm} + \left(\frac{\sigma_{\pm}}{L_p} \right)^2 \delta r_{\pm} = 0$$

See also lectures by
J.J. Barnard, [Envelope Modes and Halo](#)

- Simple harmonic oscillator equation

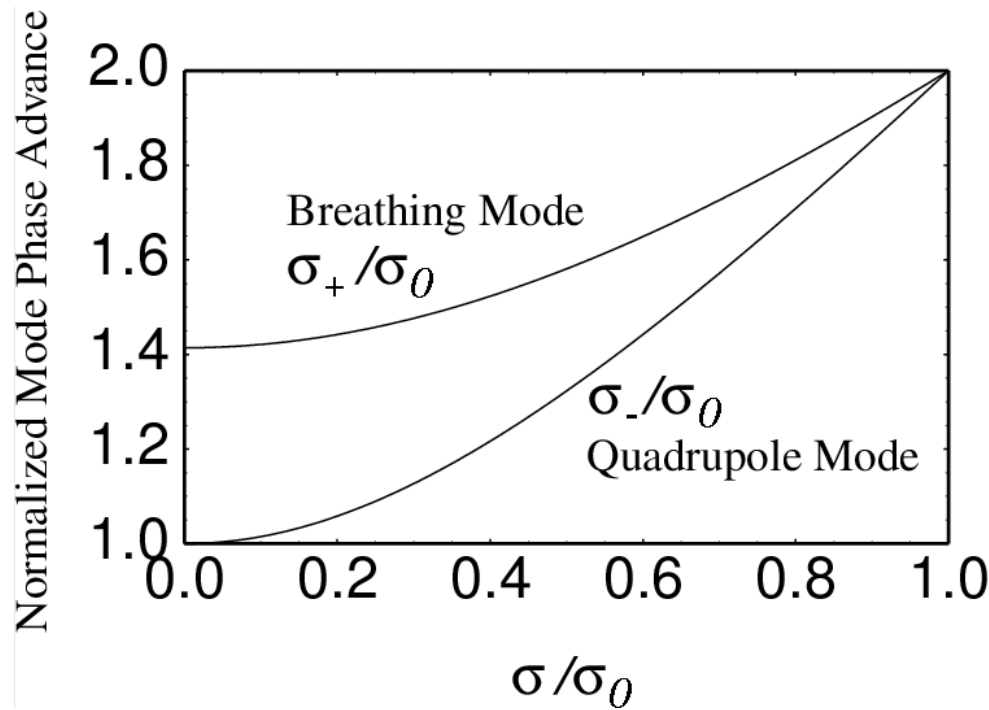
Homogeneous Solution (normal modes):

$$\delta r_{\pm}(s) = \delta r_{\pm}(s_i) \cos \left(\sigma_{\pm} \frac{s - s_i}{L_p} \right) + \frac{\delta r'_{\pm}(s_i)}{\sigma_{\pm}/L_p} \sin \left(\sigma_{\pm} \frac{s - s_i}{L_p} \right)$$

$\delta r_{\pm}(s_i), \delta r'_{\pm}(s_i)$ mode initial conditions

Properties of continuous focusing homogeneous solution: Normal Modes

Mode Phase Advances



$$\sigma_+ \equiv \sqrt{2\sigma_0^2 + 2\sigma^2}$$

$$\sigma_- \equiv \sqrt{\sigma_0^2 + 3\sigma^2}$$

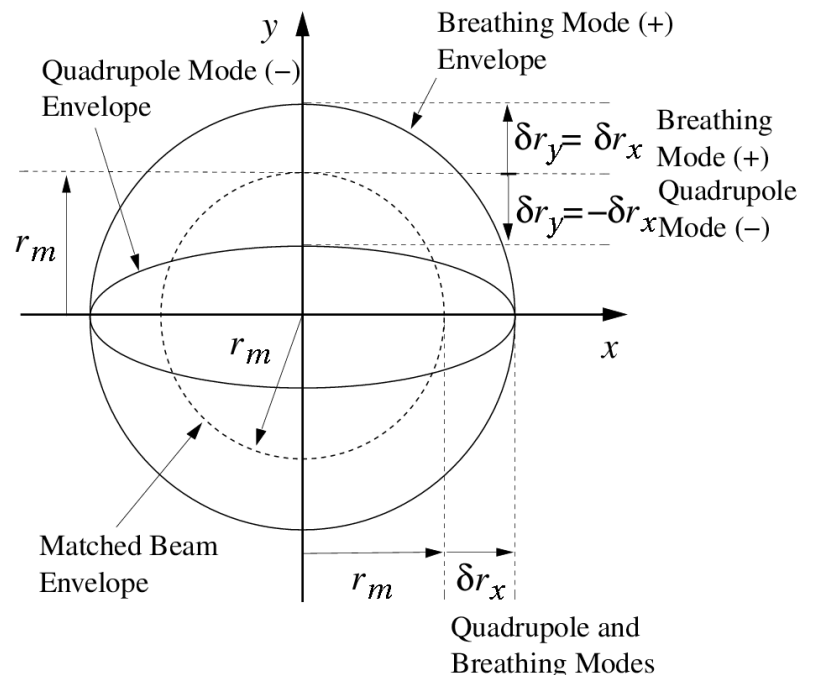
Breathing Mode:

$$\delta r_+ \equiv \frac{\delta r_x + \delta r_y}{2}$$

Quadrupole Mode:

$$\delta r_- \equiv \frac{\delta r_x - \delta r_y}{2}$$

Mode Projections



Particular Solution (driving perturbations):

Green's function form of solution derived using projections onto normal modes

- ◆ See proof that this is a valid solution is given in [Appendix A](#)

$$\frac{\delta r_{\pm}(s)}{r_m} = \frac{1}{L_p^2} \int_{s_i}^s d\tilde{s} G_{\pm}(s, \tilde{s}) \delta p_{\pm}(\tilde{s})$$

$$\delta p_+(s) = -\frac{\sigma_0^2}{2} \left[\frac{\delta \kappa_x(s)}{k_{\beta 0}^2} + \frac{\delta \kappa_y(s)}{k_{\beta 0}^2} \right] + (\sigma_0^2 - \sigma^2) \frac{\delta Q(s)}{Q} + \sigma^2 \left[\frac{\delta \varepsilon_x(s)}{\varepsilon} + \frac{\delta \varepsilon_y(s)}{\varepsilon} \right]$$

$$\delta p_-(s) = -\frac{\sigma_0^2}{2} \left[\frac{\delta \kappa_x(s)}{k_{\beta 0}^2} - \frac{\delta \kappa_y(s)}{k_{\beta 0}^2} \right] + \sigma^2 \left[\frac{\delta \varepsilon_x(s)}{\varepsilon} - \frac{\delta \varepsilon_y(s)}{\varepsilon} \right]$$

$$G_{\pm}(s, \tilde{s}) = \frac{1}{\sigma_{\pm}/L_p} \sin \left(\sigma_{\pm} \frac{s - \tilde{s}}{L_p} \right)$$

Green's function solution is *fully general*. Insight gained from simplified solutions for specific classes of driving perturbations:

- ◆ Adiabatic
- ◆ Sudden
- ◆ Ramped
- ◆ Harmonic

covered in these lectures

covered in PRSTAB Review article

Continuous Focusing – adiabatic particular solution

For driving perturbations $\delta p_+(s)$ and $\delta p_-(s)$ slow on quadrupole mode (slower mode) wavelength $\sim 2\pi L_p/\sigma_-$ the Green function solution reduces to:

$$\frac{\delta r_+(s)}{r_m} = \frac{\delta p_+(s)}{\sigma_+^2}$$

Focusing

$$= - \left[\frac{1}{2} \frac{1}{1 + (\sigma/\sigma_0)^2} \right] \frac{1}{2} \left(\frac{\delta \kappa_x(s)}{k_{\beta 0}^2} + \frac{\delta \kappa_y(s)}{k_{\beta 0}^2} \right) + \left[\frac{1}{2} \frac{1 - (\sigma/\sigma_0)^2}{1 + (\sigma/\sigma_0)^2} \right] \frac{\delta Q(s)}{Q}$$

$$+ \left[\frac{(\sigma/\sigma_0)^2}{1 + (\sigma/\sigma_0)^2} \right] \frac{1}{2} \left(\frac{\delta \varepsilon_x(s)}{\varepsilon} + \frac{\delta \varepsilon_y(s)}{\varepsilon} \right),$$

Emittance

$$\frac{\delta r_-(s)}{r_m} = \frac{\delta p_-(s)}{\sigma_-^2}$$

Focusing

$$= - \left[\frac{1}{1 + 3(\sigma/\sigma_0)^2} \right] \frac{1}{2} \left(\frac{\delta \kappa_x(s)}{k_{\beta 0}^2} - \frac{\delta \kappa_y(s)}{k_{\beta 0}^2} \right)$$

$$+ \left[\frac{2(\sigma/\sigma_0)^2}{1 + 3(\sigma/\sigma_0)^2} \right] \frac{1}{2} \left(\frac{\delta \varepsilon_x(s)}{\varepsilon} - \frac{\delta \varepsilon_y(s)}{\varepsilon} \right).$$

Emittance

Coefficients of adiabatic terms in square brackets "[]"

$\sigma_+ \equiv \sqrt{2\sigma_0^2 + 2\sigma^2}$

$\sigma_- \equiv \sqrt{\sigma_0^2 + 3\sigma^2}$

Derivation of Adiabatic Solution:

- Several ways to derive, show more “mechanical” procedure here

Use:

$$\frac{\delta r_{\pm}(s)}{r_m} = \frac{1}{L_p^2} \int_{s_i}^s d\tilde{s} G_{\pm}(s, \tilde{s}) \delta p_{\pm}(\tilde{s})$$

$$G_{\pm}(s, \tilde{s}) = \frac{1}{\sigma_{\pm}/L_p} \sin \left(\sigma_{\pm} \frac{s - \tilde{s}}{L_p} \right) = \frac{1}{(\sigma_{\pm}/L_p)^2} \frac{d}{d\tilde{s}} \cos \left(\sigma_{\pm} \frac{s - \tilde{s}}{L_p} \right)$$

Gives:

$$\begin{aligned}
 \frac{\delta r_{\pm}(s)}{r_m} &= \int_{s_i}^s d\tilde{s} \left[\frac{d}{d\tilde{s}} \cos \left(\sigma_{\pm} \frac{s - \tilde{s}}{L_p} \right) \right] \frac{\delta p_{\pm}(\tilde{s})}{\sigma_{\pm}^2} && \text{Adiabatic } \uparrow 0 \\
 &= \int_{s_i}^s d\tilde{s} \frac{d}{d\tilde{s}} \left[\cos \left(\sigma_{\pm} \frac{s - \tilde{s}}{L_p} \right) \frac{\delta p_{\pm}(\tilde{s})}{\sigma_{\pm}^2} \right] - \int_{s_i}^s d\tilde{s} \cos \left(\sigma_{\pm} \frac{s - \tilde{s}}{L_p} \right) \frac{d}{d\tilde{s}} \frac{\delta p_{\pm}(\tilde{s})}{\sigma_{\pm}^2} \\
 &= \cos \left(\sigma_{\pm} \frac{s - \tilde{s}}{L_p} \right) \frac{\delta p_{\pm}(\tilde{s})}{\sigma_{\pm}^2} \Big|_{\tilde{s}=s_i}^{\tilde{s}=s} && = \frac{\delta p_{\pm}(s)}{\sigma_{\pm}^2} - \cos \left(\sigma_{\pm} \frac{s - s_i}{L_p} \right) \frac{\delta p_{\pm}(s_i)}{\sigma_{\pm}^2} \uparrow 0 \\
 &= \frac{\delta p_{\pm}(s)}{\sigma_{\pm}^2} && \text{No Initial Perturbation}
 \end{aligned}$$

Comments on Adiabatic Solution:

- Adiabatic response is essentially a slow adaptation in the matched envelope to perturbations (solution does not oscillate due to slow changes)
- Slow envelope frequency σ_- sets the scale for slow variations required

Replacements in adiabatically adapted match:

$$r_x = r_m \rightarrow r_m + \delta r_+ + \delta r_-$$

$$r_y = r_m \rightarrow r_m + \delta r_- - \delta r_+$$

Parameter replacements in rematched beam (no longer axisymmetric):

$$\kappa_x = k_{\beta 0}^2 \rightarrow k_{\beta 0}^2 + \delta \kappa_x(s)$$

$$\kappa_y = k_{\beta 0}^2 \rightarrow k_{\beta 0}^2 + \delta \kappa_y(s)$$

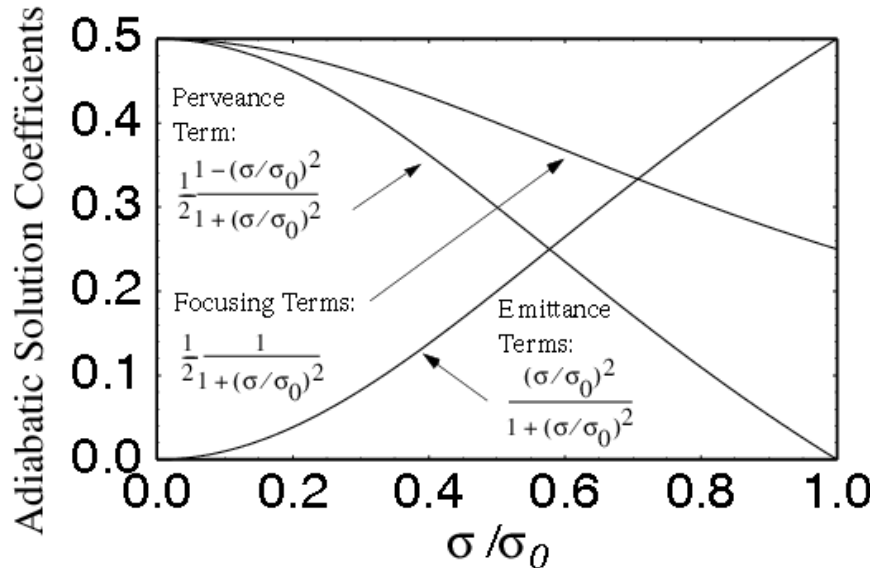
$$Q \rightarrow Q + \delta Q(s)$$

$$\varepsilon_x = \varepsilon \rightarrow \varepsilon + \delta \varepsilon_x(s)$$

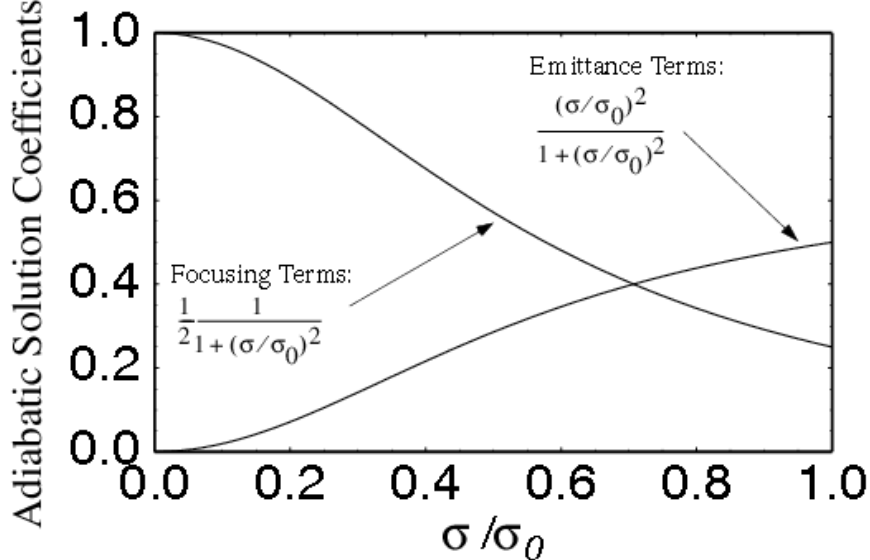
$$\varepsilon_y = \varepsilon \rightarrow \varepsilon + \delta \varepsilon_y(s)$$

Continuous Focusing – adiabatic solution coefficients

a) $\delta r_+ = (\delta r_x + \delta r_y)/2$ Breathing Mode Projection



b) $\delta r_- = (\delta r_x - \delta r_y)/2$ Quadrupole Mode Projection



Relative strength of:

- ◆ Space-Charge (Perveance)
- ◆ Applied Focusing
- ◆ Emittance

terms vary with space-charge depression (σ/σ_0) for both breathing and quadrupole mode projections

Plots allow one to read off the relative importance of various contributions to beam mismatch as a function of space-charge strength

Continuous Focusing – sudden particular solution

For sudden, step function driving perturbations of form:

$$\delta p_{\pm}(s) = \widehat{\delta p}_{\pm} \Theta(s - s_p)$$

$s = s_p$ = axial coordinate
perturbation applied

Hat quantities
are constant
amplitudes

with amplitudes:

$$\widehat{\delta p}_+ = -\frac{\sigma_0^2}{2} \left[\frac{\widehat{\delta \kappa}_x}{k_{\beta 0}^2} + \frac{\widehat{\delta \kappa}_y}{k_{\beta 0}^2} \right] + (\sigma_0^2 - \sigma^2) \frac{\widehat{\delta Q}}{Q} + \sigma^2 \left[\frac{\widehat{\delta \varepsilon}_x}{\varepsilon} + \frac{\widehat{\delta \varepsilon}_y}{\varepsilon} \right] = \text{const}$$

$$\widehat{\delta p}_- = -\frac{\sigma_0^2}{2} \left[\frac{\widehat{\delta \kappa}_x}{k_{\beta 0}^2} - \frac{\widehat{\delta \kappa}_y}{k_{\beta 0}^2} \right] + \sigma^2 \left[\frac{\widehat{\delta \varepsilon}_x}{\varepsilon} - \frac{\widehat{\delta \varepsilon}_y}{\varepsilon} \right] = \text{const}$$

The solution is given by the substitution in the expression for the adiabatic solution:

- Manipulate Green's function solution to show (similar to Adiabatic case steps)

$$\frac{\delta r_{\pm}(s)}{r_m} = \frac{\delta p_{\pm}(s)}{\sigma_{\pm}^2}$$

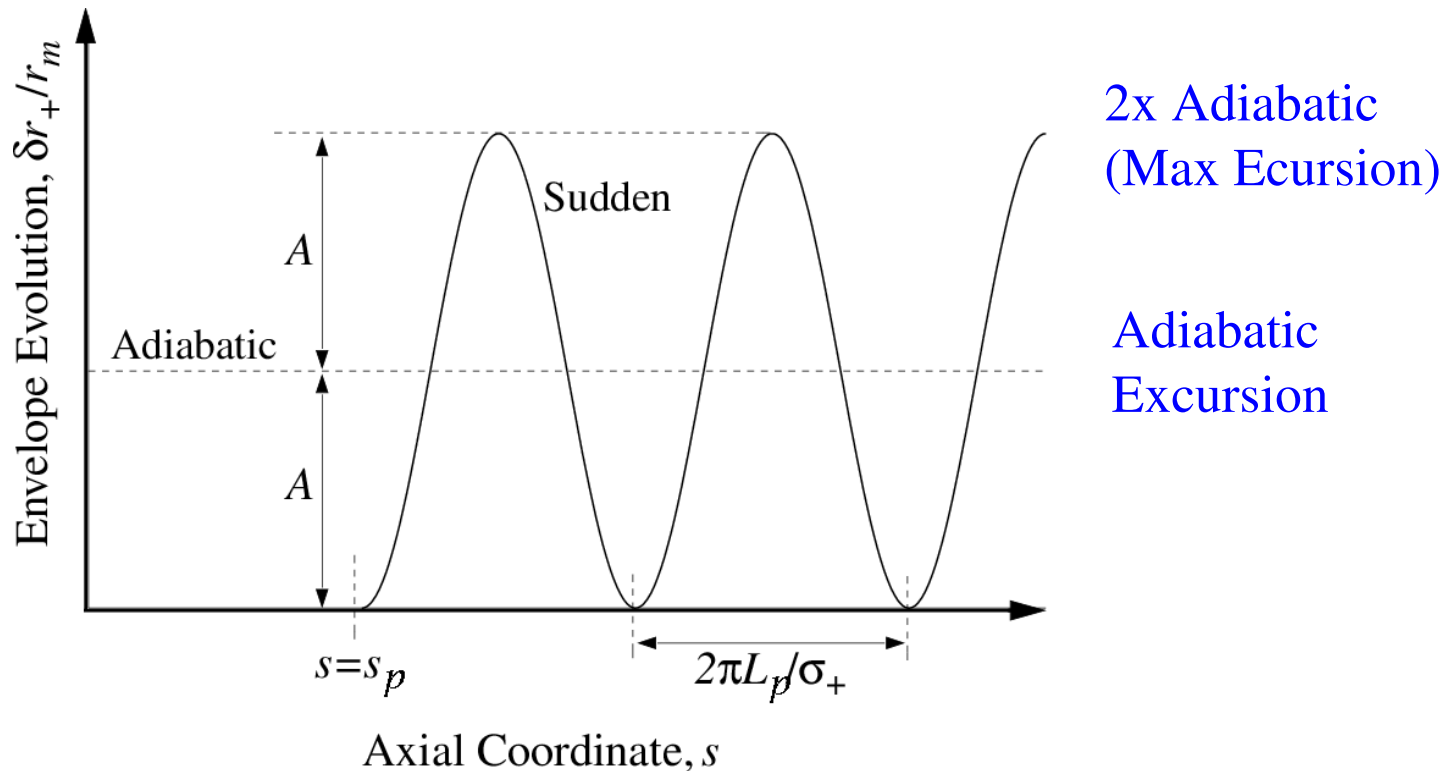
with

$$\delta p_{\pm}(s) \rightarrow \widehat{\delta p}_{\pm} \left[1 - \cos \left(\sigma_{\pm} \frac{s - s_p}{L_p} \right) \right] \Theta(s - s_p)$$

Sudden perturbation solution, substitute in previous adiabatic expressions:

$$\frac{\delta r_{\pm}(s)}{r_m} = \widehat{\delta p_{\pm}} \left[1 - \cos \left(\sigma_{\pm} \frac{s - s_p}{L_p} \right) \right] \Theta(s - s_p)$$

Illustration of solution properties for a sudden $\delta p_+(s)$ perturbation term



For the same amplitude of total driving perturbations, sudden perturbations result in 2x the envelope excursion that adiabatic perturbations produce

Continuous Focusing – Driven perturbations on a continuously focused matched equilibrium (summary)

Adiabatic Perturbations:

- ◆ Essentially a rematch of equilibrium beam if the change is slow relative to quadrupole envelope mode oscillations

Sudden Perturbations:

- ◆ Projects onto breathing and quadrupole envelope modes with 2x adiabatic amplitude oscillating from zero to max amplitude

Ramped Perturbations: (see PRSTAB article; based on Green's function)

- ◆ Can be viewed as a superposition between the adiabatic and sudden form perturbations

Harmonic Perturbations: (see PRSTAB article; based on Green's function)

- ◆ Can build very general cases of driven perturbations by linear superposition
- ◆ Results may be less “intuitive” (expressed in complex form)

Cases covered in class illustrate a range of common behavior and help build intuition on what can drive envelope oscillations and the relative importance of various terms as a function of space-charge strength

Appendix A: Particular Solution for Driven Envelope Modes

Lund and Bukh, PRSTAB 7, 024801 (2004)

Following Wiedemann (Particle Accelerator Physics, 1993, pp 106) first, consider more general *Driven Hill's Equation*

$$x'' + \kappa(s)x = p(s)$$

The corresponding homogeneous equation:

$$x'' + \kappa(s)x = 0$$

has principal solutions

$$x(s) = C_1\mathcal{C}(s) + C_2\mathcal{S}(s) \quad C_1, C_2 = \text{constants}$$

where

[Cosine-Like Solution](#)

$$\mathcal{C}'' + \kappa(s)\mathcal{C} = 0$$

$$\mathcal{C}(s = s_i) = 1$$

$$\mathcal{C}'(s = s_i) = 0$$

[Sine-Like Solution](#)

$$\mathcal{S}'' + \kappa(s)\mathcal{S} = 0$$

$$\mathcal{S}(s = s_i) = 0$$

$$\mathcal{S}'(s = s_i) = 1$$

Recall that the homogeneous solutions have the Wronskian symmetry:

- ◆ See S.M. Lund lectures on [Transverse Dynamics, S5C](#)

$$W(s) = \mathcal{C}(s)\mathcal{S}'(s) - \mathcal{C}'(s)\mathcal{S}(s) = 1$$

A particular solution to the *Driven Hill's Equation* can be constructed using a Greens' function method:

$$x(s) = \int_{s_i}^s d\tilde{s} G(s, \tilde{s}) p(\tilde{s})$$

$$G(s, \tilde{s}) = \mathcal{S}(s)\mathcal{C}(\tilde{s}) - \mathcal{C}(s)\mathcal{S}(\tilde{s})$$

Demonstrate this works by first taking derivatives:

$$x = \mathcal{S}(s) \int_{s_i}^s d\tilde{s} \mathcal{C}(\tilde{s}) p(\tilde{s}) - \mathcal{C}(s) \int_{s_i}^s d\tilde{s} \mathcal{S}(\tilde{s}) p(\tilde{s})$$

$$\begin{aligned} x' &= \mathcal{S}'(s) \int_{s_i}^s d\tilde{s} \mathcal{C}(\tilde{s}) p(\tilde{s}) - \mathcal{C}'(s) \int_{s_i}^s d\tilde{s} \mathcal{S}(\tilde{s}) p(\tilde{s}) \\ &\quad + p(s) [\mathcal{S}(s)\mathcal{C}(s) \cancel{-} \mathcal{S}(s)\mathcal{C}(s)] \end{aligned}$$

$$= \mathcal{S}'(s) \int_{s_i}^s d\tilde{s} \mathcal{C}(\tilde{s}) p(\tilde{s}) - \mathcal{C}'(s) \int_{s_i}^s d\tilde{s} \mathcal{S}(\tilde{s}) p(\tilde{s})$$

$$\begin{aligned} x'' &= \mathcal{S}''(s) \int_{s_i}^s d\tilde{s} \mathcal{C}(\tilde{s}) p(\tilde{s}) - \mathcal{C}''(s) \int_{s_i}^s d\tilde{s} \mathcal{S}(\tilde{s}) p(\tilde{s}) \\ &\quad + p(s) [\mathcal{S}'(s)\mathcal{C}(s) \cancel{-} \mathcal{C}'(s)\mathcal{S}(s)] \quad \text{Wronskian Symmetry} \end{aligned}$$

$$= p(s) + \mathcal{S}''(s) \int_{s_i}^s d\tilde{s} \mathcal{C}(\tilde{s}) p(\tilde{s}) - \mathcal{C}''(s) \int_{s_i}^s d\tilde{s} \mathcal{S}(\tilde{s}) p(\tilde{s})$$

Apply these results in the *Driven Hill's Equation*:

Definition of Principal Orbit Functions

$$\begin{aligned}
 x'' + \kappa(s)x &= p(s) + [\mathcal{S}'' + \kappa\mathcal{S}] \int_{s_i}^s d\tilde{s} \mathcal{C}(\tilde{s})p(\tilde{s}) - [\mathcal{C}'' + \kappa\mathcal{C}] \int_{s_i}^s d\tilde{s} \mathcal{S}(\tilde{s})p(\tilde{s}) \\
 &= p(s)
 \end{aligned}$$

Thereby proving we have a valid particular solution. The general solution to the *Driven Hill's Equation* is then:

- Choose constants C_1, C_2 consistent with particle initial conditions at $s = s_i$

$$x(s) = x(s_i)\mathcal{C}(s) + x'(s_i)\mathcal{S}(s) + \int_{s_i}^s d\tilde{s} G(s, \tilde{s})p(\tilde{s})$$

$$G(s, \tilde{s}) = \mathcal{S}(s)\mathcal{C}(\tilde{s}) - \mathcal{C}(s)\mathcal{S}(\tilde{s})$$

Apply these results to the driven perturbed envelope equation:

$$\frac{d^2}{ds^2} \delta r_{\pm} + \frac{\sigma_{\pm}^2}{L_p^2} \delta r_{\pm} = \frac{r_m}{L_p^2} \delta p_{\pm}$$

The homogeneous equations can be solved exactly for continuous focusing:

$$\mathcal{C}(s) = \cos\left(\sigma_{\pm} \frac{s - s_i}{L_p}\right)$$

$$\mathcal{S}(s) = \frac{L_p}{\sigma_{\pm}} \sin\left(\sigma_{\pm} \frac{s - s_i}{L_p}\right)$$

and the Green's function can be simplified as:

$$\begin{aligned} G(s, \tilde{s}) &= \mathcal{S}(s)\mathcal{C}(\tilde{s}) - \mathcal{C}(s)\mathcal{S}(\tilde{s}) \\ &= \frac{L_p}{\sigma_{\pm}} \left\{ \sin\left(\sigma_{\pm} \frac{s - s_i}{L_p}\right) \cos\left(\sigma_{\pm} \frac{\tilde{s} - s_i}{L_p}\right) - \cos\left(\sigma_{\pm} \frac{s - s_i}{L_p}\right) \sin\left(\sigma_{\pm} \frac{\tilde{s} - s_i}{L_p}\right) \right\} \\ &= \frac{L_p}{\sigma_{\pm}} \sin\left(\sigma_{\pm} \frac{s - \tilde{s}}{L_p}\right) \end{aligned}$$

Using these results the **particular solution for the driven perturbed envelope equation** can be expressed as:

- Here we rescale the Green's function to put in the form given in S8

$$\frac{\delta r_{\pm}(s)}{r_m} = \frac{1}{L_p^2} \int_{s_i}^s d\tilde{s} G_{\pm}(s, \tilde{s}) \delta p_{\pm}(\tilde{s})$$

$$G_{\pm}(s, \tilde{s}) = \frac{1}{\sigma_{\pm}/L_p} \sin\left(\sigma_{\pm} \frac{s - \tilde{s}}{L_p}\right)$$

S8: Envelope Modes in Periodic Focusing Channels

Lund and Bukh, PRSTAB 7, 024801 (2004)

Overview

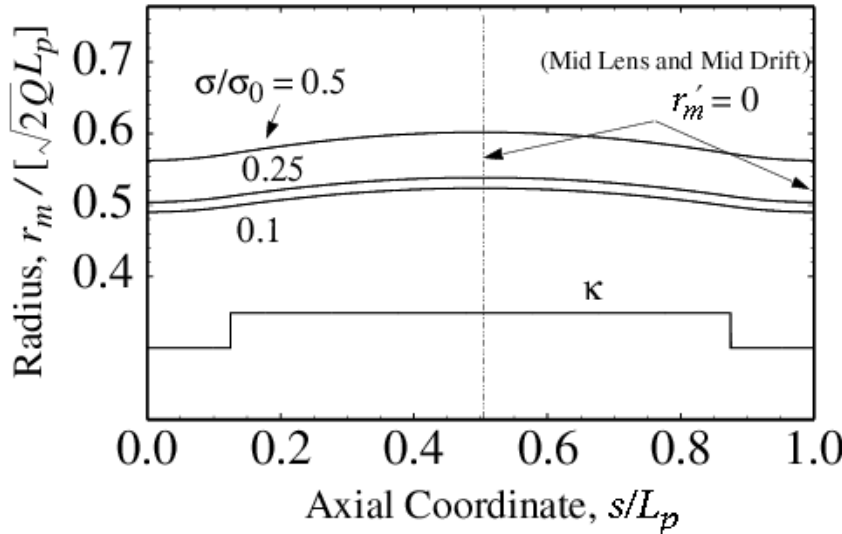
- ◆ Much more complicated than continuous focusing results
 - Lattice can couple to oscillations and destabilize the system
 - Broad **parametric instability** bands can result
- ◆ Instability bands calculated will exclude wide ranges of parameter space from machine operation
 - Exclusion region depends on focusing type
 - Will find that alternating gradient quadrupole focusing tends to have more instability than high occupancy solenoidal focusing due to larger envelope flutter driving stronger, broader instability
- ◆ Results in this section are calculated numerically and summarized parametrically to illustrate the full range of normal mode characteristics
 - Driven modes not considered but should be mostly analogous to CF case
 - Results presented in terms of phase advances and normalized space-charge strength to allow broad applicability
 - Coupled 4x4 eigenvalue problem and mode symmetries identified in **S6** are solved numerically and analytical limits are verified
 - Carried out for piecewise constant lattices for simplicity (fringe changes little)
- ◆ More information on results presented can be found in the PRSTAB review

Procedure

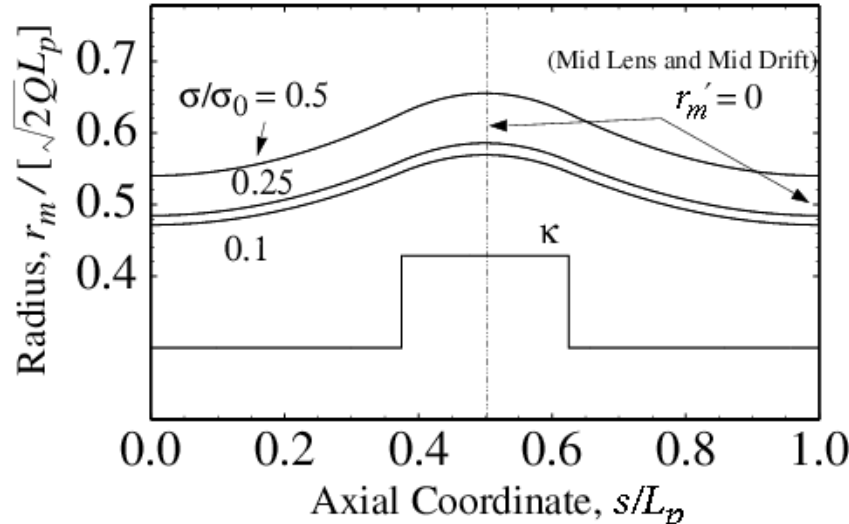
- 1) Specify periodic lattice to be employed and beam parameters
- 2) Calculate undepressed phase advance σ_0 and characterize focusing strength in terms of σ_0
- 3) Find matched envelope solution to the KV envelope equation and depressed phase advance σ to estimate space-charge strength
 - ◆ Procedures described in: Lund, Chilton and Lee, PRSTAB **9**, 064201 (2006)
can be applied to greatly simplify analysis, particularly where lattice is unstable
 - Instabilities complicate calculation of matching conditions
- 4) Calculate 4x4 envelope perturbation transfer matrix $\mathbf{M}_e(s_i + L_p | s_i)$ through one lattice period and calculate 4 eigenvalues
- 5) Analyze eigenvalues using symmetries to characterize mode properties
 - ◆ Instabilities
 - ◆ Stable mode characteristics and launching conditions

Solenoidal Focusing – Matched Envelope Solution

a) $\sigma_\theta = 80^\circ$ and $\eta = 0.75$ High Occupancy



b) $\sigma_\theta = 80^\circ$ and $\eta = 0.25$ Low Occupancy



Focusing:

$$\kappa_x(s) = \kappa_y(s) = \kappa(s)$$

$$\kappa(s + L_p) = \kappa(s)$$

Matched Beam:

$$\varepsilon_x = \varepsilon_y = \varepsilon = \text{const}$$

$$r_{xm}(s) = r_{ym}(s) = r_m(s)$$

$$r_m(s + L_p) = r_m(s)$$

Comments:

- ◆ Envelope flutter a strong function of occupancy η
 - Flutter also increases with higher values of σ_0
- ◆ Space-charge expands envelope but does not strongly modify periodic flutter

Envelope Flutter Scaling of Matched Envelope Solution

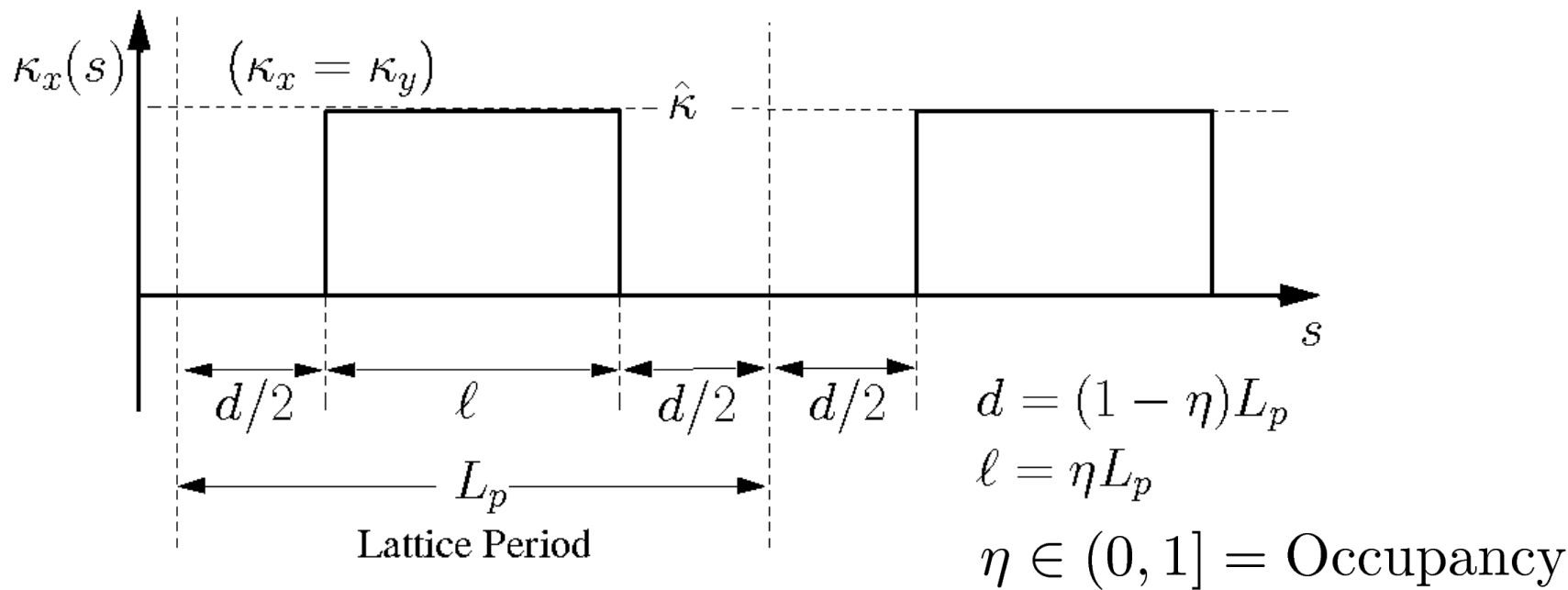
Add material explaining scaling better in future editions

Using a transfer matrix approach on undepressed single-particle orbits set the strength of the focusing function for specified undepressed particle phase advance by solving:

- ◆ See: S.M. Lund, lectures on **Transverse Particle Dynamics**
- ◆ Particle phase-advance is measured in the rotating Larmor frame

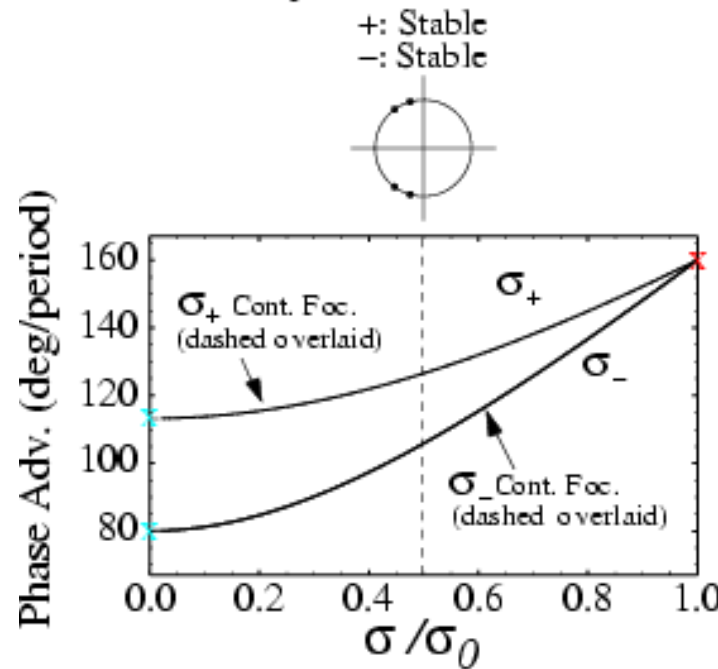
Solenoidal Focusing - piecewise constant focusing lattice

$$\cos \sigma_0 = \cos(2\Theta) - \frac{1 - \eta}{\eta} \Theta \sin(2\Theta) \quad \Theta \equiv \frac{\sqrt{\hat{\kappa}} L_p}{2}$$

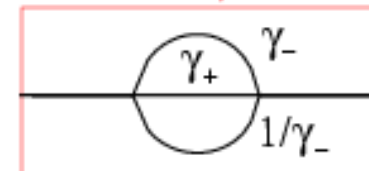
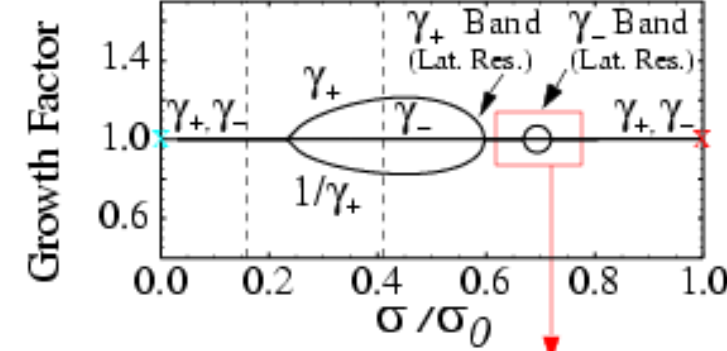
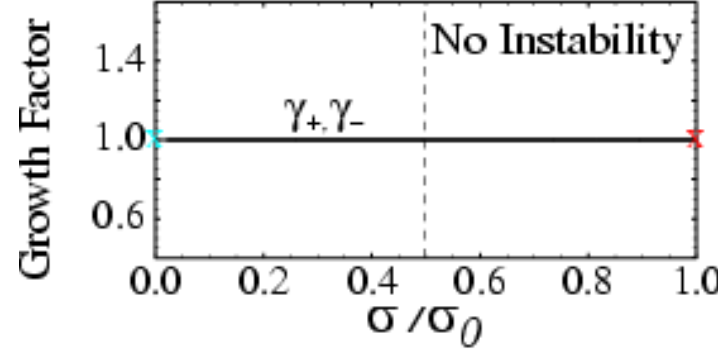
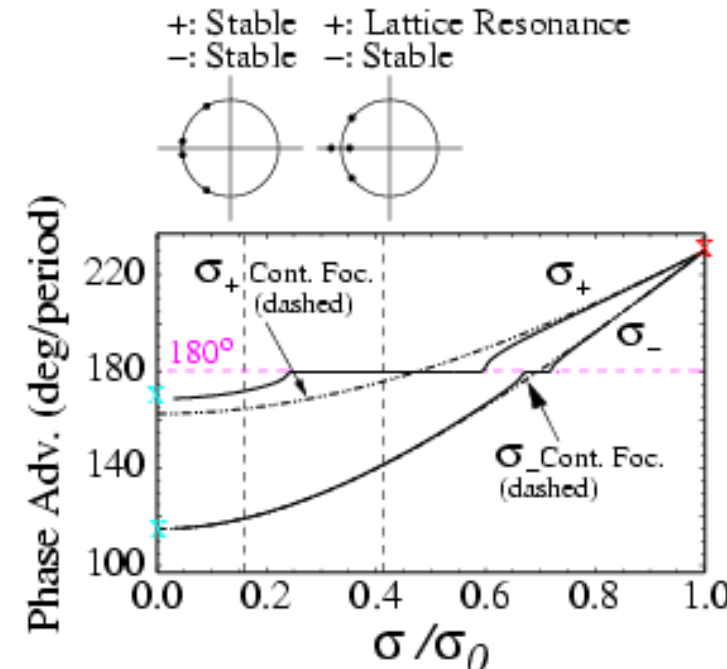


Solenoidal Focusing – parametric plots of breathing and quadrupole envelope mode phase advances two values of undepressed phase advance

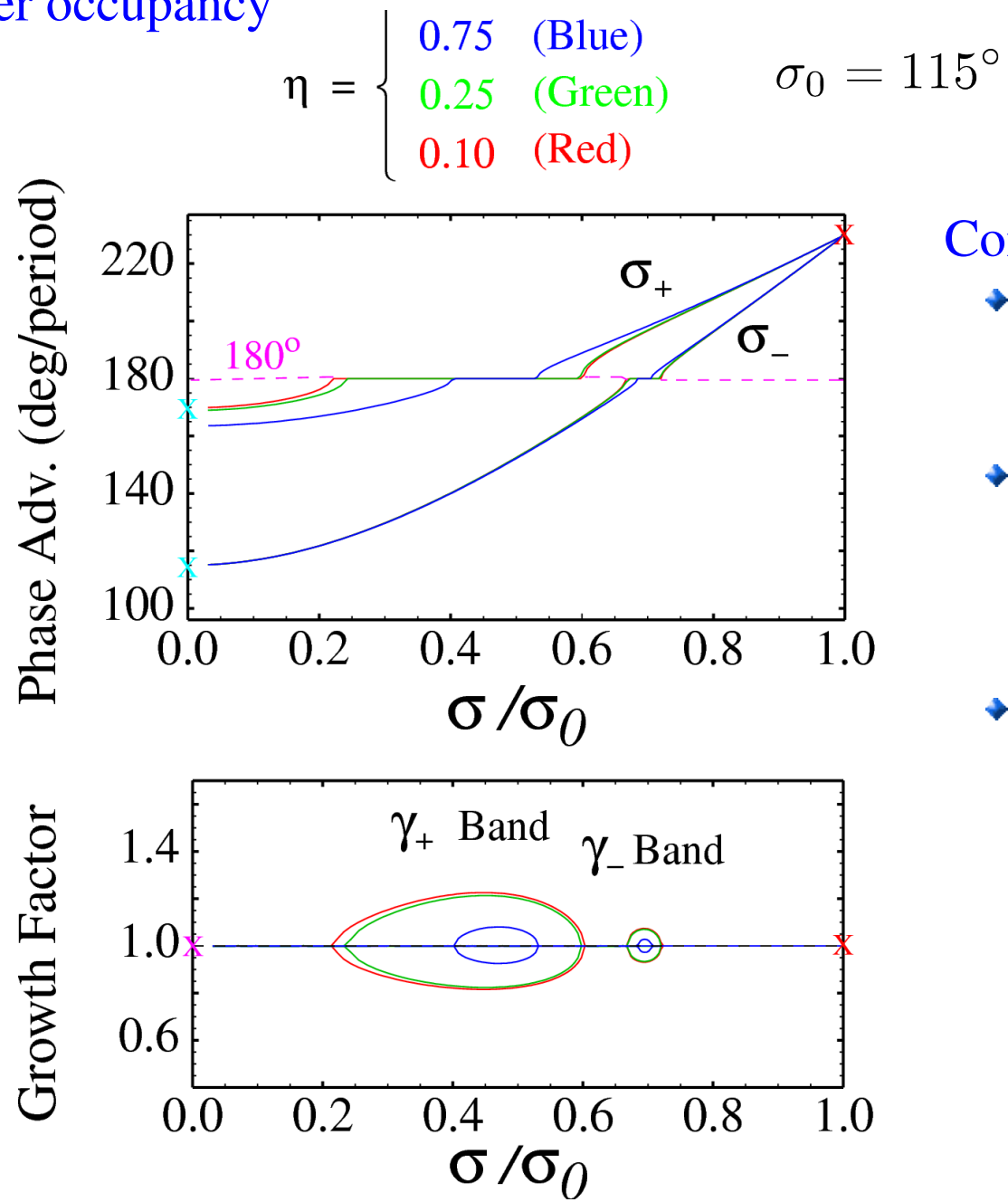
a) $\eta = 0.25, \sigma_0 = 80^\circ$



b) $\eta = 0.25, \sigma_0 = 115^\circ$



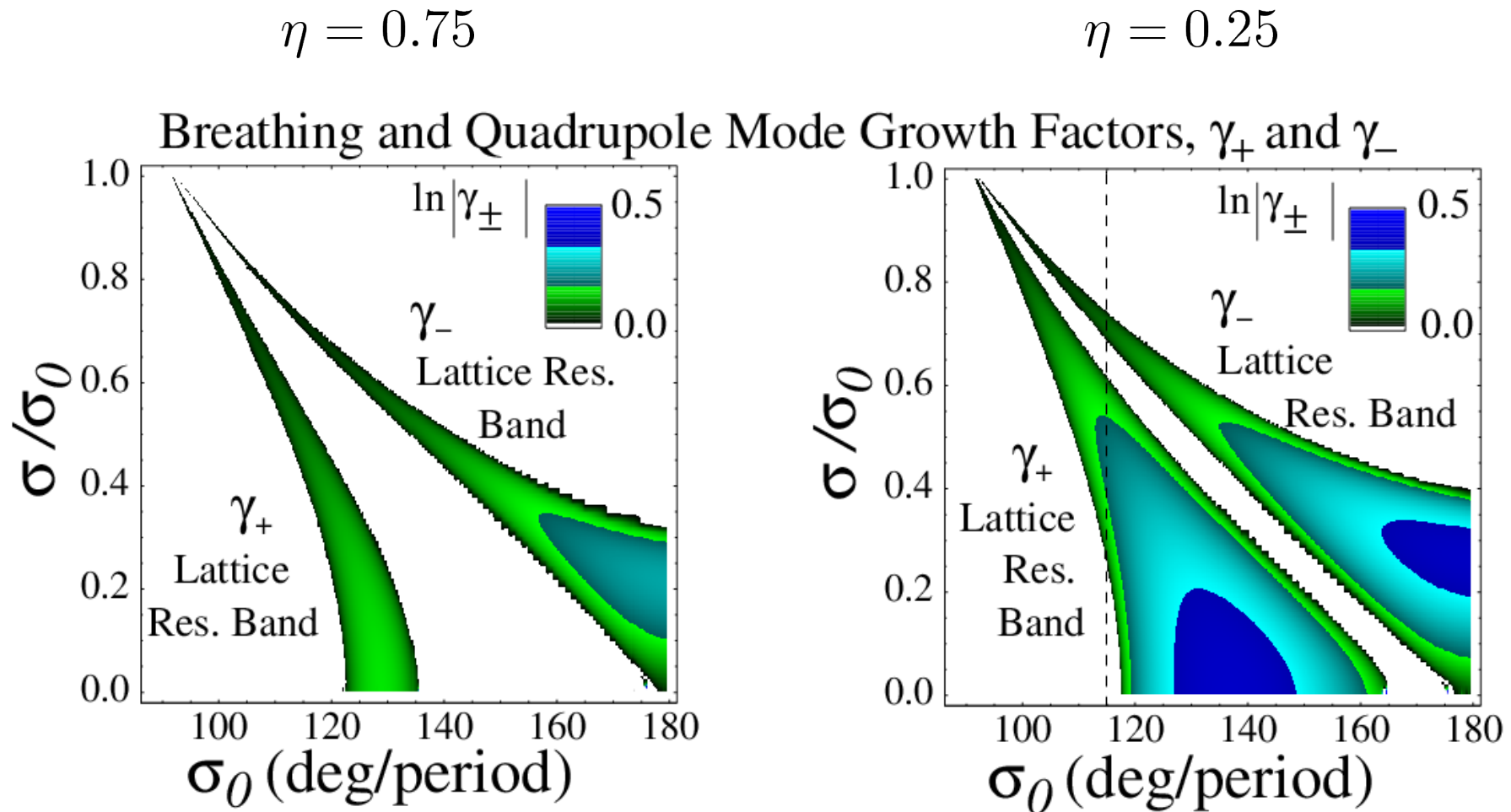
Solenoidal Focusing – mode instability bands become wider and stronger for smaller occupancy



Comments:

- ◆ Mode phase advance in instability band 180 degrees per lattice period
- ◆ Significant deviations from continuous model even outside the band of instability when space-charge is strong
- ◆ Instability band becomes stronger/broader for low occupancy and weaker/narrower for high occupancy
 - Disappears at full occupancy (continuous limit)

Solenoidal Focusing – broad ranges of parametric instability are found for the breathing and quadrupole bands that must be avoided in machine operation:
 Contour unstable parameters for breathing and quadrupole modes to clarify



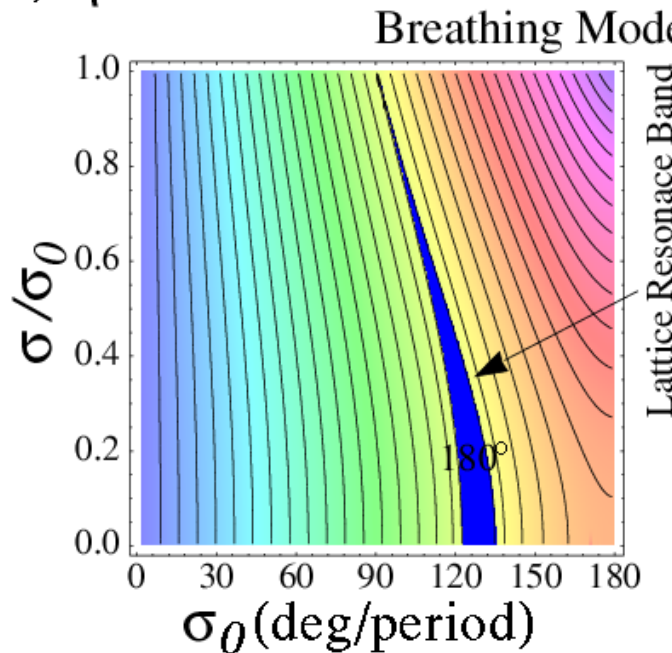
Eigenvalues in unstable regions:

$$\lambda_{\pm} = \gamma_{\pm} e^{i\pi}$$

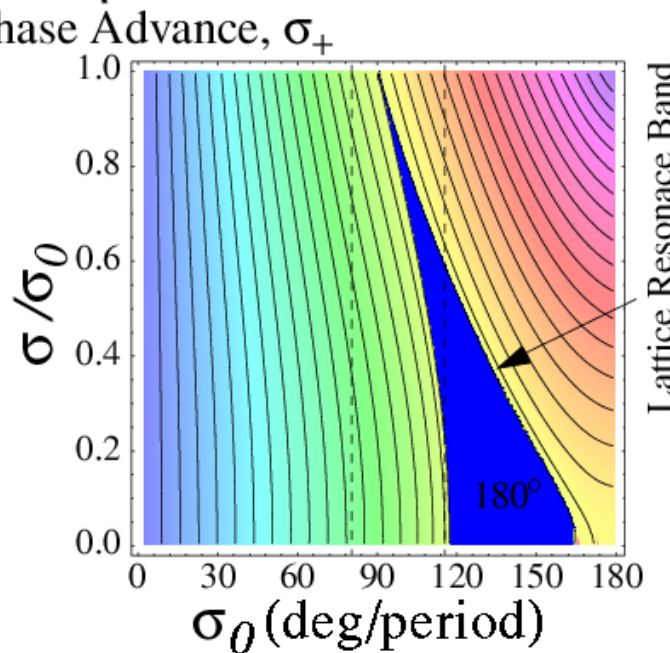
$\gamma_{\pm} > 1$ for unstable growing mode
 $\ln \gamma_{\pm}$ = *e*-folds of growth per period

Solenoidal Focusing – parametric mode properties of band oscillations

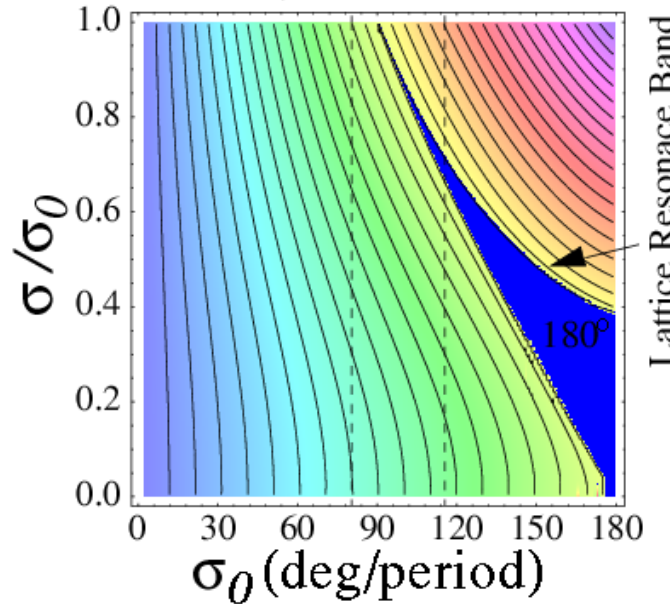
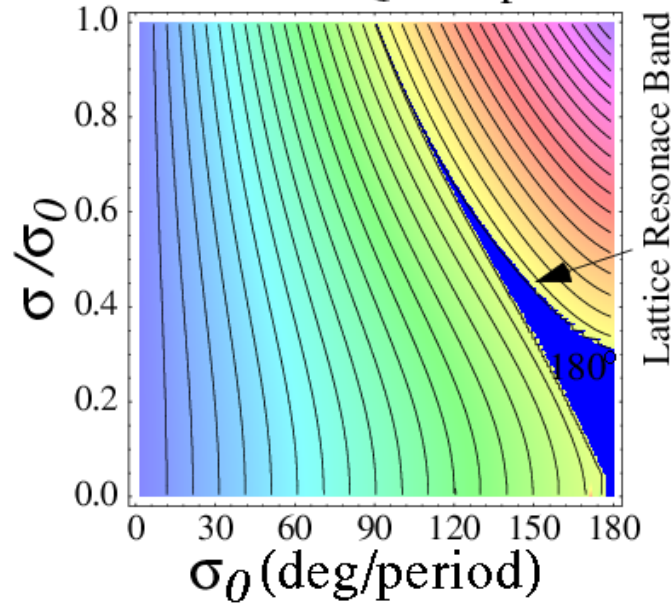
a) $\eta = 0.75$



b) $\eta = 0.25$



Quadrupole Mode Phase Advance, σ_-



Parametric scaling of the boundary of the region of instability

Solenoid instability bands identified as a [Lattice Resonance Instability](#) corresponding to a 1/2-integer parametric resonance between the mode oscillation frequency and the lattice

Estimate normal mode frequencies for weak focusing from continuous focusing theory:

$$\sigma_+ \simeq \sqrt{2\sigma_0^2 + 2\sigma^2}$$

$$\sigma_- \simeq \sqrt{\sigma_0^2 + 3\sigma^2}$$

This gives (measure phase advance in degrees):

Breathing Band:

$$\sigma_+ = 180^\circ$$

$$\Rightarrow \sqrt{2\sigma_0^2 + 2\sigma^2} = 180^\circ$$

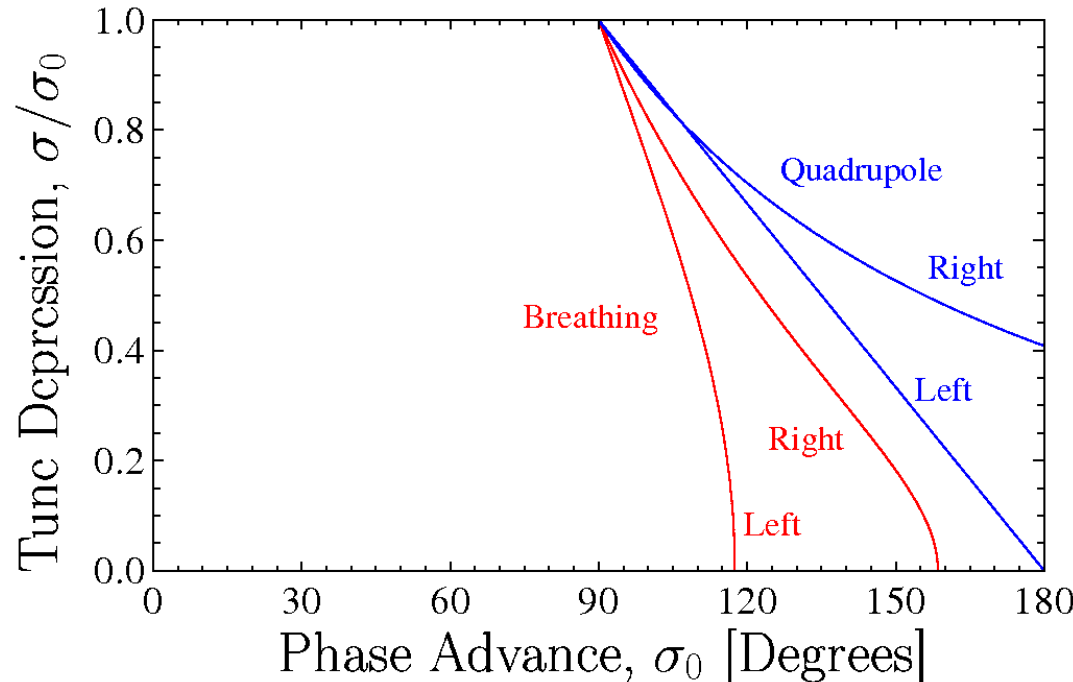
Quadrupole Band:

$$\sigma_- = 180^\circ$$

$$\Rightarrow \sqrt{\sigma_0^2 + 3\sigma^2} = 180^\circ$$

- ◆ Predictions poor due to inaccurate mode frequency estimates
 - Predictions nearer to left edge of band rather than center (expect resonance strongest at center)
- ◆ Simple resonance condition cannot predict width of band
 - Important to characterize width to avoid instability in machine designs
 - Width of band should vary strongly with solenoid occupancy η

To provide an approximate guide on the location/width of the breathing and quadrupole envelope bands, many parametric runs were made and the instability band boundaries were quantified through curve fitting:



Breathing Band Boundaries:

$$\sigma^2 + f\sigma_0^2 = (90^\circ)^2(1 + f)$$

$$f = f(\sigma_0, \eta) =$$

$$\begin{cases} 1.113 - 0.413\eta + 0.00348\sigma_0, & \text{left-edge} \\ 1.046 + 0.318\eta - 0.00410\sigma_0, & \text{right-edge} \end{cases}$$

Quadrupole Band Boundaries:

$$\text{Left: } \sigma/\sigma_0 + g \frac{\sigma_0}{90^\circ} = 1 + g$$

$$\text{Right: } \sigma + g\sigma_0 = 90^\circ(1 + g)$$

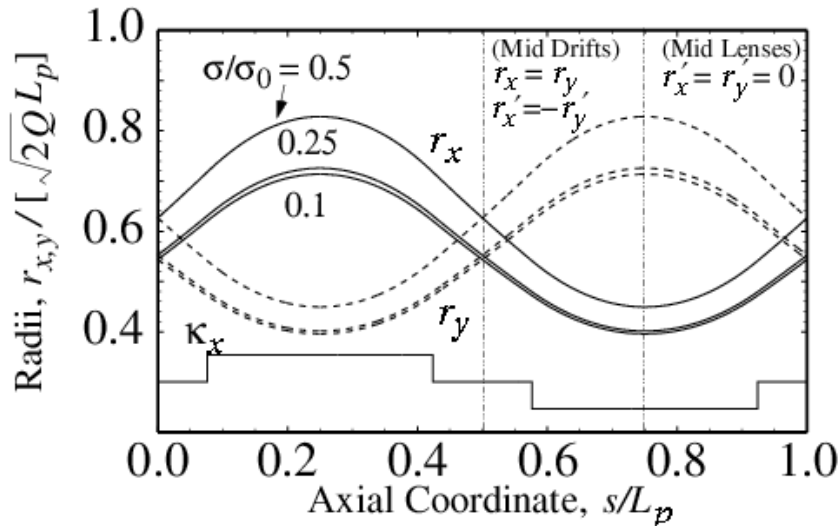
$$g = g(\eta) = \begin{cases} 1, & \text{left-edge} \\ 0.227 - 0.173\eta, & \text{right-edge} \end{cases}$$

- ◆ Breathing band: maximum errors $\sim 5 / \sim 2$ degrees on left/right boundaries
- ◆ Quadrupole band: maximum errors $\sim 8 / \sim 3$ degrees on left/right boundaries

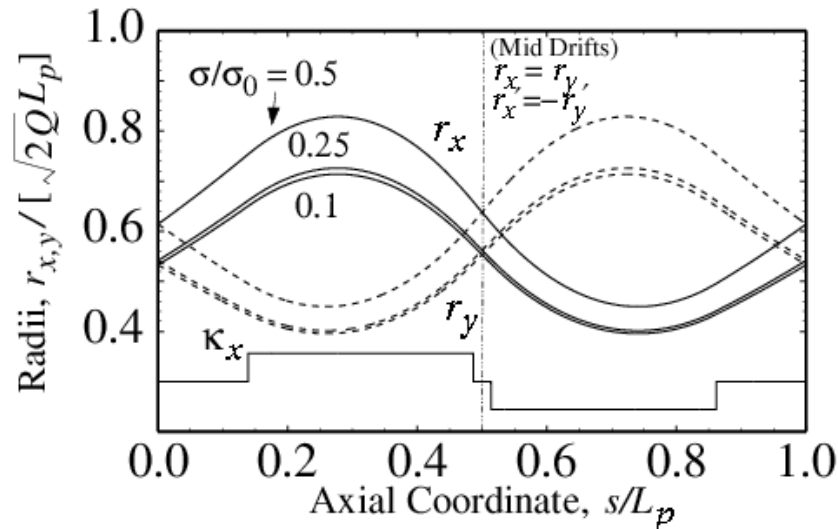
Quadrupole Doublet Focusing – Matched Envelope Solution

FODO and Syncopated Lattices

a) $\sigma_0 = 80^\circ$, $\eta = 0.6949$, and $\alpha = 1/2$ FODO



b) $\sigma_0 = 80^\circ$, $\eta = 0.6949$, and $\alpha = 0.1$ Syncopated



Focusing:

$$\kappa_x(s) = -\kappa_y(s) = \kappa(s)$$

$$\kappa(s + L_p) = \kappa(s)$$

Matched Beam:

$$\varepsilon_x = \varepsilon_y = \varepsilon = \text{const}$$

$$r_{xm}(s + L_p) = r_{xm}(s)$$

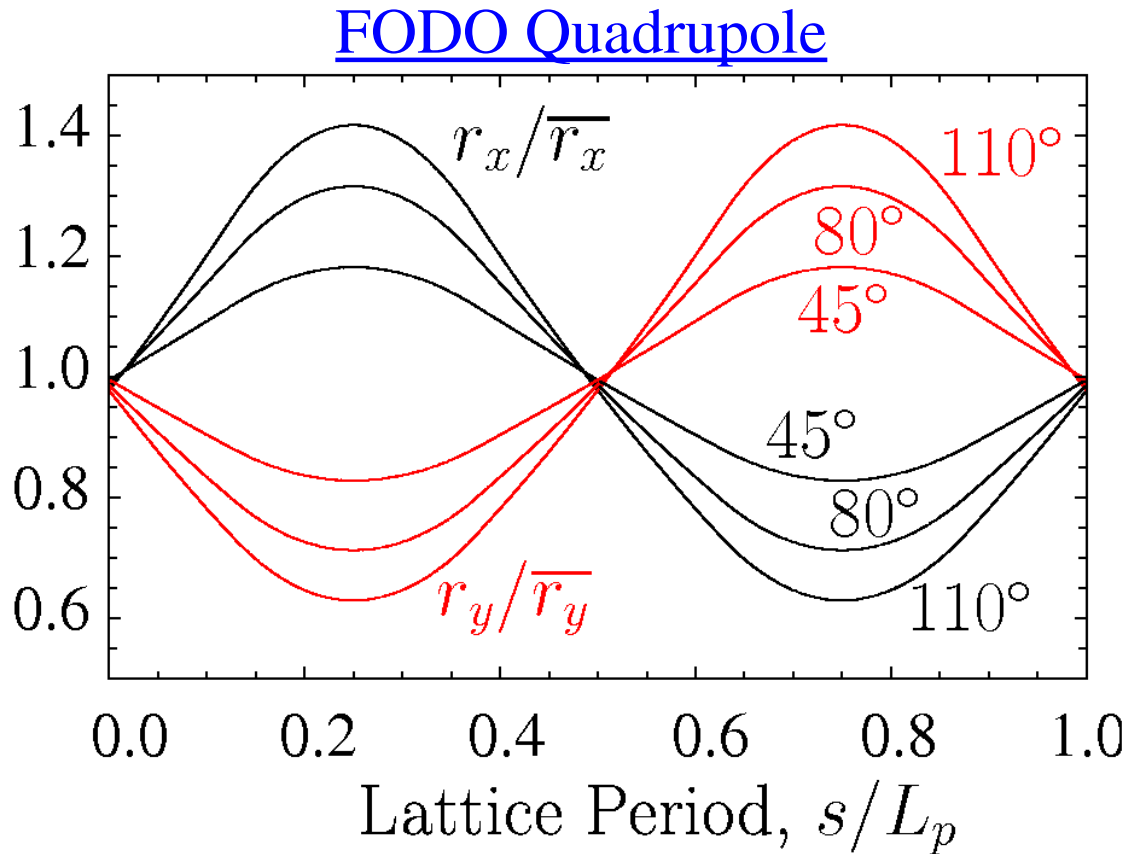
$$r_{ym}(s + L_p) = r_{ym}(s)$$

Comments:

- ◆ Envelope flutter a *weak* function of occupancy η
- ◆ Syncopation factors $\alpha \neq 1/2$ reduce envelope symmetry and can drive more instabilities
- ◆ Space-charge expands envelope

Envelope Flutter Scaling of Matched Envelope Solution

For FODO quadrupole transport, plot relative matched beam envelope excursions for a fixed form focusing lattice and fixed beam perveance as the strength of applied focusing strength increases as measured by σ_0



$$\bar{r}_x = \int_0^{L_p} \frac{ds}{L_p} r_x(s)$$
$$\eta = 0.5 \quad L_p = 0.5 \text{ m}$$
$$Q = 5 \times 10^{-4}$$
$$\varepsilon_x = \varepsilon_y = 50 \text{ mm-mrad}$$

σ_0	σ/σ_0
45°	0.20
80°	0.26
110°	0.32

- ◆ Larger matched envelope “flutter” corresponds to larger σ_0
 - More flutter results in higher prospects for instability due to transfer of energy from applied focusing
- ◆ Little dependence of flutter on quadrupole occupancy η

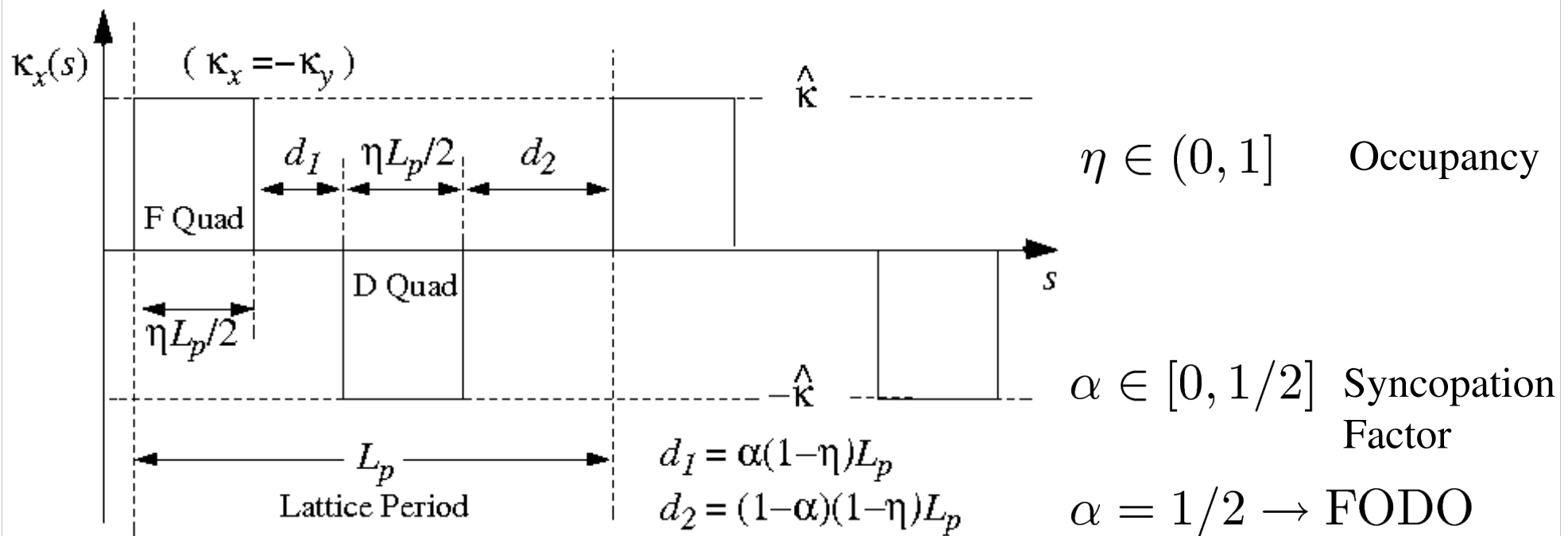
Using a transfer matrix approach on undepressed single-particle orbits set the strength of the focusing function for specified undepressed particle phase advance by solving:

- ◆ See: S.M. Lund, lectures on **Transverse Particle Dynamics**

Quadrupole Doublet Focusing - piecewise constant focusing lattice

$$\cos \sigma_0 = \cos \Theta \cosh \Theta + \frac{1-\eta}{\eta} \theta (\cos \Theta \sinh \Theta - \sin \Theta \cosh \Theta) - 2\alpha(1-\alpha) \frac{(1-\eta)^2}{\eta^2} \Theta^2 \sin \Theta \sinh \Theta$$

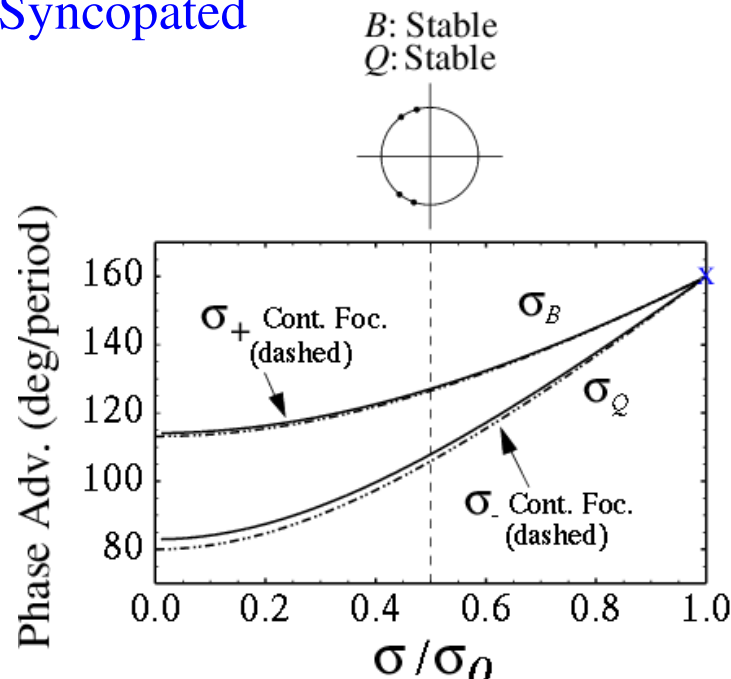
$$\Theta \equiv \frac{\sqrt{|\hat{\kappa}|} L_p}{2}$$



Quadrupole Focusing – parametric plots of breathing and quadrupole envelope mode phase advances two values of undepressed phase advance

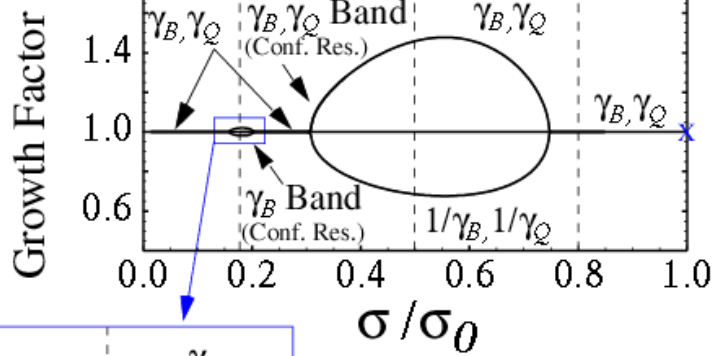
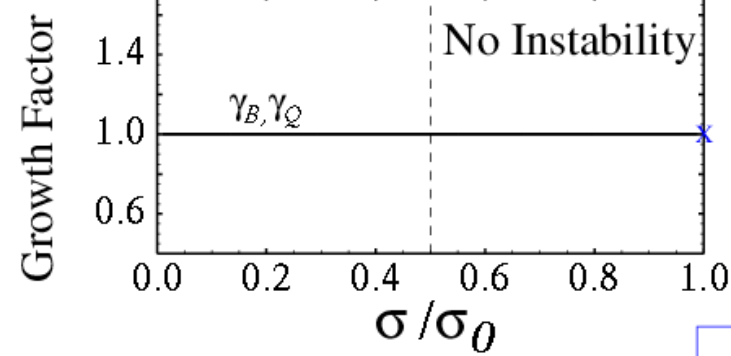
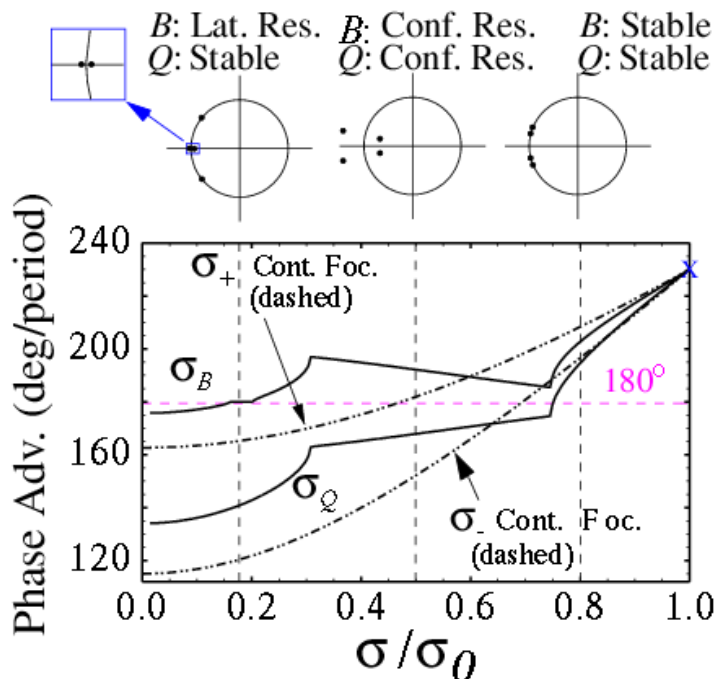
a) $\eta = 0.6949$, $\alpha = 0.1$, $\sigma_0 = 80^\circ$

Syncopated



b) $\eta = 0.6949$, $\alpha = 0.1$, $\sigma_0 = 115^\circ$

Syncopated



Important point:

For quadrupole focusing the normal mode coordinates are *NOT*

$$\delta r_{\pm} = \frac{\delta r_x \pm \delta r_y}{2} \quad \begin{aligned} \delta r_+ &\Leftrightarrow \text{Breathing Mode} \\ \delta r_- &\Leftrightarrow \text{Quadrupole Mode} \end{aligned}$$

- Only works for axisymmetric focusing ($\kappa_x = \kappa_y = \kappa$) with an axisymmetric matched beam ($\varepsilon_x = \varepsilon_y = \varepsilon$)

However, for low σ_0 we will find that the two stable modes correspond closely in frequency with continuous focusing model breathing and quadrupole modes even though they have different symmetry properties in terms of normal mode coordinates. Due to this, we denote:

$$\begin{array}{lll} \text{Subscript B} & \Leftrightarrow & \text{Breathing Mode} \\ \text{Subscript Q} & \Leftrightarrow & \text{Quadrupole Mode} \end{array}$$

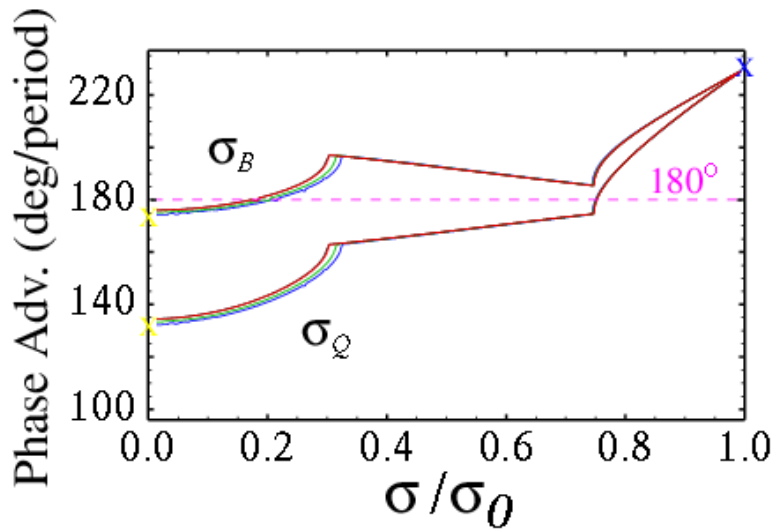
- Label branches breathing and quadrupole in terms of low σ_0 branch frequencies corresponding to breathing and quadrupole frequencies from continuous theory
- Continue label to larger values of σ_0 where frequency correspondence with continuous modes breaks down

Quadrupole Focusing – mode instability bands vary little/strongly with occupancy for FODO/syncopated lattices

a) $\alpha = 1/2$ (FODO), $\sigma_0 = 115^\circ$

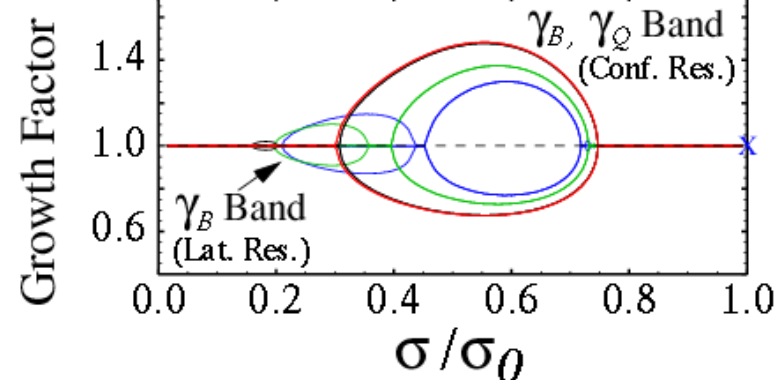
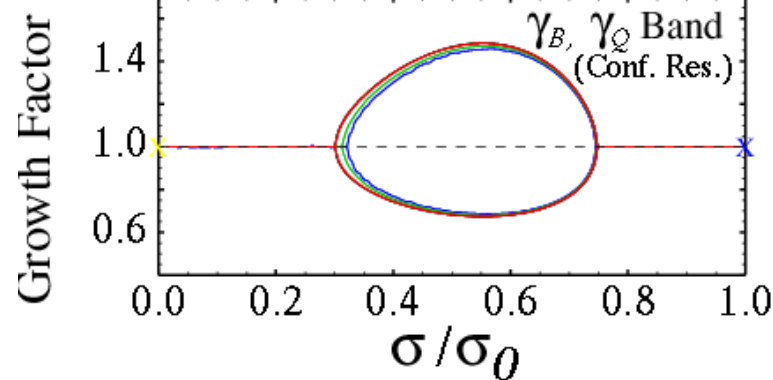
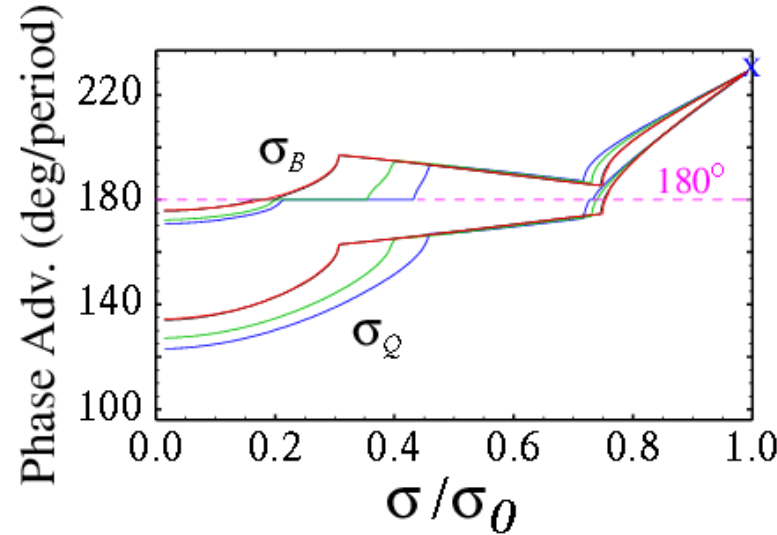
FODO

$$\eta = \begin{cases} 0.90 & \text{(Blue)} \\ 0.6949 & \text{(Black)} \\ 0.25 & \text{(Green)} \\ 0.10 & \text{(Red)} \end{cases}$$



b) $\alpha = 0.1$, $\sigma_0 = 115^\circ$

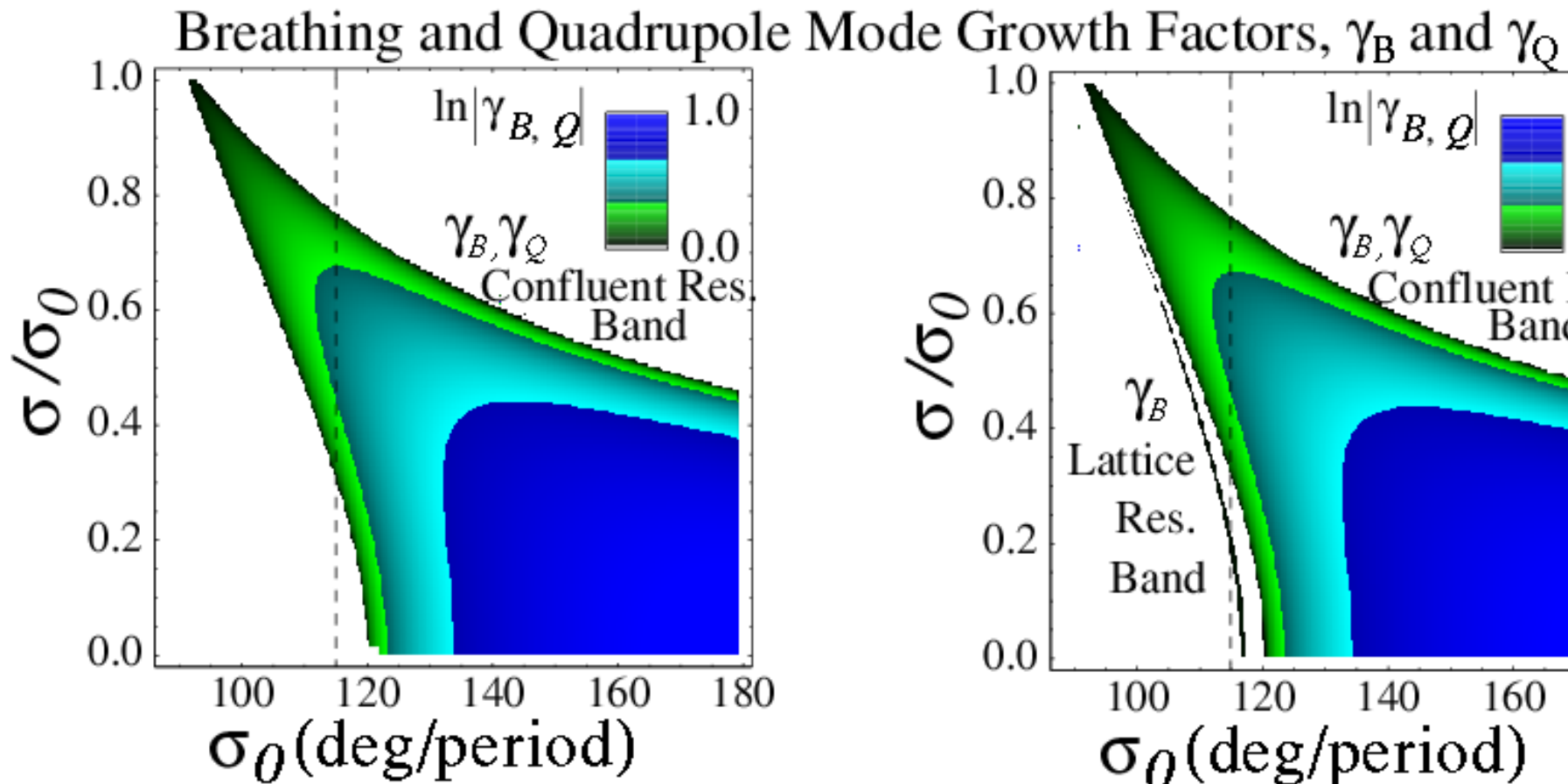
Syncopated



Quadrupole Focusing – broad ranges of parametric instability are found for the breathing and quadrupole bands that must be avoided in machine operation: Contour parameter ranges of instability to clarify

FODO Lattice

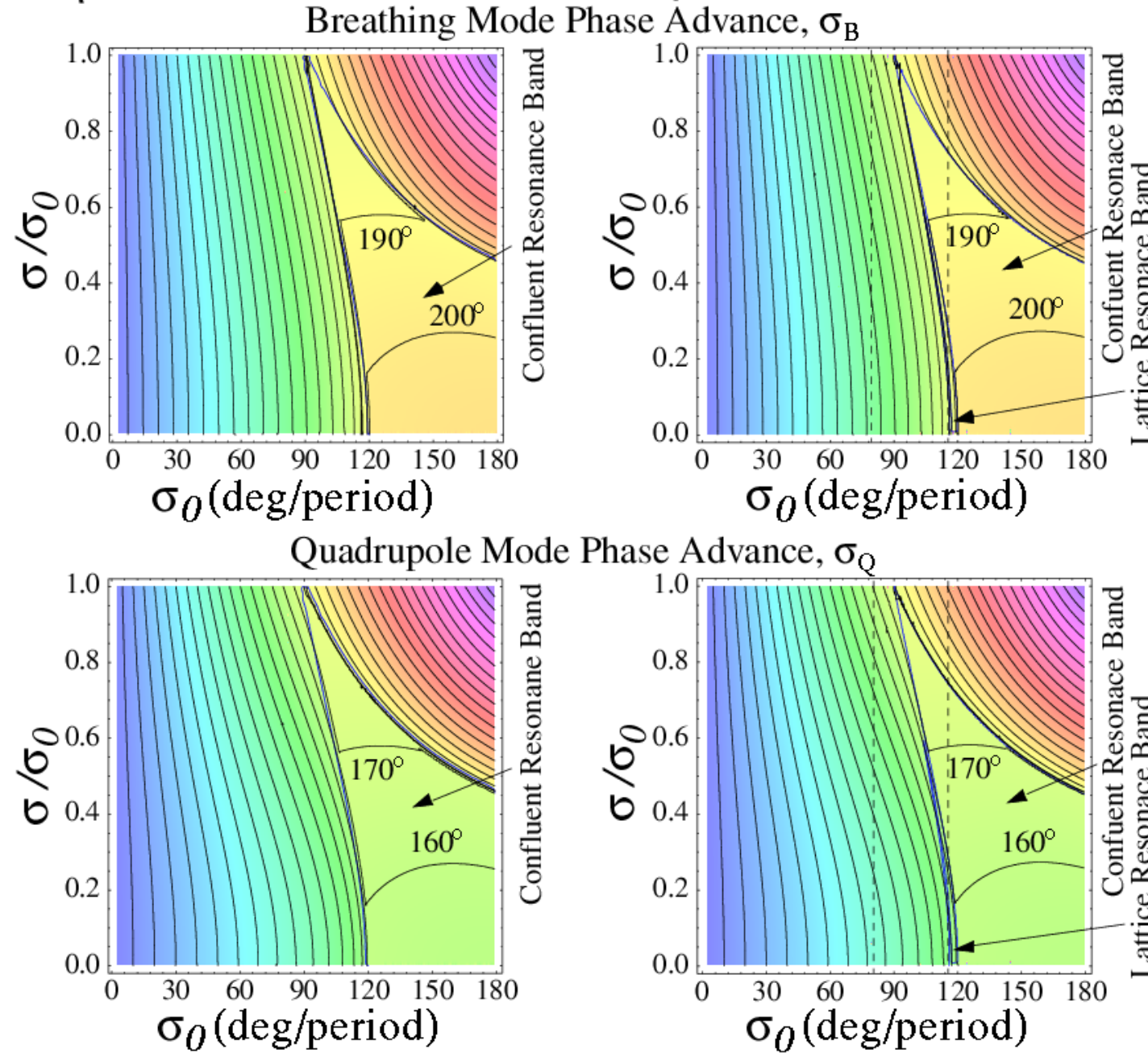
$$\eta = 0.6949, \alpha = 1/2$$



$\ln|\gamma_{B,Q}| = e$ -folds of growth per period of unstable mode

Quadrupole Focusing – parametric mode properties of band oscillations

a) $\eta = 0.6949, \alpha = 1/2$ FODO b) $\eta = 0.6949, \alpha = 0.1$ Syncopated



Parametric scaling of the boundary of the region of instability

Quadrupole instability bands identified:

- ◆ **Confluent Band**: 1/2-integer parametric resonance between *both* breathing and quadrupole modes and the lattice
- ◆ **Lattice Resonance Band** (Syncopated lattice only): 1/2-integer parametric resonance between *one* envelope mode and the lattice

Estimate mode frequencies for weak focusing from continuous focusing theory:

$$\sigma_B = \sigma_+ = \sqrt{2\sigma_0^2 + 2\sigma^2}$$

$$\sigma_Q = \sigma_- = \sqrt{\sigma_0^2 + 3\sigma^2}$$

This gives (measure phase advance in degrees):

Confluent Band:

$$(\sigma_+ + \sigma_-)/2 = 180^\circ$$

$$\Rightarrow \sqrt{2\sigma_0^2 + 2\sigma^2} + \sqrt{\sigma_0^2 + 3\sigma^2} = 360^\circ$$

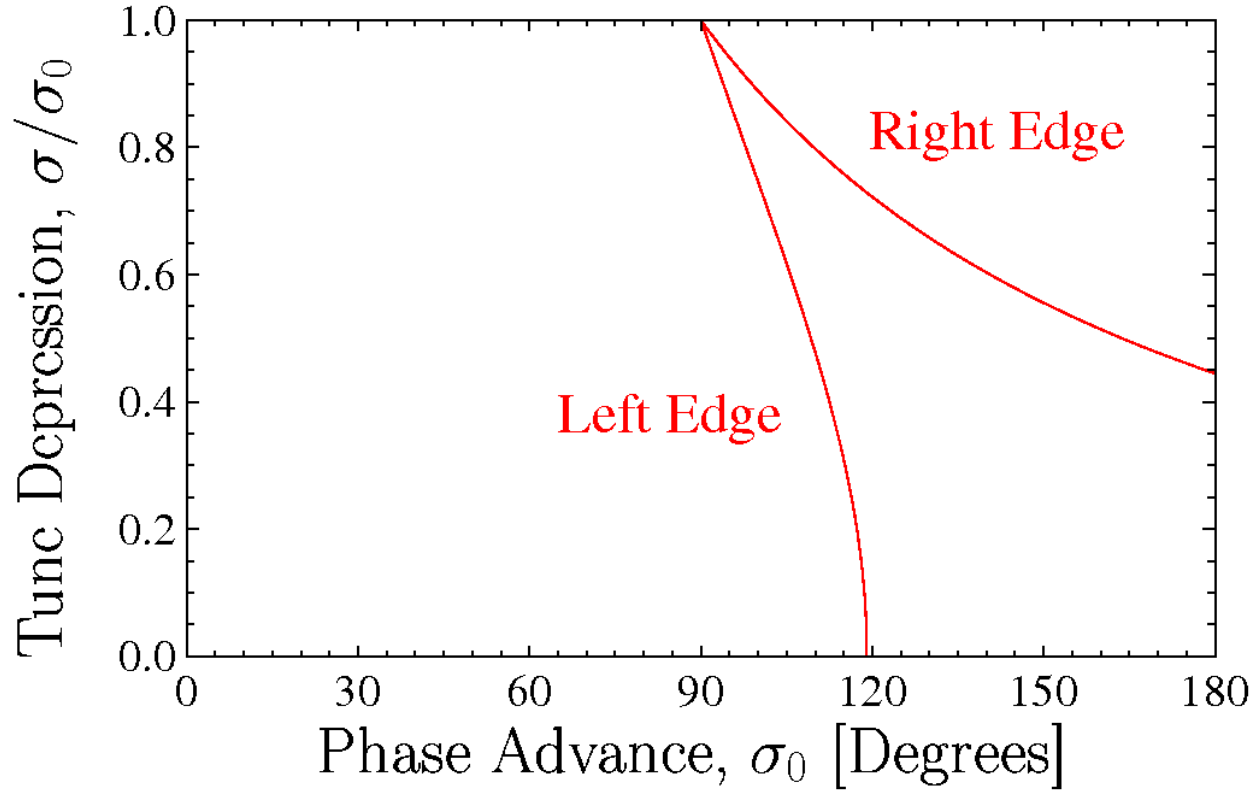
Lattice Resonance Band:

$$\sigma_+ = 180^\circ$$

$$\Rightarrow \sqrt{2\sigma_0^2 + 2\sigma^2} = 180^\circ$$

- ◆ Predictions poor due to inaccurate mode frequency estimates from continuous model
 - Predictions nearer to edge of band rather than center (expect resonance strongest at center)
- ◆ Cannot predict width of band
 - Important to characterize to avoid instability

To provide a rough guide on the location/width of the important **FODO confluent instability band**, many parametric runs were made and the instability region boundary was quantified through curve fitting:



Left Edge Boundary:

$$\sigma^2 + f(\eta)\sigma_0^2 = (90^\circ)^2[1 + f(\eta)]$$

$$f(\eta) = \frac{4}{3}$$

Right Edge Boundary:

$$\sigma + g(\eta)\sigma_0 = 90^\circ[1 + g(\eta)]$$

$$g(\eta) = \frac{1}{9}$$

- ◆ Negligible variation in quadrupole occupancy η is observed
- ◆ Formulas have a maximum error ~ 5 and ~ 2 degrees on left and right boundaries

Pure mode launching conditions for quadrupole focusing

Launching a pure breathing (B) or quadrupole (Q) mode in alternating gradient quadrupole focusing requires specific projections that generally require an eigenvalue/eigenvector analysis of symmetries to carry out

- ♦ See eigenvalue symmetries given in S6

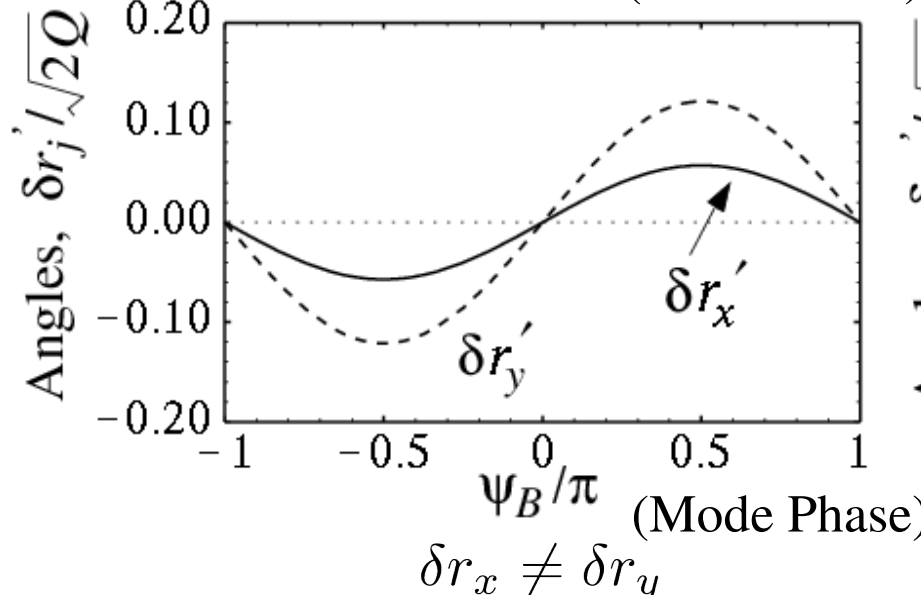
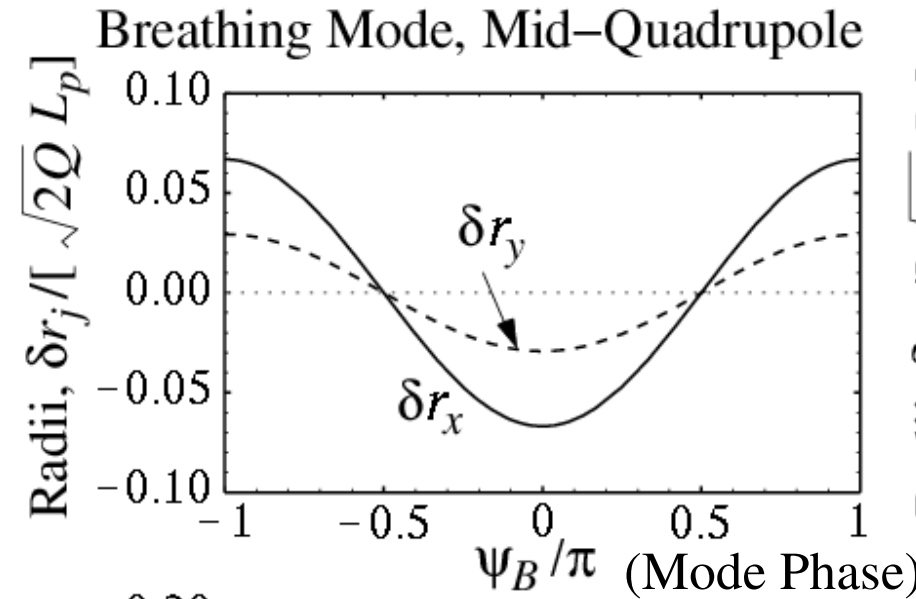
Show example launch conditions for:

$$\text{FODO Lattice} \quad \eta = 0.6949$$

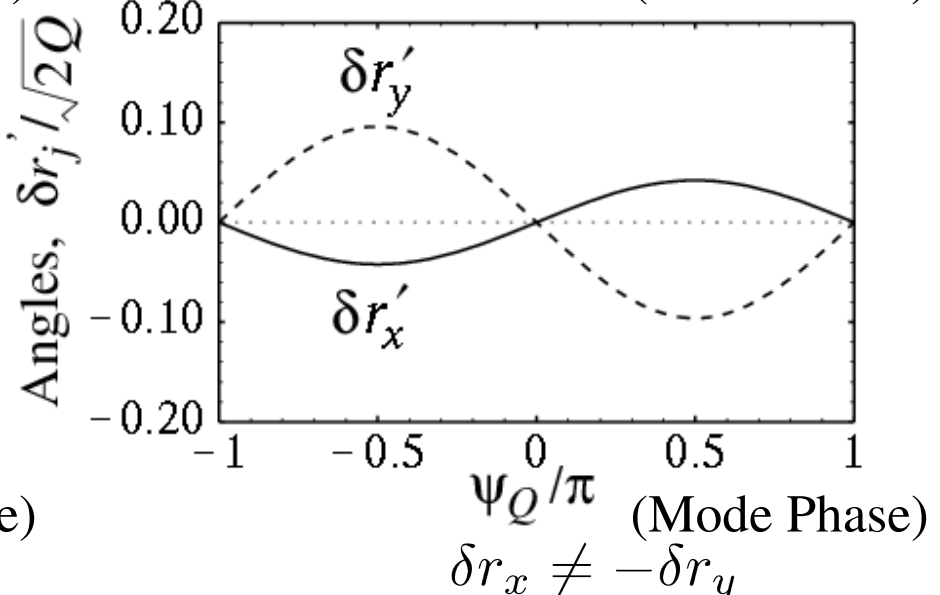
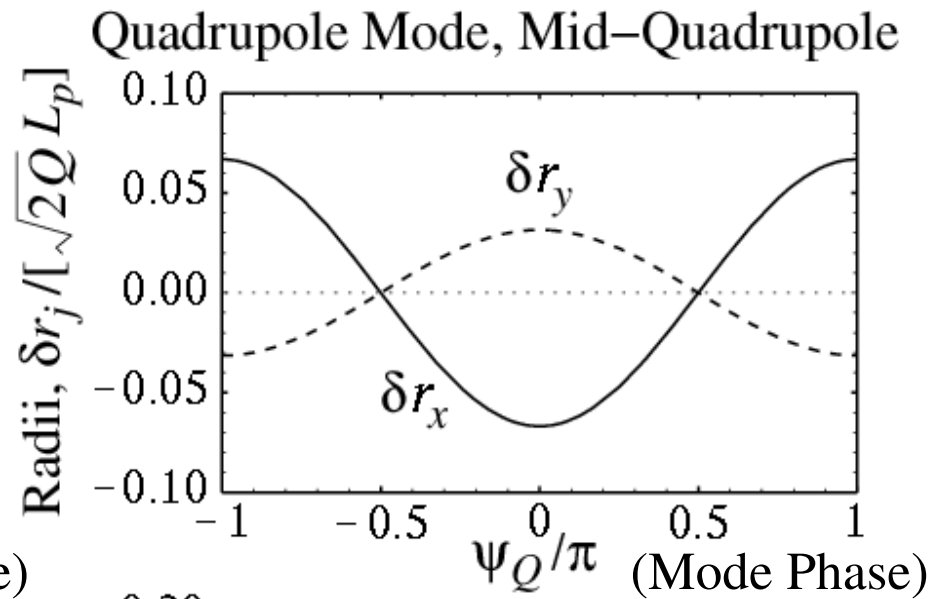
$$\sigma_0 = 80^\circ$$

$$\sigma/\sigma_0 = 0.2$$

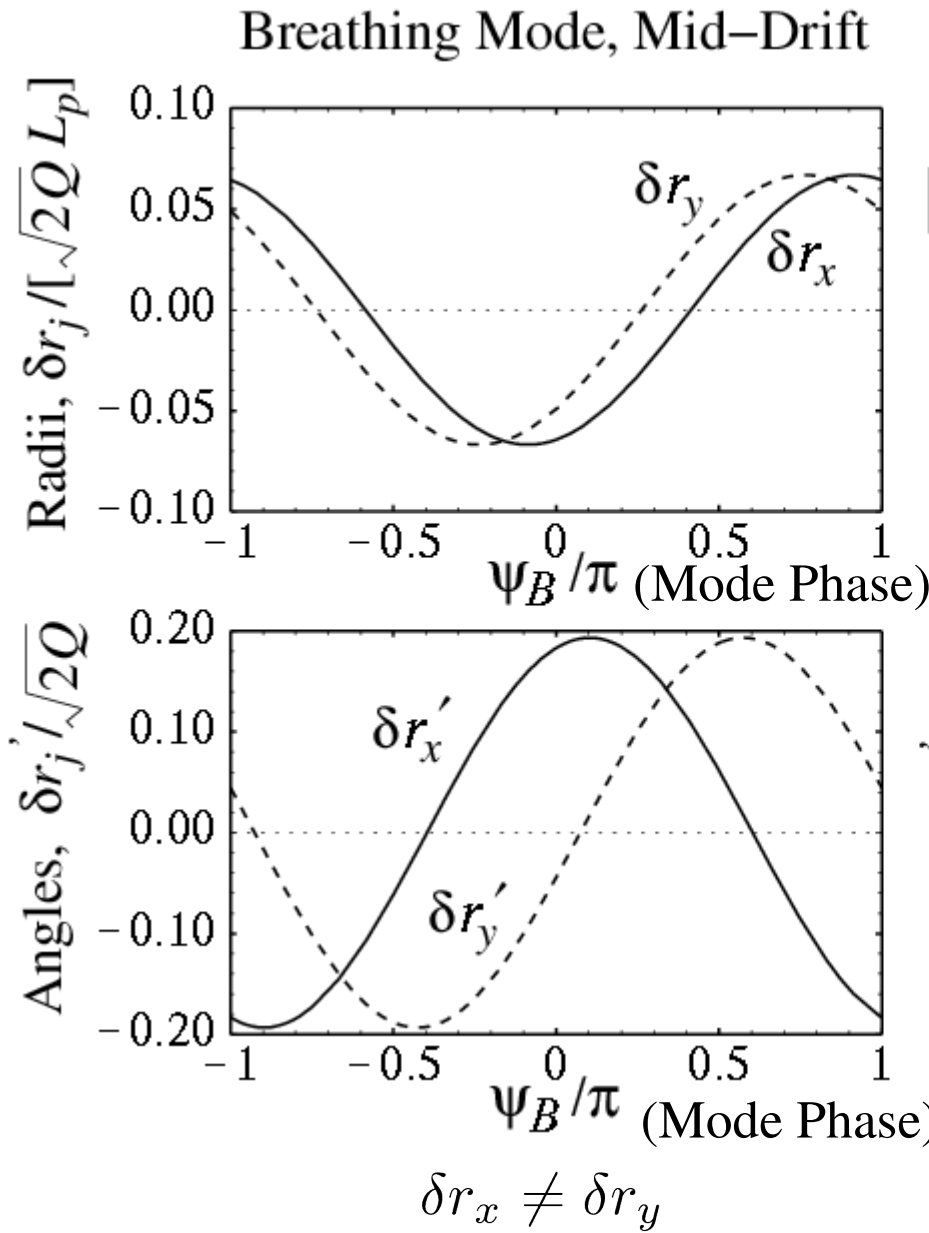
Quadrupole Focusing – projections of perturbations on pure modes varies strongly with mode phase and the location in the lattice (FODO example)



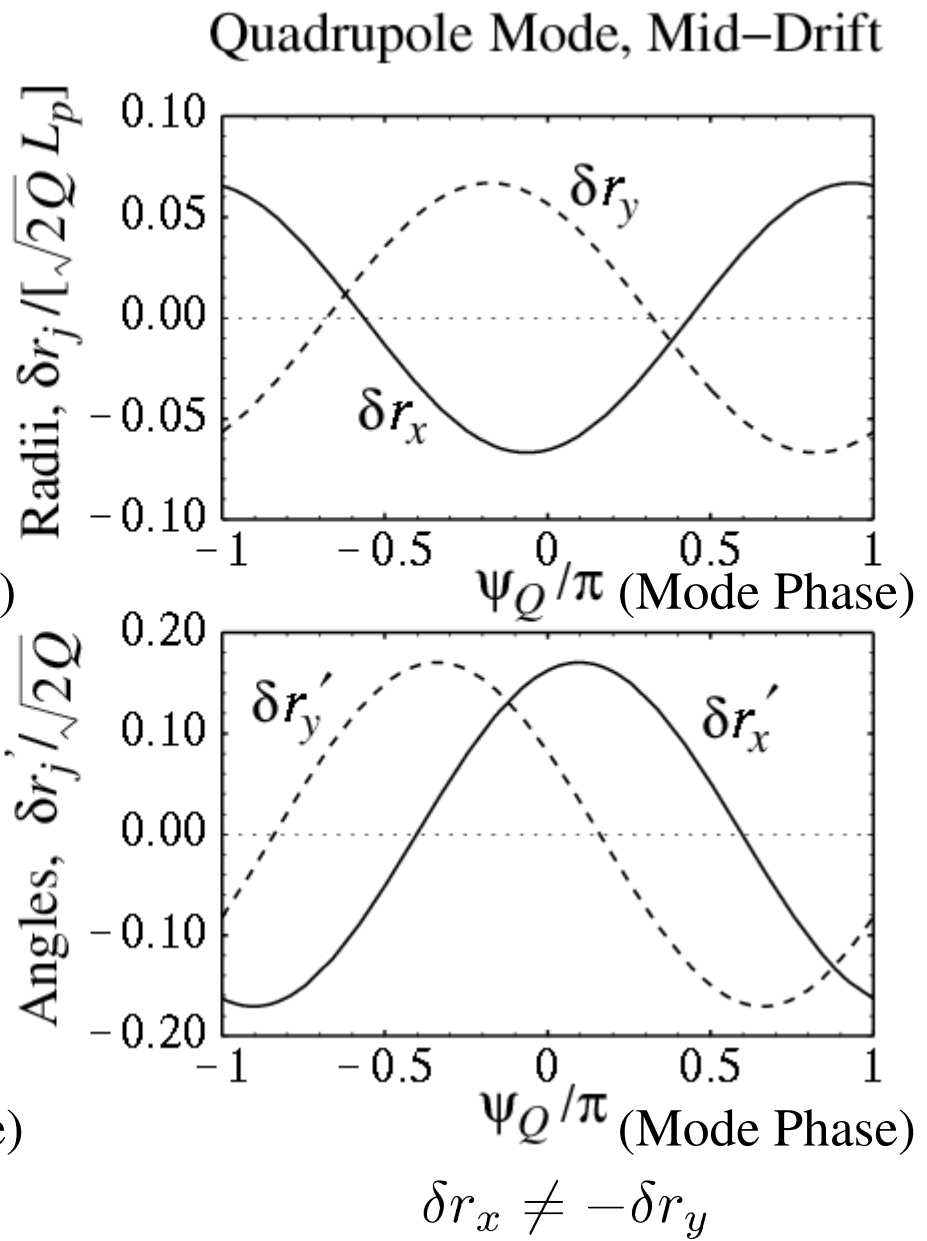
generally not exact
breathing symmetry



generally not exact
quadrupole symmetry



generally not exact
breathing symmetry

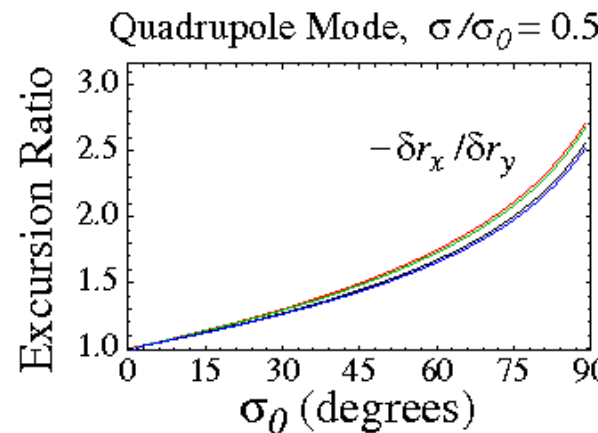
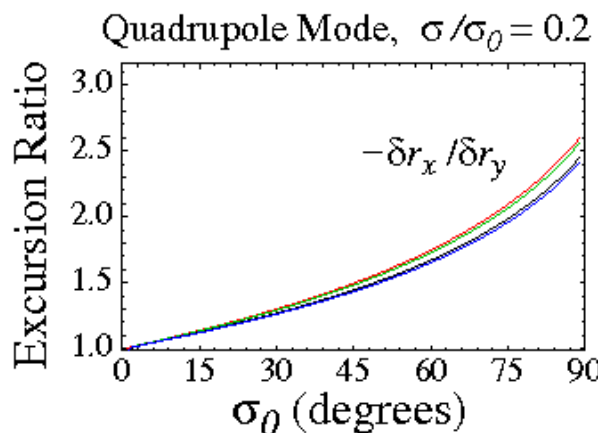
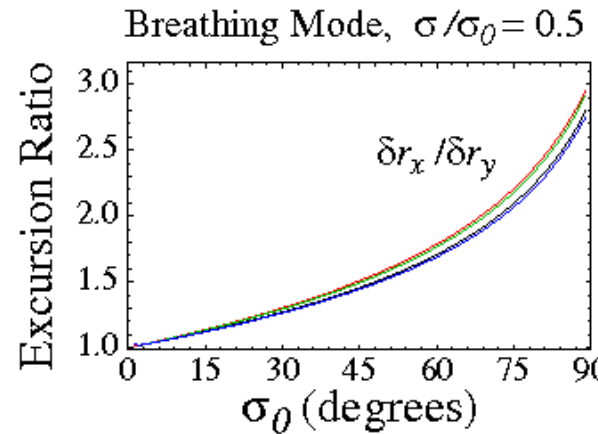
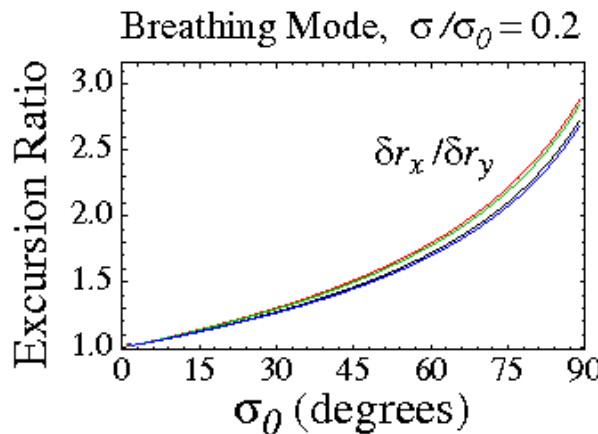


generally not exact
quadrupole symmetry

As a further guide in **pure mode launching**, summarize FODO results for:

- ◆ Mid-axial location of an x -focusing quadrupole with the additional choice $\delta r'_j = 0$
- ◆ Specify ratio of $\delta r_x / \delta r_y$ to launch pure mode
- ◆ Plot as function of σ_0 for $\sigma_0 < 90^\circ$
 - Results vary little with occupancy η or σ/σ_0

$$\eta = \begin{cases} 0.90 & \text{(Blue)} \\ 0.6949 & \text{(Black)} \\ 0.25 & \text{(Green)} \\ 0.10 & \text{(Red)} \end{cases}$$



Specific mode phase in this case due to the choice $\delta r'_x = 0 = \delta r'_y$ at launch location

Comments:

- For quadrupole transport using the axisymmetric equilibrium projections on the breathing (+) mode and quadrupole (-) mode will *NOT* generally result in nearly pure mode projections:

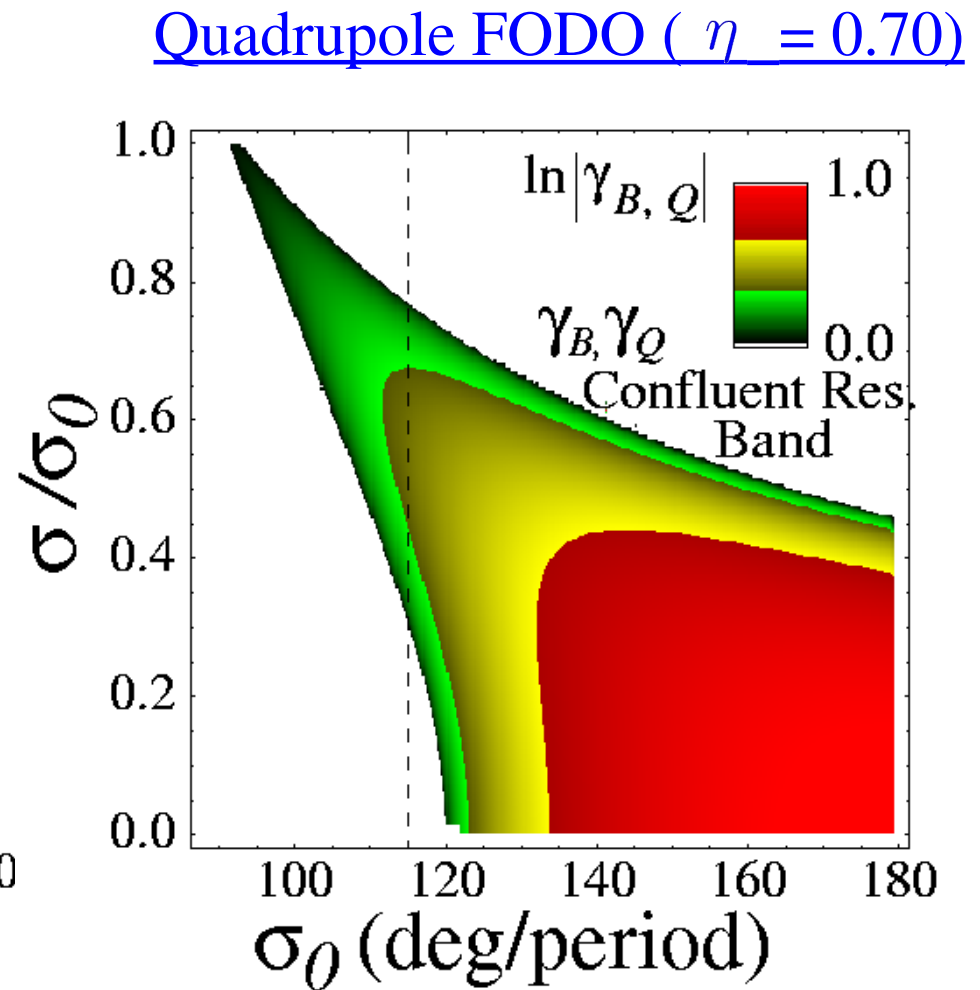
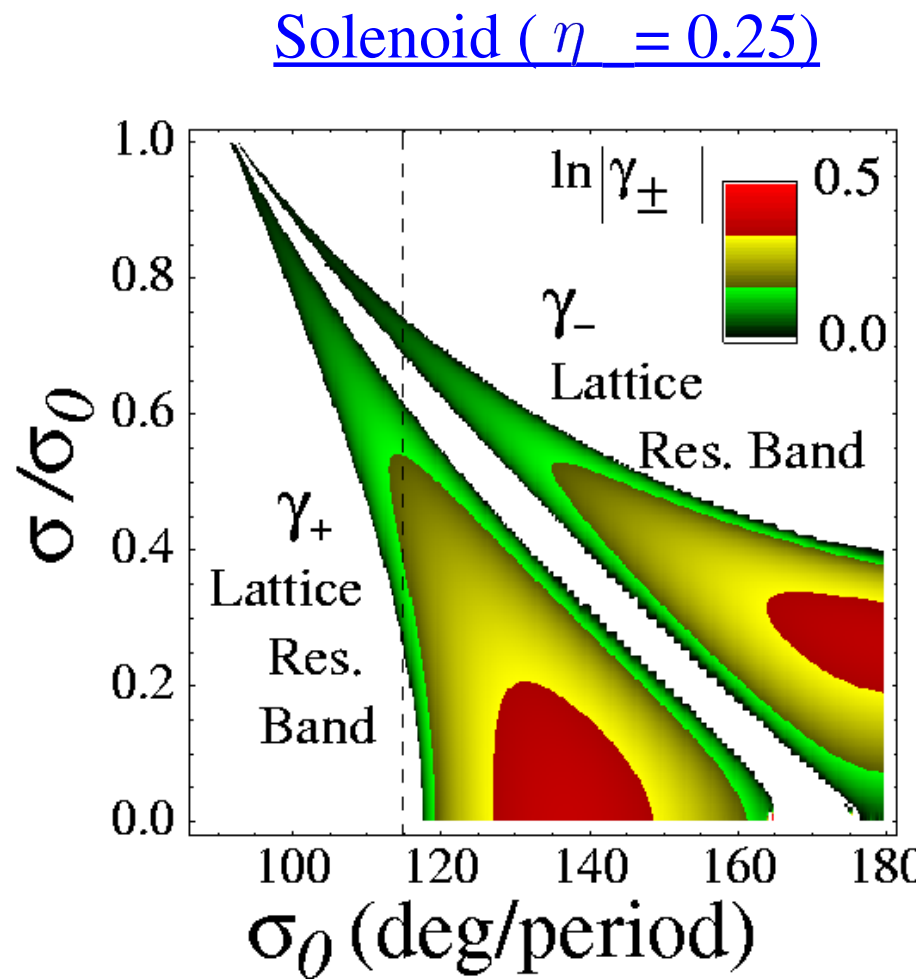
$$\delta r_+ \equiv \frac{\delta r_x + \delta r_y}{2} \neq \text{Breathing Mode Projection}$$

$$\delta r_- \equiv \frac{\delta r_x - \delta r_y}{2} \neq \text{Quadrupole Mode Projection}$$

- Mistake can be commonly found in research papers and can confuse analysis of supposedly pure classes of envelope oscillations which are not.
- Recall: reason denoted generalization of breathing mode with a subscript B and quadrupole mode with a subscript Q was an attempt to avoid confusion by overgeneralization
- Must solve for eigenvectors of 4x4 envelope transfer matrix through one lattice period calculated from the launch location in the lattice and analyze symmetries to determine proper projections (see **S6**)
- Normal mode coordinates can be found for the quadrupole and breathing modes in AG quadrupole focusing lattices through analysis of the eigenvectors but the expressions are typically complicated
 - Modes have underlying Courant-Snyder invariant but it will be a complicated

Summary: Envelope band instabilities and growth rates for periodic solenoidal and quadrupole doublet focusing lattices have been described

Envelope Mode Instability Growth Rates



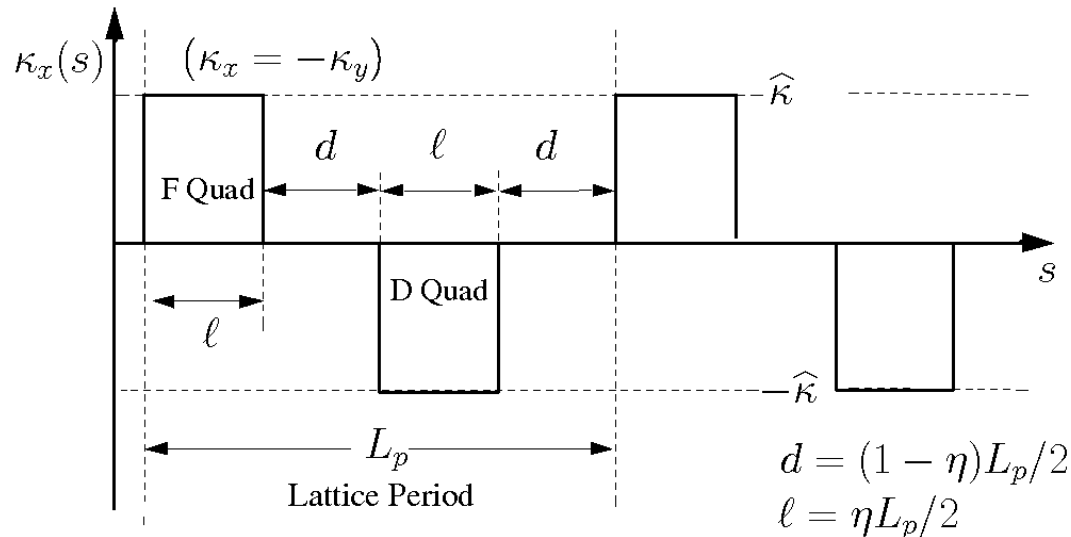
S9: Transport Limit Scaling Based on Matched Beam Envelope Models for Periodic Focusing

For high intensity applications, scaling of the max beam current (or perveance Q) that can be transported for particular focusing technology is important when designing focusing/acceleration lattices. Analytical solutions can provide valuable guidance on design trade-offs. When too cumbersome, numerical solutions of the envelope equation can be applied.

- ◆ Transport limits inextricably linked to technology limitations
 - Magnet field limits
 - Electric breakdown
 - Vacuum
 - ...
- ◆ Higher-order stability constraints (i.e., parameter choices to avoid kinetic instabilities) must ultimately also be explored to verify viability of results for applications: not covered in this idealized case

Review example covered in **Intro Lectures** adding more details: Transport Limits of a Periodic FODO Quadrupole Transport Channel

Lattice:



Parameters:

$L_p = 2L$ = Lattice Period

L = Half-Period

$\eta \in (0, 1]$ = Occupancy

$\hat{\kappa}$ = Strength

Characteristics:

$\eta L = \ell = \text{F/D Len}$

$(1 - \eta)L = d = \text{Drift Len}$

Matched beam envelope equations :

$$r''_{xm}(s) + \kappa_x(s)r_{xm}(s) - \frac{2Q}{r_{xm}(s) + r_{ym}(s)} - \frac{\varepsilon_x^2}{r_{xm}^3(s)} = 0$$

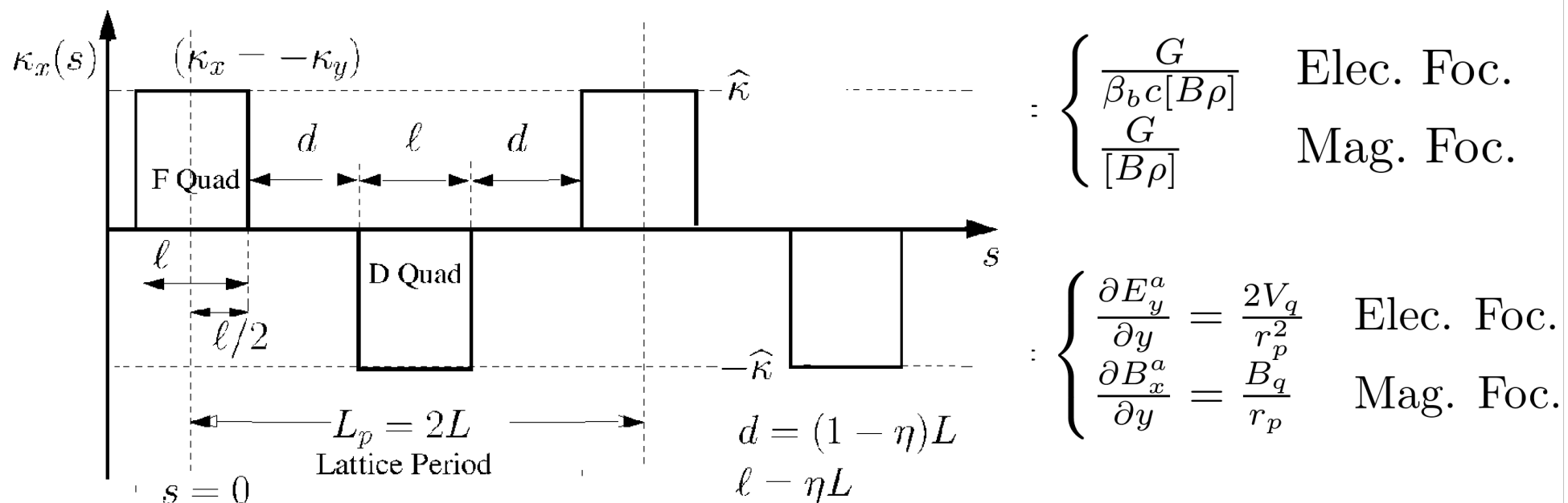
$$r''_{ym}(s) + \kappa_y(s)r_{ym}(s) - \frac{2Q}{r_{xm}(s) + r_{ym}(s)} - \frac{\varepsilon_y^2}{r_{ym}^3(s)} = 0$$

$$r_{xm}(s + L_p) = r_{xm}(s) \quad r_{xm}(s) > 0$$

$$r_{ym}(s + L_p) = r_{ym}(s) \quad r_{ym}(s) > 0$$

Expand the periodic $\kappa_x(s)$ as a Fourier series:

- Choose coordinate zero in s -middle of a x -focusing quadrupole so that can be expanded as an even function in s
- Make symmetrical as possible to simplify analysis to the extent possible!



with this choice :

$$\kappa_x(s) = \sum_{n=1}^{\infty} \kappa_n \cos \left(\frac{n\pi s}{L} \right)$$

$$\kappa_n = \frac{1}{L} \int_0^{2L} \kappa_x(s) \cos \left(\frac{n\pi s}{L} \right) = \frac{2\hat{\kappa}}{n\pi} [1 - (-1)^n] \sin \left(\frac{n\pi\eta}{2} \right)$$

Take : $(\gamma_b \beta_b)' = 0 \iff$ No Acceleration

$\varepsilon_x = \varepsilon_y \equiv \varepsilon \iff$ Isotropic Beam

Expand the periodic matched envelope according to:

$$r_{xm} = r_b [1 + \Delta \cos(\pi s/L)] + \sum_{n=2}^{\infty} \Delta_{xn} \cos(n\pi s/L)$$

$$r_{ym} = r_b [1 - \Delta \cos(\pi s/L)] + \sum_{n=2}^{\infty} \Delta_{yn} \cos(n\pi s/L)$$

$r_b = \text{const} =$ Average Beam Radius

$$|\Delta| = \text{const} < 1$$

Δ_{xn}, Δ_{yn} = constants with $|\Delta_{xn}|, |\Delta_{yn}| \ll |\Delta|$

Insert expansions in the matched envelope eqn and neglect:

- All terms order Δ^2 and higher
- Fast oscillation terms $\sim \cos(n\pi s/L)$ with $n > 2$

To obtain two independent matched beam constraint equations:

Average (const): $\frac{2\Delta\hat{\kappa}}{\pi}r_b \sin(\pi\eta/2) - \frac{Q}{r_b} - \frac{\varepsilon^2}{r_b^3} = 0$

Fundamental:
 $(\propto \cos(\pi s/L))$ $-\Delta \left(\frac{\pi}{L}\right)^2 r_b + \frac{4\hat{\kappa}r_b}{\pi} \sin(\pi\eta/2) + \frac{2\Delta\varepsilon^2}{r_b^3} = 0$

These equations can be solved to express the matched envelope edge excursion (beam size) as:

$$\text{Max}[r_{xm}] = \text{Max}[r_{ym}] \simeq r_b(1 + |\Delta|) = r_b \left\{ 1 + \frac{4|\hat{\kappa}|L^2}{\pi^3} \frac{\sin(\pi\eta/2)}{\left(1 - \frac{3L^2\varepsilon^2}{\pi^2r_b^4}\right)} \right\}$$

and the beam permeance (i.e., transportable current) as:

$$Q = 8 [\sin(\pi\eta/2)]^2 \frac{\hat{\kappa}^2 L^2 r_b^2}{\left(1 - \frac{3L^2\varepsilon^2}{\pi^2r_b^4}\right)} - \frac{\varepsilon^2}{r_b^2}$$

Lattice Design Strategy:

Outline for FODO quadrupole focusing in context with the previous derivation, but pattern adaptable to other cases

Step 1) Choose a lattice period $2L$, occupancy η , clear bore “pipe” radius r_p consistent with focusing technology employed.

- Here estimate in terms of hard-edge equivalent idealization

Step 2) Choose the largest possible focus strength $\hat{\kappa}$ (i.e., quadrupole current or voltage excitation) possible for beam energy with undepressed particle phase advance:

$$\sigma_0 \lesssim 80^\circ/\text{Period}$$

“Tiefenback Limit”

See Lectures on **Transverse Kinetic Stability**

- Larger phase advance corresponds to stronger focus and smaller beam cross-sectional area for given values of: Q , ε_x
- Weaker focusing/smaller phase advance tends to suppress various envelope and kinetic instabilities for more reliable transport
- Specific lattices likely have different focusing limits for stability:
For example, solenoid focusing tends to have less instability

Step 3) Choose beam-edge to aperture clearance factor Δ_p :

$$r_p = \text{Max}[r_{xm}] + \Delta_p \quad \Delta_p = \text{Clearance}$$

To account for:

- Centroid offset (from misalignments + initial value)
- Limit scraping of halo particles outside the beam core
- Nonlinear fields effects (from magnet fill factor + image charges)
- Vacuum needs (gas propagation time from aperture to beam ...)
- + Other effects

Step 4) Evaluate choices made using theory, numerical simulations, etc. Iterate choices to meet performance needs and optimize cost.

Effective application of this procedure requires extensive practical knowledge:

- Nonideal effects: collective instabilities, halo, electron and gas interactions (Species contamination, ...)
- Technology limits: voltage breakdown, normal and superconducting magnet limits,

Details and limits vary with choice of focusing and application needs.

Maximum Current Limit of a quadrupole FODO lattice

At the space-charge limit, the beam is “cold” and the emittance defocusing term is negligible relative to space-charge. Neglect the emittance terms in the previous equations to find the maximum transportable current for a FODO lattice

$$\lim_{\varepsilon_x \rightarrow 0} \sigma_x = 0$$

$$\implies$$

$$\lim_{\varepsilon_y \rightarrow 0} \sigma_y = 0$$

Full space-charge
Depression

In this limit, the maximum transportable perveance (current) is obtained:

$$\lim_{\varepsilon_x, \varepsilon_y \rightarrow 0} Q \equiv Q_{\max}$$

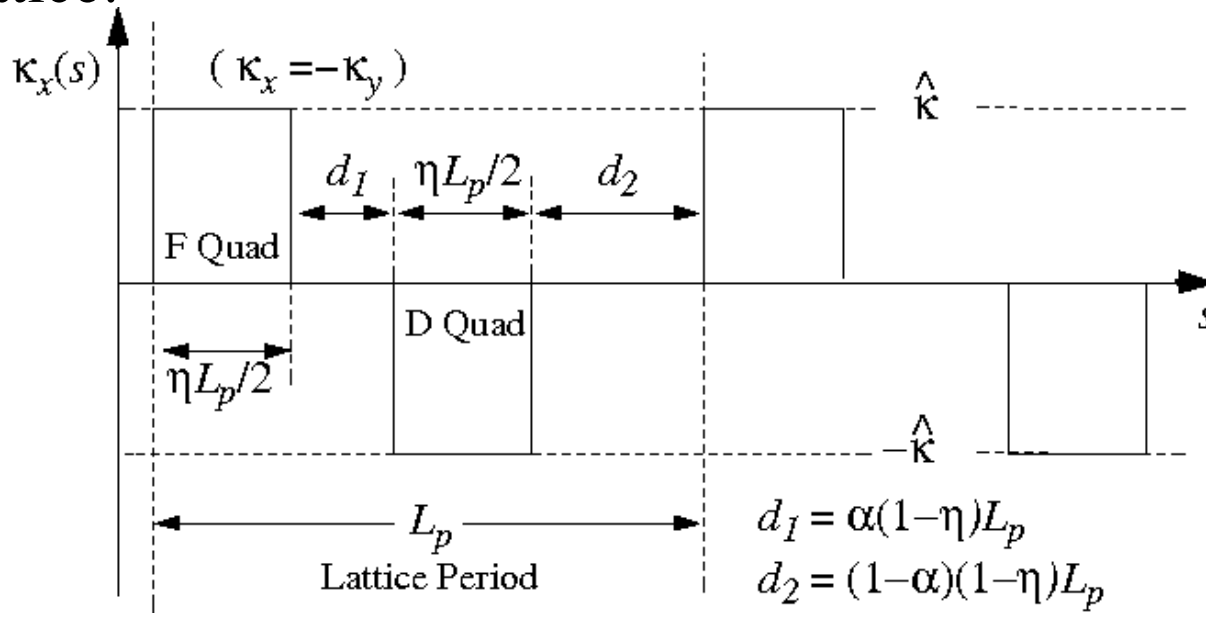
Taking this limit in our previous results for a FODO quadrupole lattice obtains:

$$\lim_{\varepsilon \rightarrow 0} \text{Max}[r_{xm}] = r_b \left\{ 1 + \frac{4|\hat{\kappa}|L^2}{\pi^3} \sin(\pi\eta/2) \right\}$$

$$\lim_{\varepsilon \rightarrow 0} Q = Q_{\max} = 8 [\sin(\pi\eta/2)]^2 \hat{\kappa}^2 L^2 r_b^2$$

Transport Limits of syncopated quadrupole FODO transport channel

Lattice:



$$\eta \in (0, 1] \quad \text{Occupancy}$$

$$\alpha \in [0, 1/2] \quad \text{Syncopation Factor}$$

$$\alpha = 1/2 \rightarrow \text{FODO}$$

Material to be added from based on
supplemental 2008 pdf scan USPAS notes

- ◆ Not simple analytical calculation but summary of results to illustrate how results change in situations with less symmetry

Transport Limits of a Solenoidal Transport Channel

Covered in homework!

- ♦ Much easier than quadrupole cases!
- ♦ May summarize results from homework here in future notes for completeness

S10: Centroid and Envelope Descriptions via 1st Order Coupled Moment Equations

When constructing centroid and moment models, it can be efficient to simply write moments, differentiate them, and then apply the equation of motion. Generally, this results in lower order moments coupling to higher order ones and an infinite chain of equations. But the hierarchy can be truncated by:

- ◆ Assuming a fixed functional form of the distribution in terms of moments
- ◆ And/Or: neglecting coupling to higher order terms

Resulting first order moment equations can be expressed in terms of a closed set of moments and advanced in s or t using simple (ODE based) numerical codes. This approach can prove simpler to include effects where invariants are not easily extracted to reduce the form of the equations (as when solving the KV envelope equations in the usual form).

Examples of effects that might be more readily analyzed:

- ◆ Skew coupling in quadrupoles
- ◆ Chromatic effects in final focus
- ◆ Dispersion in bends

See: references at end of notes and
J.J. Barnard, lecture on
Heavy-Ion Fusion and Final Focusing

Resulting 1st order form of coupled moment equations:

$$\frac{d}{ds} \mathbf{M} = \mathbf{F}(\mathbf{M})$$

\mathbf{M} = vector of moments, and their s derivatives, generally infinite

\mathbf{F} = vector function of \mathbf{M} , generally nonlinear

- System advanced from a specified initial condition (initial value of \mathbf{M})

Transverse moment definition:

$$\langle \dots \rangle_{\perp} \equiv \frac{\int d^2x_{\perp} \int d^2x'_{\perp} \dots f_{\perp}}{\int d^2x_{\perp} \int d^2x'_{\perp} f_{\perp}}$$

Can be generalized if other variables such as off momentum are included in distribution f

Differentiate moments and apply equations of motion:

$$\frac{d}{ds} \langle \dots \rangle_{\perp} \equiv \frac{\int d^2x_{\perp} \int d^2x'_{\perp} \left[\frac{d}{ds} \dots \right] f_{\perp}}{\int d^2x_{\perp} \int d^2x'_{\perp} f_{\perp}}$$

+ apply equations of motion to simplify $\frac{d}{ds} \dots$

When simplifying the results, if the distribution form is frozen in terms of moments (Example: assume uniform density elliptical beam) then we use constructs like:

$$n = \int d^2x'_\perp f_\perp = n(\mathbf{M})$$

to simplify the resulting equations and express the RHS in terms of elements of \mathbf{M}

1st order moments:

$$\mathbf{X}_\perp = \langle \mathbf{x}_\perp \rangle_\perp \quad \text{Centroid coordinate}$$

$$\mathbf{X}'_\perp = \langle \mathbf{x}'_\perp \rangle_\perp \quad \text{Centroid angle}$$

+ possible others if more variables. Example

$$\Delta = \left\langle \frac{\delta p_s}{p_s} \right\rangle = \langle \delta \rangle \quad \text{Centroid off-momentum}$$

⋮

⋮

2nd order moments:

It is typically convenient to subtract centroid from higher-order moments

$$\tilde{x} \equiv x - X \quad \tilde{x}' \equiv x' - X'$$

$$\tilde{y} \equiv y - Y \quad \tilde{y}' \equiv y' - Y'$$

$$\tilde{\delta} \equiv \delta - \Delta$$

x-moments	y-moments	x-y cross moments	dispersive moments
$\langle \tilde{x}^2 \rangle_{\perp}$	$\langle \tilde{y}^2 \rangle_{\perp}$	$\langle \tilde{x}\tilde{y} \rangle_{\perp}$	$\langle \tilde{x}\tilde{\delta} \rangle, \langle \tilde{y}\tilde{\delta} \rangle$
$\langle \tilde{x}\tilde{x}' \rangle_{\perp}$	$\langle \tilde{y}\tilde{y}' \rangle_{\perp}$	$\langle \tilde{x}'\tilde{y} \rangle_{\perp}, \langle \tilde{x}\tilde{y}' \rangle_{\perp}$	$\langle \tilde{x}'\tilde{\delta} \rangle, \langle \tilde{y}'\tilde{\delta} \rangle$
$\langle \tilde{x}'^2 \rangle_{\perp}$	$\langle \tilde{y}'^2 \rangle_{\perp}$	$\langle \tilde{x}'\tilde{y}' \rangle_{\perp}$	$\langle \tilde{\delta}^2 \rangle$

3rd order moments: Analogous to 2nd order case, but more for each order

$$\langle \tilde{x}^3 \rangle_{\perp}, \langle \tilde{x}^2\tilde{y} \rangle_{\perp}, \dots$$

Many quantities of physical interest are expressed in transport can then be expressed in terms of moments calculated when the equations are numerically advanced in s and their evolutions plotted to understand behavior

- ◆ Many quantities of physical interest are expressible in terms of 1st and 2nd order moments

Example moments often projected:

Statistical beam size:
(rms edge measure)

$$r_x = 2\langle \tilde{x}^2 \rangle_{\perp}^{1/2}$$

$$r_y = 2\langle \tilde{y}^2 \rangle_{\perp}^{1/2}$$

Statistical emittances:
(rms edge measure)

$$\varepsilon_x = 4 [\langle \tilde{x}^2 \rangle_{\perp} \langle \tilde{x}'^2 \rangle_{\perp} - \langle \tilde{x}\tilde{x}' \rangle_{\perp}^2]^{1/2}$$

$$\varepsilon_y = 4 [\langle \tilde{y}^2 \rangle_{\perp} \langle \tilde{y}'^2 \rangle_{\perp} - \langle \tilde{y}\tilde{y}' \rangle_{\perp}^2]^{1/2}$$

Kinetic longitudinal temperature:
(rms measure)

$$T_s = \text{const} \times \langle \tilde{\delta}^2 \rangle$$

Illustrate approach with the familiar KV model

Truncation assumption: unbunched uniform density elliptical beam in free space

- ◆ $\delta = 0$, no axial velocity spread
- ◆ All cross moments zero, i.e. $\langle \tilde{x}\tilde{y} \rangle_{\perp} = 0$

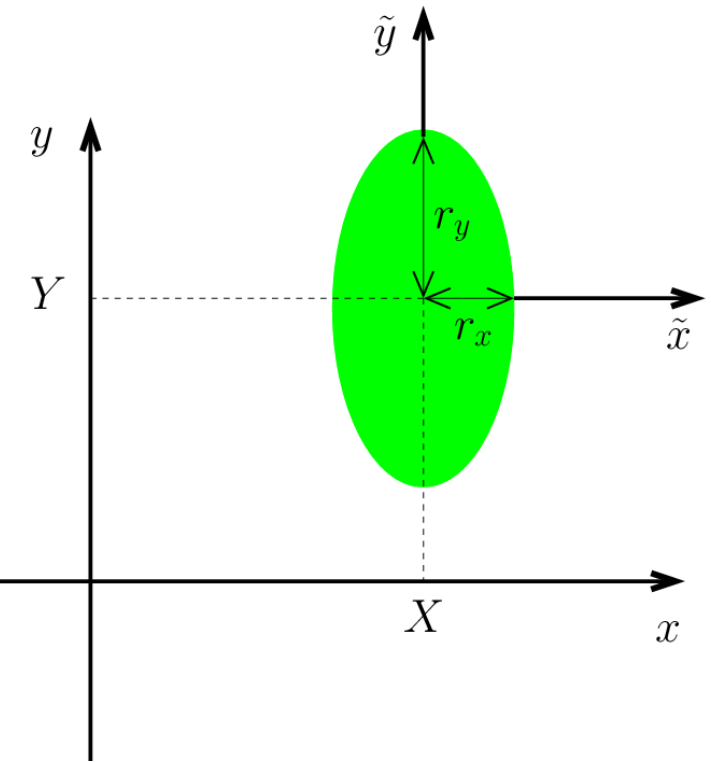
$$\frac{d}{ds} \langle x \rangle_{\perp} = \langle x' \rangle_{\perp}$$

$$\frac{d}{ds} \langle x^2 \rangle_{\perp} = 2 \langle xx' \rangle_{\perp}$$

$$\frac{d}{ds} \langle x' \rangle_{\perp} = \langle x'' \rangle_{\perp}$$

$$\frac{d}{ds} \langle x'^2 \rangle_{\perp} = 2 \langle x'x'' \rangle_{\perp}$$

$$\vdots$$

$$\vdots$$


Use particle equations of motion within beam, neglect images, and simplify

- ◆ Apply equations in S2 with $\mathbf{E}_{\perp}^i = 0$

$$x'' + \frac{(\gamma_b \beta_b)'}{(\gamma_b \beta_b)} x' + \kappa_x x - \frac{2Q}{(r_x + r_y)r_x} (x - \langle x \rangle_{\perp}) = 0$$

$$y'' + \frac{(\gamma_b \beta_b)'}{(\gamma_b \beta_b)} y' + \kappa_y y - \frac{2Q}{(r_x + r_y)r_y} (y - \langle y \rangle_{\perp}) = 0$$

Resulting system of 1st and 2nd order moments

1st order moments:

$$\frac{d}{ds} \begin{bmatrix} \langle x \rangle_{\perp} \\ \langle x' \rangle_{\perp} \\ \langle y \rangle_{\perp} \\ \langle y' \rangle_{\perp} \end{bmatrix} = \begin{bmatrix} \langle x' \rangle_{\perp} \\ -\kappa_x(s) \langle x \rangle_{\perp} \\ \langle y' \rangle_{\perp} \\ -\kappa_y(s) \langle y \rangle_{\perp} \end{bmatrix}$$

2nd order moments:

$$\frac{d}{ds} \begin{bmatrix} \langle \tilde{x}^2 \rangle_{\perp} \\ \langle \tilde{x}\tilde{x}' \rangle_{\perp} \\ \langle \tilde{x}'^2 \rangle_{\perp} \\ \langle \tilde{y}^2 \rangle_{\perp} \\ \langle \tilde{y}\tilde{y}' \rangle_{\perp} \\ \langle \tilde{y}'^2 \rangle_{\perp} \end{bmatrix} = \begin{bmatrix} 2\langle \tilde{x}\tilde{x}' \rangle_{\perp} \\ \langle \tilde{x}'^2 \rangle_{\perp} - \kappa_x(s) \langle \tilde{x}^2 \rangle_{\perp} + \frac{Q \langle \tilde{x}^2 \rangle_{\perp}^{1/2}}{2[\langle \tilde{x}^2 \rangle_{\perp}^{1/2} + \langle \tilde{y}^2 \rangle_{\perp}^{1/2}]} \\ -2\kappa_x(s) \langle \tilde{x}\tilde{x}' \rangle_{\perp} + \frac{Q \langle \tilde{x}\tilde{x}' \rangle_{\perp}}{\langle \tilde{x}^2 \rangle_{\perp}^{1/2} [\langle \tilde{x}^2 \rangle_{\perp}^{1/2} + \langle \tilde{y}^2 \rangle_{\perp}^{1/2}]} \\ 2\langle \tilde{y}\tilde{y}' \rangle_{\perp} \\ \langle \tilde{y}'^2 \rangle_{\perp} - \kappa_y(s) \langle \tilde{y}^2 \rangle_{\perp} + \frac{Q \langle \tilde{y}^2 \rangle_{\perp}^{1/2}}{2[\langle \tilde{x}^2 \rangle_{\perp}^{1/2} + \langle \tilde{y}^2 \rangle_{\perp}^{1/2}]} \\ -2\kappa_y(s) \langle \tilde{y}\tilde{y}' \rangle_{\perp} + \frac{Q \langle \tilde{y}\tilde{y}' \rangle_{\perp}}{\langle \tilde{y}^2 \rangle_{\perp}^{1/2} [\langle \tilde{x}^2 \rangle_{\perp}^{1/2} + \langle \tilde{y}^2 \rangle_{\perp}^{1/2}]} \end{bmatrix}$$

- ◆ Express 1st and 2nd order moments separately in this case since uncoupled
- ◆ Form truncates due to frozen distribution form: all moments on LHS on RHS
- ◆ Integrate from initial moments values of s and project out desired quantities

Using 2nd order moment equations we can show that

$$\frac{d}{ds} \varepsilon_x^2 = 0 = \frac{d}{ds} \varepsilon_y^2$$

$$\begin{aligned} \varepsilon_x^2 &= 16 [\langle x^2 \rangle_{\perp} \langle x'^2 \rangle_{\perp} - \langle xx' \rangle_{\perp}^2] = \text{const} \\ \implies \varepsilon_y^2 &= 16 [\langle y^2 \rangle_{\perp} \langle y'^2 \rangle_{\perp} - \langle yy' \rangle_{\perp}^2] = \text{const} \end{aligned}$$

Using this, the 2nd order moment equations can be equivalently expressed in the standard KV envelope form:

$$\begin{aligned} \frac{dr_x}{ds} &= r'_x ; \quad \frac{d}{ds} r'_x + \kappa_x r_x - \frac{2Q}{r_x + r_y} - \frac{\varepsilon_x^2}{r_x^3} = 0 \\ \frac{dr_y}{ds} &= r'_y ; \quad \frac{d}{ds} r'_y + \kappa_y r_y - \frac{2Q}{r_x + r_y} - \frac{\varepsilon_y^2}{r_y^3} = 0 \end{aligned}$$

- ◆ Moment form fully consistent with usual KV model as it must be
- ◆ Moment form generally easier to put in additional effects that would violate the usual emittance invariants

Relative advantages of the use of coupled matrix form versus reduced equations can depend on the problem/situation

Coupled Matrix Equations

$$\frac{d}{ds} \mathbf{M} = \mathbf{F}(\mathbf{M})$$

\mathbf{M} = Moment Vector

\mathbf{F} = Force Vector

- ◆ Easy to formulate
 - Straightforward to incorporate additional effects
- ◆ Natural fit to numerical routine
 - Easy to numerically code/solve

Reduced Equations

$$X'' + \kappa_x X = 0$$

$$r_x'' + \kappa_x r_x - \frac{2Q}{r_x + r_y} - \frac{\varepsilon_x^2}{r_x^3} = 0$$

etc.

Reduction based on identifying invariants such as
 $\varepsilon_x^2 = 16 \left[\langle \tilde{x}^2 \rangle_{\perp} \langle \tilde{x}'^2 \rangle_{\perp} - \langle \tilde{x} \tilde{x}' \rangle_{\perp}^2 \right]$ helps understand solutions

- ◆ Compact expressions can help analytical understanding

Corrections and suggestions for improvements welcome!

These notes will be corrected and expanded for reference and for use in future editions of US Particle Accelerator School (USPAS) and Michigan State University (MSU) courses. Contact:

Prof. Steven M. Lund
Facility for Rare Isotope Beams
Michigan State University
640 South Shaw Lane
East Lansing, MI 48824

lund@frb.msu.edu
(517) 908 – 7291 office
(510) 459 - 4045 mobile

Please provide corrections with respect to the present archived version at:

https://people.nscl.msu.edu/~lund/uspas/bpisc_2015

Redistributions of class material welcome. Please do not remove author credits.

References: For more information see:

These course notes are posted with updates, corrections, and supplemental material at:

https://people.nscl.msu.edu/~lund/uspas/bpisc_2015

Materials associated with previous and related versions of this course are archived at:

JJ Barnard and SM Lund, *Beam Physics with Intense Space-Charge*, USPAS:

http://hifweb.lbl.gov/USPAS_2011 2011 Lecture Notes + Info

https://people.nscl.msu.edu/~lund/uspas/bpisc_2011/

<http://uspas.fnal.gov/programs/past-programs.shtml> (2008, 2006, 2004)

JJ Barnard and SM Lund, *Interaction of Intense Charged Particle Beams with Electric and Magnetic Fields*, UC Berkeley, Nuclear Engineering NE290H

<http://hifweb.lbl.gov/NE290H> 2009 Lecture Notes + Info

References: Continued (2):

Image charge couplings:

E.P. Lee, E. Close, and L. Smith, “SPACE CHARGE EFFECTS IN A BENDING MAGNET SYSTEM,” Proc. Of the 1987 Particle Accelerator Conf., 1126 (1987)

Seminal work on envelope modes:

J. Struckmeier and M. Reiser, “Theoretical Studies of Envelope Oscillations and Instabilities of Mismatched Intense Charged-Particle Beams in Periodic Focusing Channels,” Particle Accelerators **14**, 227 (1984)

M. Reiser, *Theory and Design of Charged Particle Beams* (John Wiley, 1994, 2008)

Extensive review on envelope instabilities:

S.M. Lund and B. Bukh, “Stability properties of the transverse envelope equations describing intense ion beam transport,” PRSTAB **7** 024801 (2004)

Efficient, Fail-Safe Generation of Matched Envelope Solutions:

S.M. Lund and S.H. Chilton, and E.P. Lee, “Efficient computation of matched solutions of the Kapchinskij-Vladimirskij envelope equations,” PRSTAB **9**, 064201(2006)

A highly flexible Mathematica -based implementation is archived on the course web site with these lecture notes. This was used to generated many plots in this course.

KV distribution:

F. Sacherer, *Transverse Space-Charge Effects in Circular Accelerators*, Univ. of California Berkeley, Ph.D Thesis (1968)

I. Kaphinskij and V. Vladimirsij, in *Proc. Of the Int. Conf. On High Energy Accel. and Instrumentation* (CERN Scientific Info. Service, Geneva, 1959) p. 274

S.M. Lund, T. Kikuchi, and R.C. Davidson, “Generation of initial kinetic distributions for simulation of long-pulse charged particle beams with high space-charge intensity,” PRSTAB **12**, 114801 (2009)

Symmetries and phase-amplitude methods:

A. Dragt, *Lectures on Nonlinear Orbit Dynamics in Physics of High Energy Particle Accelerators*, (American Institute of Physics, 1982), AIP Conf. Proc. No. 87, p. 147

E. D. Courant and H. S. Snyder, “Theory of the Alternating-Gradient Synchrotron,” Annals of Physics **3**, 1 (1958)

Analytical analysis of matched envelope solutions and transport scaling:

E. P. Lee, “Precision matched solution of the coupled beam envelope equations for a periodic quadrupole lattice with space-charge,” Phys. Plasmas **9**, 4301 (2005)

O.A. Anderson, “Accurate Iterative Analytic Solution of the KV Envelope Equations for a Matched Beam,” PRSTAB, **10** 034202 (2006)

Coupled Moment Formulations of Centroid and Envelope Evolution:

- J.J. Barnard, H.D. Shay, S.S. Yu, A. Friedman, and D.P. Grote, “Emittance Growth in Heavy-Ion Recirculators,” 1992 PAC Proceedings, Ontario, Canada, p. 229
- J.J. Barnard, J. Miller, I. Haber, “Emittance Growth in Displaced Space Charge Dominated Beams with Energy Spread,” 1993 PAC Proceedings, Washington, p. 3612 (1993)
- J.J. Barnard, “Emittance Growth from Rotated Quadrupoles in Heavy Ion Accelerators,” 1995 PAC Proceedings, Dallas, p. 3241 (1995)
- R.A. Kishek, J.J. Barnard, and D.P. Grote, “Effects of Quadrupole Rotations on the Transport of Space-Charge-Dominated Beams: Theory and Simulations Comparing Linacs with Circular Machines,” 1999 PAC Proceedings, New York, TUP119, p. 1761 (1999)
- J.J. Barnard, R.O. Bangerter, E. Henestroza, I.D. Kaganovich, E.P. Lee, B.G. Logan, W.R. Meier, D. Rose, P. Santhanam, W.M. Sharp, D.R. Welch, and S.S. Yu, “A Final Focus Model for Heavy Ion Fusion System Codes,” NIMA **544** 243-254 (2005)
- J.J. Barnard and B. Losic, “Envelope Modes of Beams with Angular Momentum,” Proc. 20th LINAC Conf., Monterey, MOE12 (2000)

Acknowledgments:

These lecture notes reflect input from numerous scientists and engineers who helped educate the author in accelerator physics over many years. Support enabling the long hours it took to produce these lecture notes were provided by the Facility for Rare Isotope Beams (FRIB) at Michigan State University (MSU), Lawrence Livermore National Laboratory (LLNL), and Lawrence Berkeley National Laboratory (LBNL). Special thanks are deserved to:

Rodger Bangerter	Martin Berz	John Barnard	
Oliver Boine-Frankenheim		Richard Briggs	Ronald Davidson
Mikhail Dorf	Andy Faltens	Bill Fawley	Giuliano Franchetti
Alex Friedman	Dave Grote	Irving Haber	Klaus Halbach
Enrique Henestroza		Ingo Hoffmann	Dave Judd
Igor Kagonovich	Takashi Kikuchi	Rami Kishek	Joe Kwan
Ed Lee	Daniela Leitner	Steve Lidia	
Guillaume Machicoane		Felix Marti	Hiromi Okamoto
Eduard Pozdeyez	Martin Reiser	Lou Reginato	Robert Ryne
Gian-Luca Sabbi	Peter Seidl	William Sharp	Peter Spiller
Edward Startsev	Ken Takayama	Jean-Luc Vay	Will Waldron
Tom Wangler	Jie Wei	Yoshi Yamazaki	Simon Yu
Pavel Zenkovich	Yan Zhang	Qiang Zhao	